I-82 Prosser Landslide Investigation
Benton City, WA

Technical Report

Prepared by:
Jessica Jamsgard
Master's Candidate
MESSAGe Program
University of Washington

Date:
December 6, 2013

Mentor: Tom Badger,
Washington Department of Transportation

Coordinator: Kathy Troost
University of Washington

Reading Committee: Juliet Crider, Tom Badger

Report Number: 006

A report prepared in partial fulfillment of the requirements for the degree of Master of Science, Earth and Space Sciences: Applied Geosciences, University of Washington, December 2013

Date: 12/6/2013
To: Tom Badger
CC: Juliet Crider, Kathy Troost
From: Jessica Jamsgard

Re: Prosser Landslide site MP 91.9, I-82, Benton City, WA

At your request, I have prepared the following technical report in partial fulfillment the degree requirements for the Department of Earth and Space Sciences Master's in Applied Geoscience at the University of Washington.

The scope of this technical report is to help Tom Badger of the WSDOT Geotechnical Office establish the mechanisms by which the eastbound lanes of Interstate 82 at mile post (MP) 91.9 near Benton City continue to deform. Within the WSDOT, the area is known as the Prosser Landslide and has been an ongoing concern since the 1980s. Results from previous technical investigations have been conflicted or inconclusive as to whether landslide movement persists beneath or through the shear key-buttress or that pavement distress is related to swelling of a clay-rich unit that underlies the slope and interstate.

For this report, the following steps were taken. First, I conducted a desk review of archived reports, memos, data, and drill logs from the original construction of I-82 and previous geotechnical investigations commissioned by WSDOT. Findings of this desk review are reported in Part III. Second, at Tom Badger's request, WSDOT drillers drilled two new boreholes at the Prosser Landslide site above the buttress and instrumentation was installed within the boreholes. Borehole logs produced from the 2013 drilling can be found in Appendix A of this report. Material retrieved from the suspected failure zone during drilling was tested at the WSDOT Materials Lab by WSDOT personnel for its mechanical properties including Atterberg limits, grain-size analysis, and residual shear strength (Appendix B). Samples were also analyzed for mineral content using X -ray powder diffraction (XRD). These data and observations are reported in Part III and Appendix C. Finally, using drill logs produced by WSDOT from the latest drilling and from historic drilling campaigns, I constructed a 2-D geologic model of the landslide site. This model is the basis for slope stability analysis reported in Part IV and Appendix D.

This study concludes that the deformation observed in the eastbound lanes of I-82 could be the result of continued landslide movement, despite previous remediation efforts.

I am pleased to present the following technical report on my findings at the Prosser Landslide site.

Respectfully,

Jessica Jamsgard

Table of Contents

Part I: Introduction and Geologic Setting

Introduction

The Prosser Landslide is small, reactivated portion of a larger, ancient landslide which originally came to the attention of WSDOT in 1987 during the realignment of Interstate 82 (I-82, also known as SR-82). Since then, a bump has continuously formed in the eastbound lanes of the realigned portion of I-82 in the vicinity of the original reactivated portion of the landslide. The deformation the road has been a continual concern for WSDOT South Central Region and as of yet, WSDOT has not remediated the deformation permanently

The key question about this site is whether the landslide is causing the deformation of the road, or if some other mechanism, such as swelling clays or frost heave, is responsible.

The landslide is located immediately adjacent to I-82 in south central Washington, in Benton County between Prosser and Kiona (Figure 1a, Figure 1b) along a section of the highway which runs along the base of the Horse Heaven Hills. The area where the most deformation has occurred in the roadway is at mile post (MP) 91.9 (Figure 1a, Figure 1b).

Beginning with the construction of I-82 between Prosser and Kiona in 1986, WSDOT encountered multiple areas where excavation caused significant upslope movement and deformation which in turn impacted construction efforts, including other areas near MP 84, 88, and 90. The Prosser Landslide area at MP 91.9 required the construction of a shear key buttress to arrest upslope landslide movement and allow for completion of the interstate. Since construction, this site has also required the most ongoing monitoring and remediation out of all the problem locations encountered during the realignment.

Since the construction in the 1980s, WSDOT personnel have noticed multiple areas of deformation above the buttress and a bump which formed in the roadbed of the eastbound lanes of I-82. This ongoing deformation has precipitated several internal geotechnical investigations. Since this deformation has persisted, the road surface of the eastbound lane was replaced and repaired multiple times. However, no action beyond construction of the original shear key-buttress has been was taken to stabilize the slope.

In 2006, WSDOT partnered with the Federal Highway Administration, who released a study to investigate the efficacy of using InSAR (Interferometric Synthetic Aperture Radar) to characterize ground deformation of landslides. The Prosser Landslide site was chosen along with two other test sites the InSAR study. InSAR data between 1992 and 2005 were used at the Prosser Landslide site to assess vertical ground displacement. The study concluded that was not able to discern movement with the methods employed during the 1992-2005 time period (FHWA, 2006).

Also in 2006, a geotechnical report was released by C-Core, a contractor, on behalf of the Federal Highway Administration (FHWA) and in conjunction with WSDOT, as part of the InSAR study. Relying on new 200-2004 WSDOT borings, C-Core performed finite element and limit equilibrium analyses of the slide. The study concluded that the slide is effectively stable

and that another mechanism must be responsible for the ongoing deformation of the eastbound lanes (C-Core, 2006).

Since 2006, the South Central Region has continually graded and repaired the bump in the eastbound lanes. Concerned that the site characterization, engineering properties of the failure zone, and landslide analyses to date may not wholly correct, WSDOT has since concluded that further analysis of the site is necessary to finding a way to more confidently characterize the nature of the problem and develop a permanent solution.

Scope of Work

As part of an effort to better characterize the cause of the ongoing deformation of the eastbound lanes of I-82, WSDOT has generously offered this project as an opportunity for an internship.

The mentor for this project is Tom Badger, the chief engineering geologist with WSDOT at the WSDOT Geotechnical Office located in its headquarters at WSDOT Materials Lab in Tumwater, WA.

The scope of this project is to assist Tom Badger and WSDOT in identifying the mechanism by which the eastbound lanes continues to deform and provide an adequate body of work from which WSDOT personal can use for permanently remediating the deformation. To this end, the following steps were taken. First, a desk review was conducted of archived reports, memos, data, and drill logs from the original construction of I-82 and previous geotechnical investigations commissioned by WSDOT. Tom Badger requested and received all archived materials from the Washington State Archives related to the Prosser Landslide and the original construction work between Prosser and Kiona. These materials were provided to me for the desk review. Second, two new boreholes were drilled at the Prosser Landslide site above the buttress and instrumentation was installed within the boreholes. Drill logs produced from the 2013 drill can be found in Appendix A: Drill Logs. Disturbed and undisturbed samples (Shelby tubes), as well as rock core retained during drilling were transmitted to the WSDOT Materials Lab for sample review and testing. Clay-rich material retrieved with the Shelby tubes taken within the suspected failure zone of the landslide was tested by WSDOT personnel for its mechanical properties including Atterberg limits, grain size analysis, and residual shear strength which can be found in Appendix B: Atterberg Limit and Shear Ring Testing Results of this report. Additionally, I analyzed samples taken with from the Shelby tubes for mineral content using X-ray powder diffraction (XRD) (Appendix C: X-Ray Diffraction Mineralogy). Finally, using drill logs produced from the latest drilling and from historic drilling campaigns by WSDOT, I constructed a 2-D geologic cross section of the landslide which I used for slope stability analysis found within this report. The slope stability analyses were intended to test the viability of a landslide failure mechanism in order to explain the observed deformation using reasonable material strengths and measured groundwater conditions. Results from the slope stability analysis can be found in Appendix D: Slope Stability Analysis Results.

This technical report will be filed with WSDOT as an internal document. History drill logs, reports, memos, and laboratory test results may be requested from the Washington State Archives under WSDOT projects XL-1725, OL-1517, and C-3204.

Additionally, completion of this technical report represents partial fulfillment of the author's program requirements for conferral of a Master's Degree in the Earth and Space Sciences Department's Masters in Earth and Space Science Applied Geoscience (MESSAGe) program at the University of Washington.

A presentation of findings from this technical report will be given by me at the University of Washington on December 5th, 2013 to the public.

Site Conditions

Physiography

The Prosser Landslide is situated on Department of Natural Resources (DNR)-controlled land. As I observed during my site visits, cheatgrass and wild sage cover the majority of the site and surrounding hillsides. Areas of bare broken rock can be seen on the hillslopes surrounding the landslide mass.

The site can be accessed via I-82 or W Yakitat Road above the engineered shear-key buttress at the base of the slide. Several barbed wire fences inhibit access around the site, including the top of the buttress immediately adjacent to I-82, and are in good repair. Another barbed wire fence restricts access to the upslope portions of the slide mass.

W Yakitat Road lies immediately above the buttress and used to serve as part of I-82 prior to the 1980s realignment. Traffic is minimal along the road, and it provides easy and safer access to the site that the shoulder of I-82. Benton County recently resurfaced W Yakitat Road with chip seal, as evidenced by the black color and fresh condition of the road material.

A Kennewick Irrigation District (KID) irrigation canal traverses the site from west to east. The canal enters the site from the west, and carries water via a syphon from the south side of I-82 to the north side at the westernmost end of the buttress. The canal then exits the site to the exit, traveling along the downslope side of I-82. The KID canal as it is presently consists of unlined concrete panels. Of interest is a small lined section approximately 150 feet long (Figure 2).

Buttress

The shear key buttress (Figure 3) consists of angular basalt rip rap which abuts the south shoulder of the eastbound land of I-82 for approximately 1000 feet. The buttress rises about 20 feet off the road surface at an angle. At the time of the most recent site visit (8-21-2013), there did not appear to be any raveling or displacement of buttress material onto the shoulder. A rain gauge is situated on top of the buttress on the eastern end.

Boreholes

Since the 1980s and even into the 1970s, there has been drilling activity on the Prosser Landslide site. However, many borehole locations have been lost since the beginning of interest in the site,

especially uninstrumented boreholes from the 1980s and 1970s. Since the renewed geotechnical interest in the 1990s and into the early 2000s, WSDOT has maintained much better control over borehole locations (Figure 4) and continues to maintain several serviceable inclinometers.

Of the 1980s geotechnical work, information regarding the locations of 5 boreholes remains. Holes H-01-84 and H-03-84 are located on the westernmost side of the buttress above the KID irrigation canal syphon, and possibly contain serviceable inclinometers. H-06-87 is located the syphon output and the northern shoulder of the westbound land of I-82. H-06-87 contains a functional slope inclinometer. H-05-87 and H-09-87 are located in the slide mass above W Yakitat Road.

Boreholes from the 1990s geotechnical campaign are all located. H-01-93 and H-01-94 are located on the south shoulder of W Yakitat Road on the west and east ends of the buttress respectively. H-01-94 has sheared off and is no longer serviceable. H-02-93 is located immediately in front of the buttress on the east end. H-02-94 is located in the slide mass upslope of W Yakitat Road between boreholes H-05-87 and H-09-87.

Four holes are locatable from the 2002 geotechnical study. H-03a-02, H-04a-02, H-05ab-02, and H-06a-02 are located immediately in front of the buttress. Borehole H-05ab-02 is actually two holes drilled side by side. H-05a-02, has a functional slope inclinometer. Borehole H-05b-02 contains a vibrating wire piezometer.

As a part of the current work in 2013, WSDOT drilled two holes immediately above the buttress on the eastern side between holes H-05ab-02, H-02-93, and H-01-94. The boreholes, H-100-13 and H-101-13 were drilled side by side over the summer on 8-20-2013 and 8-21-2013. Borehole H-100-13 contains a slope inclinometer. Borehole H-101-13 contains a vibrating wire piezometer.

Borehole data indicate that the water table is developed in the fractured basalt beneath the gravels about 25 feet below the road surface.

Geologic Setting

The Prosser Landslide site is situated at the north flank of the Horse Heaven Hills, just south of the Hanford Nuclear Reserve and at the southeast end of the Yakima Valley (Figure 5). The Horse Heaven Hills area is part of a system of anticlinal ridges and synclinal valleys which form the Yakima Fold and Thrust Belt (YFTB), a sequence of faults and folds with Holocene slip history (REF). Other notable features in the vicinity are the Rattlesnake Hills to the north, the Pasco Basin to the northeast, and Wallula Gap to the southeast. The Prosser Landslide located just barely within the limits of the Olympic-Wallowa Lineament (OWL), another enigmatic active tectonic feature (Hagood, 1986).

Regional History

The surface geology of the Yakima Valley and Pasco Basin, of which the Prosser Landslide lies at the intersection, consists largely of units related to the Columbia River Flood Basalts (CRB) of

the Miocene and the sediments which cover them. The CRB units in this area are part of the Saddle Mountains Basalt (Reidel and Fecht, 1994; Hagood, 1986). Sediments deposited between Saddle Mountains Basalt flows and immediately on top of the final basalt flow are known as the Ellensburg Formation sediments (Hagood, 1986; Smith, 1988). The Ringold and Hanford formations are deposited atop the Ellensburg Formation (Figure 6). Both of these formations are related to the flooding of the Columbia Basin during the Missoula Floods (Smith, 1988; Lindsay and Gaylord, 1990). The YFTB has deformed the Saddle Mountains CRB, Ellensburg Formation units, Ringold Formation, and Hanford Formation (Hagood, 1986; Smith, 1988, Repasky et al., 2009). (Figure 7).

The Horse Heaven Hills are part of the larger YFTB system of NW and SW-trending, roughly north-vergent folds and thrust faults which range from north-central Oregon into central Washington on the Columbia Plateau and Columbia Basin. The Prosser Landslide is located at the intersection of three anticlines (Figure 8): The Chandler Anticline, the Kiona Anticline, and the Badlands Anticline. The landslide and Quaternary deposits conceal the intersection, so it is difficult to understand how these three structures interact (Hagood, 1986).

The YFTB began to develop at the earliest in the Miocene around 12 Ma coeval with the eruptions of the CRB and has been continuous since that time (Reidel, 1984). Eruption and emplacement of CRB and Ellensburg interbed sediments record deformation progressively throughout their history, meaning that older units are more deformed than younger units (Reidel, 1984; Smith, 1988). Changes in the interbed facies likely record not only the growth of the YFTB, but its effect on the paleo-Yakima and –Columbia River systems as well (Smith, 1988). Results from Repasky et al., 2009 indicate that suprabasalt sediments, including the more recent Hanford Formation, are deformed as well, supporting Reidel, 1984.

In the Horse Heaven Hills, YFTB folding is expressed as northwest and northeast trending, north-vergent en echelon anticlines and monoclines. Northwest-trending structures roughly parallel the alignment of the OWL. At the intersection of the trends, the northeast-trending structures are truncated by the northwest-trending structures (Hagood, 1986). Uplift was concentrated along the major folds of the hills during the middle to late Miocene and occurred along both northwest and northeast fold trends (Hagood, 1986). The Horse Heaven Hills likely achieved its current relief during the Late Miocene to Pleistocene (Hagood, 1986). Development of other major folds in the area, such as the Yakima Valley syncline, appears coeval with development of the folding within the Horse Heaven Hills (Hagood, 1986).

Depositional History

The stratigraphy of the Prosser Landslide area consists of the uppermost Saddle Mountains Basalt member (the Elephant Mountain Member) and interlayered gravels and fine sediments. However, the stratigraphy and deposition history of the surrounding regions are important because of WSDOT's interest in the origin of clay material within the units overlaying the basalt.

The basement of the Prosser Landslide site consists of several members of Saddle Mountains Basalt. Four members, from oldest to youngest, are recognized as part of the Saddle Mountains Basalt: the Umatilla Member, the Esquatzel Member, the Pomona Member, and the Elephant

Mountain Member (Hagood, 1986). Each member of the Saddle Mountains basalt is a sedimentary unit (Hagood, 1986; Smith, 1988). These sedimentary units are assigned to the Ellensburg Formation (Hagood, 1986; Smith, 1988).

The sediments deposited atop the Elephant Mountain Member are likely fluvial sediments related to the migration of the Yakima and Columbia rivers in the late Miocene to early Quaternary (DOE, 2009; Smith, 1988). Large influxes of volcanoclastic sediments and ash from the Cascade Range during that time were incorporated into fluvial sediments deposited along the Yakima Valley but are best preserved in the upper portions of the valley (Smith, 988). Regional lakes forming in the Pasco Basin likely extended into the surrounding valleys, including the Yakima Valley, and brought with it lacustrine sediments of the uppermost Ellensburg Formation (Smith, 1988). However, as Smith, 1988 also points out, the amount of fluvial activity as well as the formation of YFTB complicates facies identification because of both aerial and vertical variation of the sediments deposited during this time.

Upper Ellensburg and Ringold Formation sediments are associated with the phase of lake formation in the Early Quaternary (Smith, 1988; Lindsay and Gaylord, 1990).The Miocene-Pliocene Ringold Formation is largely confined to the basin and pinches out at the margins (Lindsay and Gaylord, 1990). Ringold Formation sediments are both active fluvial and overbank deposits related to the migration of the Columbia River into its current position (Lindsey and Gaylord, 1990). Sediments range from bedded muds to interlayered gravels and cobbles (Lindsey and Gaylord, 1990). Ringold-equivalent sediments have been mapped further outside the basin (Lindsay and Gaylord, 1990).

The Hanford Formation has been mapped outside of the basin (USGS, 1977) and is related to Missoula Flood. The glacial-aged Missoula Floods deposited much of the surface material seen in the valley bottom to the north of the Prosser Landslide (USGS, 1977). These deposits are locally known as the Hanford Formation. Hanford Formation deposits have been incorporated into the regional stratigraphic unit corresponding to Quaternary Missoula flood deposits (Qfs) (Reidel and Fecht, 1994). Earlier Hanford Formation deposits consist of basalt-dominated gravels and sands (DOE, 2002). Fines and clays are generally absent of the formation save for at the margins of the Pasco Basin, where flood waters were depleted of coarser clasts (DOE, 2002). However, in area further from and higher than the Pasco Basin likely preserve fines deposited during the formation of Lake Lewis as cataclysmic flood waters backed up behind the Wallula Gap (DOE, 2002). Ashes from Miocene-aged or younger eruptions of the Cascade arc volcanoes also have been preserved within the Missoula flood deposits (Reidel and Fecht, 1994), and help constrain the age of the deposits to 13 ka at the youngest.

Local

Based on what I observed on my visits to the site, the soils developed on the slide mass at the site are loosely consolidated, and sometimes with desiccation cracking present at the surface. Soils are pale and powdery. I observed that root development through the soil is shallow, ending approximately 8 inches from the surface. There appeared to be the development of caliche is seen 18 inches from the surface, followed by matrix-supported angular basalt clasts.

A basalt outcrop is located across the road from the buttress (Figure 3). Several other outcrops of basalt can be seen in the hills above the landslide as well. Basalt has been mapped previously in the hills above the Prosser Landslide across the Chandler Anticline hinge (USGS, 1977; Harris and Schuster, 2000) and are hypothesized to underlie the Prosser Landslide (Hagood, 1986).

WSDOT borehole data from the site shows that much of the area consists of coarse, subrounded to subangular basalt-dominated gravels with fines (Appendix A: Drill Logs). Fines generally consist of silts. Gravel deposits appear to have little bedding or stratification, and seem locally variable. Likewise, clays, silts, and sands also appear largely unstratified.

Material composing the slide mass generally consists of silts, sands, angular basalt gravels, and basalt fragments (Appendix A). Cobbles and boulders are found sparsely. Slide mass material can be differentiated from gravel packages by the larger amount of silty matrix and presence of matrix-supported basalt fragments (Appendix A).

Because of multiple phases of fluvial activity near the project site (Ancestral Columbia and Yakima River systems, and the Missoula Floods), assigning sediments to named formations is difficult. Hagood, 1986 names laminated silts and clays found in the vicinity of the project area as part of an undifferentiated package of Ellensburg Formation sediments. However, surface deposits at similar elevations and in close proximity to deposits seen under the landslide site have been associated with the Hanford Formation (USGS, 1977; Reidel and Fecht, 1994).

During excavation of the buttress in the 1987, workers encountered a clay unit local to the buttress. Buttress cross section designs by Todd Harrison of WSDOT show the buttress key interrupting the clay layer. Similarly, previous drilling in 1993-1994 and 2002 intercepted a clay unit local to the buttress. Drill logs also indicate fresh to highly fractured and weathered basalt underlies the gravel package (Appendix A).

Surface deposits immediately surrounding the Prosser Landslide have been assigned to the Hanford Formation or the regional equivalent Qfs unit (USGS, 1977; Reidel and Fecht, 1994). Please see the Discussion for my interpretation of the origin of key units in the Prosser Landslide.

Part II: Desk Review and Site History

In this section, I review the history of construction and deformation at the Prosser Landslide based on documents obtained from the Washington State Archives by Tom Badger. Except where explicitly noted, I generated the following summary using information from documents relating to WSDOT projects XL-1725, OL-1517, and C-3204. The goal of this section is to give a detailed synopsis of the events which caused WSDOT's initial concern with the Prosser Landslide area and WSDOT's ongoing effort to understand the cause of renewed deformation. I placed particular emphasis on documenting the dispute over the construction of shear-key buttress and the justifications used by WSDOT personnel to support their working hypotheses for the ongoing deformation of I-82.

A note about conventions: Projects along the I-82 corridor use both milepost (MP) and project stationing to denote where a site is located along the roadbed. Project stationing is in engineering stationing convention. There are several lines along which WSDOT denotes stations along the I-82 alignment; however, for the purposes of this project, the most pertinent lines are the eastbound (LE) and westbound (LW) centerlines.

A memo dated September 27, 2002 to Rich Burrows of the FHWA from Steve Lowell, Jim Cuthbertson, Tom Badger, and Doug Anderson of WSDOT states that plans for the realignment of I-82 from Prosser to Kiona began in the 1970s. The memo also states that it was known by WSDOT at the time that the realignment would traverse several prehistoric landslides along the north flank of the Horse Heaven Hills.

<u>Initial I-82 Realignment 1986 – 1988</u>

Initial excavation and construction at the Prosser Landslide site began in 1987 with the eastward propagation of the newly constructed I-82 from MP in 89.8 Prosser to MP 95.39 the vicinity of Kiona. Beginning on December 26, 1986, the construction of I-82 was fraught with difficulties along the northern front of the Horse Heaven Hills as the project crossed multiple ancient, deep-seated landslides. This resulted in several work stoppages and, in one case, the purchase of private property, as construction destabilized upslope sections of the northern flank of the Horse Heaven Hills. Deformation and sliding were noted along sections near MP 82, 88, and 90 west of the Prosser Landslide site.

The project through the MP 91.9 vicinity consisted of construction of the I-82 road bed, an interchange between I-82 and the KID canal, a borrow pit between the I-82 road bed and W Yakitat Road, and an aggregate crusher north of the roadbed construction. The contractor Acme Concrete used the borrow pit as a source for road aggregate at the site and crushed it on-site at the crusher downhill from the project site (Figure 9).

Problems at what would become the Prosser Landslide site were first noted January 19, 1987 when workers on site noticed a landslide headscarp had formed above the construction of the KID canal syphon in the project station LE 512+00 vicinity (MP 91.9 vicinity). No action was taken by either WSDOT or contractors Steelman-Duff and Acme Concrete until February 16, 1987 when a change order from WSDOT directed Acme Concrete to provide heavy, loose rip-

rap for the construction of a buttress from LE 509+50 to LE 510+00. Steelman-Duff then completed the buttress on February 19, 1987.

Crushing for the subsurface base commenced February 24, 1987. The subcontractor, Eucon Corporation, borrowed material from the road prism along the section from LE 515+00 to 520+00.

However, new deformation features were noted on February 27, 1987 in the form of road heave near the crushing operation downslope of the I-82 construction site as well as new tension cracks in the road above the site near the LE 515+00. Crushing continued until March 2, 1987, when mining was discontinued at the borrow pit. The next day, March 3, 1987, WSDOT geotechnical engineers produced a stability analysis for the Prosser Landslide site, including analysis of a shear key buttress designed to be constructed at the site. WSDOT issued a force change order to Steelman-Duff for the construction of the buttress on March 11, 1987 and construction began shortly thereafter. WSDOT deemed the deformation at the site a hazard to the public on March 13, 1987 and directed Steelman-Duff to work 24 hours a day on the buttress until March 18, 1987 when sliding was deemed by the State to be under control.

Construction on the shear key buttress began on the east side of the site at project station Le 517+00 and continued westward until LE 512+00 near MP 91.9 where the previous buttress ended. The buttress was designed for a Factor of Safety (FS) of 1.25 with an assumed buttress material φ angle of 45º. The buttress was intended to be keyed 2 feet below the clay layer encountered at 30 feet below the ground surface (Figure 10, Figure 11).

Undated field notes from Tom Badger of WSDOT during the time of buttress construction chronicle ongoing challenges construction of the site faced as the hillslope deformed daily in response to the buttress key excavation. He noted that the deformation was both dramatic and rapid in onset from the beginning of the buttress construction, including new tension cracks with 1-2 feet of vertical offset located hundreds of feet upslope of the project site and 5-6 feet of subsidence of the existing roadbed with similar horizontal offset downslope. Badger noted that the site inspector, Dave Fassler, observed that rapid deformation began in the slope with the beginning of buttress construction and followed the construction as it propagated westward.

Of important note during this time is an internal WSDOT memo dated March 20, 1987 from Dave Jenkins and Steve Lowell to the Project File of Contract 3204 with the following subject: "Contract 3204 I-82 Landslide Vicinity Gibbon Road to Kiona I/C". The memo states that in addition to their assigned tasks of identifying and mapping recent landslide scarps and developing a survey-controlled landslide monitoring grid at the Prosser Landslide site, they also noted a serious discrepancy in the location of the constructed shear key buttress and its specified design sections, namely that the buttress was constructed above the specified elevation. Specifically, they note that the buttress was constructed 5 to 7 feet above the low elevation in the ditch on site where it was designed to be constructed (Figure 12). In addition to the photos, they also attached an annotated to-scale drawing of the buttress as it was designed by Todd Harrison. The annotated portions show that the buttress is not seated below the clay layer and is instead resting on the sediments several feet above it.

That the buttress lacks a key below the clay layer is consistent with observations made by Tom Badger in his undated field notes from the time of buttress construction, which state that much of the buttress east of the KID canal crossing has no key below the clay and is in fact resting upon alluvial sediments. However, as also noted in the March 20, 1987 memo, statements from the site inspector, Dave Fassler, contradict what is stated in both the March 20, 1987 memo by Dave Jenkins and Steve Lowell and Tom Badger's field notes, namely that the buttress was constructed to specifications and is keyed below the clay layer in dense gravels. Additionally, Dave Fassler's construction diaries do not mention that the buttress was not built to specifications, except to say that the key excavation was exceptionally difficult.

Steelman-Duff completed the shear key buttress on March 24, 1987. WSDOT continued to closely monitor the site for three months following the completion of the buttress, during which time the instruments in the area showed little movement.

Geotechnical Investigation 1993 – 1995

After observing a renewal of deformation in 1993, WSDOT initiated an internal geotechnical assessment of the Prosser Landslide site (C-Core, 2006). Maintenance crews noted fresh tension cracks in the road surface of W Yakitat Road above the buttress (Power et al., 2006) and a bump in the eastbound lanes of I-82 (Figure 3) on the east side of the buttress. However, since the construction of the buttress, no new motion was detected beneath the buttress by the remaining slope inclinometers under the buttress at that time (Power et al., 2006).

WSDOT conducted new drilling in1993 and 1994 with the addition of several new holes and slope inclinometers. Plasticity index and direct shear tests were performed on clay-rich material retrieved within the failure zone from several holes. Testing determined that the silty clays retrieved had plasticity indices between 80 and 105, indicating the material to be a fat clay.

Most concerning for both the South Central Region and WSDOT Geotechnical Office was that the bump which had formed in the eastbound lanes on the east end of the shear key buttress was becoming a hazard for the traveling public. The original road surface in the bump area consisted of Portland cement concrete (PCC) panels. However, ongoing deformation had caused the panels to rise out of their positions, posing a hazard to traffic.

Beginning in 1995, a series of memos circulated within WSDOT about the possible mechanism causing the new deformation. First appearing in early 1995, Arnie Korynta (WSDOT South Central Region Materials Engineer) proposed that instead of slope failure being the cause of the deformation in the roadbed, swelling clays beneath the road were to blame. He hypothesized that the shear key was acting as a reservoir which provides water to the swelling clays below the roadbed. Arnie Korynta proposed that water flowing from upslope was migrating to the slide area, which then pooled in the buttress key. Swelling clays present beneath the roadbed (Figure 13) were then hydrated from water in the buttress key, leading to swelling and subsequent deformation of the road surface. Furthermore, he stated that the buttress was indeed keyed 6 to 12 feet below the roadbed and 2 feet below the clays, contradicting earlier reports of buttress not being keyed in 1987 by Tom Badger, Dave Jenkins, and Steve Lowell. Finally, Arnie Korynta recommended the I-82 roadbed around the bump be remediated, either by paving the PCC panels

with asphaltic concrete pavement (ACP) Class G, or removing the PCC panels and replacing the road surface with ACP Class A. He also recommended that the buttress be pressure grouted to prevent further infiltration to the buttress key and thus the clays.

WSDOT decided to verify the integrity of the waterproofing membrane installed beneath the roadbed in the 1980s. In 1995, a portion of the roadbed shoulder in front of the buttress was excavated to the membrane. The membrane was found to be intact. However, workers observed water pooling on the top of the membrane and that the channels draining the membrane under the road surface had been deformed. They concluded that the membrane was successfully preventing water from infiltrating the subgrade from above.

An internal geotechnical memo dated September 7, 1995 from Jim Cuthbertson and Tony Allen to Arnie Korynta and Richard Larson summarizes the Department's plan for addressing the bump in the eastbound lanes. Jim Cuthbertson and Tony Allen conclude that the slide was still in motion above the buttress but that the bump was thought to be due to swelling clays in the subgrade of the roadbed. They supported this conclusion with the observation that deformation recorded by inclinometers above the buttress was above the elevation of the road bed, that the slide appeared to be in a northwesterly direction, and that deformation was not observed in the slope inclinometer situated in front of the buttress between the buttress and the road. Jim Cuthbertson and Tony Allen recommended that the county road (W Yakitat Road) above the buttress be repaired as needed to prevent further infiltration to the slide mass. However, they were averse to recommending pressure grouting of the buttress, hypothesizing that grouting could focus groundwater elsewhere around the roadbed.

WSDOT eventually decided against pressure grouting the buttress. 12 panels of PCC in the eastbound lanes of I-82 road surface were eventually replaced with ACP Class A in response to the deformation. The subgrade was left undisturbed during the surface replacement.

Internal Geotechnical Memos 2002-2004

Since the replacement of the road surface in the 1990s, maintenance crews continued to grind and repave the MP 91.9 section in response to continuous deformation of the road surface (Power et al., 2006). WSDOT drilled additional holes in 2002 around the site and installed a slope inclinometer and piezometer in front of the buttress near the east end, where pavement deformation was most severe.

A memo dated September 27, 2002 from Steve Lowell, Jim Cuthbertson, Tom Badger, and Doug Anderson to Rich Burrows of the Western Federal Lands division of the FHWA gives a detailed account of previous geotechnical investigations, including an investigation in 1972 prior to the realignment of I-82. The memo goes on to say that the buttress was not designed with a drain in the shear key, and that it is possible that the shear key was not embedded deep enough during construction. However, the authors of the memo conceded that they only had verbal accounts of the latter. Maintenance's accounts of the bump, according to the memo, allege that the formation of the bump did not appear to correlate with seasonal fluctuations of precipitation. Finally, the memo noted that neither the buttress nor the roadway showed any horizontal deformation, but

that displacement of the concrete panels lining the KID canal to the north may be interpreted as horizontal moment.

The September 27, 2002 memo goes on to outline a proposed InSAR study of the Prosser Landslide site, including the use of CYRAX and LIDAR, to determine whether or not the landslide is moving or whether expansive soils are the culprit. The memo proposed that the study be conducted with the assistance of the FHWA.

Sometime in 2002, WSDOT drilled 5 new boreholes in the shoulder in front of the buttress. 2 slope inclinometers, a vibrating wire piezometer, and moisture content reflectometers were installed as well. WSDOT drill crews avoided the use of water for drilling so that in situ moisture content could be evaluated.

Samples of silty clay material from an elevation below the roadbed were sent back to the WSDOT Materials Lab for testing for expansion potential.

Early in 2004, Doug Anderson, a WSDOT engineering geologist, preformed slope stability modeling of the Prosser Landslide site in XTABL using the Janbu method (Janbu, Bjerrum, and Kjaernsli, 1956) (Janbu Simplified Method or Janbu Corrected Method is not distinguished). Doug Anderson's model was a of a slide of much larger aerial extent than the original back analysis slide modeling conducted in 1987, as he took into account the slide scarps developed further uphill of the buttress. This is in contrast to the modeling conducted in 1987, which only modeled movement between I-82 and immediately above W Yakitat Road.

On April 9th, 2004 Jim Cuthbertson and Tony Allen submitted a memo to R. Yates of the WSDOT South Central Region detailing their conclusions regarding the Prosser Landslide. They conclude that the deformation in the eastbound lanes at MP 91.9 is due to continued landslide movement. They based their reasoning on stability modeling using the commercial slope stability modeling software XSTABL and inclinometer data from 2002. They also note that inclinometer data show that the movement of the landslide upslope of the buttress has shifted eastward perpendicular to the original northward movement of the slide mass and that Region Maintenance reported that formation of the road bump does not appear to be seasonal.

New boreholes were proposed for the site in 2004 but were never drilled.

C-Core Geotechnical Report 2006

In 2006, C-Core was contacted by the FHWA for a study to evaluate the potential for using InSAR as a tool for remotely investigating deformation of landslides compared to traditional geotechnical investigations, and to establish guidelines for the use of InSAR in future transportation-related applications. For their part, C-Core was tasked with compiling and synthesizing existing traditional geotechnical data from the Prosser Landslide, which was chosen among 2 other sites around the US, as a pilot area for InSAR evaluation.

C-Core reviewed existing data from the 1980s and 1990s geotechnical investigations and conducted additional stability modeling of the landslide using finite element modeling and limit

equilibrium analysis techniques. A critical section developed by C-Core perpendicular to the buttress (Figure 14, Figure 15) describes 4 units within the slide mass: a silty clay with cobbles (SC), a clean porous gravel or talus (G), a gravel with a silty sandy matrix (G_m), and the basalt bedrock unit (Figure 16). C-Core concluded that the slide plane followed the silty clay-clean gravel interface, reasoning that the low hydraulic conductivity (low K-value) of the silty clay unit created confined aquifer conditions within the lower gravel unit, which has high hydraulic conductivity (high K-value). Their conclusion is also based on inclinometer data (See C-Core, 2006 Annex A).

When modeling the Prosser Landslide, C-Core varied assumed groundwater conditions (which were never measured or detected in previous investigations), slope angle, rapid pore pressure increase, and landslide toe excavation. Despite the critical section they constructed as mentioned in the previous paragraph, C-Core further simplified the geometry of the Prosser Landslide into planar-shaped, inclined beds (Figure 17) for plastic finite-element modeling (FEM) based on Mohr-Coulomb failure criteria. The silty clay unit was assumed to have a minimum φ angle of 16º. C-Core modeled the Prosser Landslide using the commercial software GeoSlope. No model accounted for the buttress.

Modeling efforts by C-Core resulted in the conclusion that the slide was effectively stable unless there are near-artesian levels of water pressure along the silty clay-clean gravel interface (C-Core, 2006).

C-Core also conducted preliminary analysis of the possibility of frost heaving or swelling clays as the culprit for the deformation. C-Core modeled the ability of a frost front to penetrate the road subgrade using annual temperature data collected from Benton City, WA. They found that frost could penetrate only approximately 0.2 m (8 inches) below the pavement layer into the sandy silty gravel subgrade, and would only displace the road surface a total of less than 8 mm (0.3 inches) throughout the entire 3 month winter season (C-Core, 2006). In addition, after calculating the swelling potential of silty clays obtained from the 2002 drilling, C-Core concluded that the total swelling potential of the clay is 28 mm (1.1 inches), which they deemed insignificant compared to the pavement movement observed.

Federal Highway Administration InSAR Report 2006

The FHWA, in conjunction with WSDOT, published a study in 2006 on the use of InSAR in evaluating potential landslide hazards (FHWA, 2006). As stated previously, WSDOT originally proposed a standalone InSAR, CYRAX, and LIDAR-based remote sensing project in 2002 in conjunction with the FHWA, the original proposal of which became the basis of the 2006 FWHA investigation. However, neither CYRAX nor LIDAR were included as part of the 2006 FHWA project and were never conducted.

The overall goal of the FHWA InSAR report was to evaluate the effectiveness of InSAR remote sensing compared to traditional geotechnical surveys, and establish cost-effective and reliable procedures for implementing InSAR as an investigation tool. The FHWA investigated three landslide sites along highways around the country for the study.

Investigation sites were individually evaluated for landslide potential within the scope of the InSAR report and using past geotechnical work. The Prosser Landside was evaluated simultaneously by the FHWA using InSAR and by C-Core using historic data. A smaller summary report, Power et al., 2006, was issued alongside the larger FHWA (2006) report covering the site-specific investigation results only. The FWHA used satellite-based data obtained by the European Space Agency's Earth Remote Sensing (ERS) satellites and the Canadian Space Agency's RADARSAT satellites.

Due to the poor coherence of the ERS data and lack of consistent displacement signatures in the interferograms, the FHWA report concluded that no slope movement appeared to be detected during the period the ERS data covers (FHWA, 2006). Despite good temporal coherence for the RADARSAT data, the magnitude of the deformation observed within the slope fell within the margin of error for the data (less than 10 mm or 0.4 inches) and located above the buttress adjacent to the highway (Figure 18) (FHWA, 2006). Cumulative measurements of deformation between the ERS and RADARSAT data total only 25 mm (Power et al., 2006). From this, the FHWA concluded that no obvious movement was measured as well (FHWA, 2006). Given the lack of evidence of movement of the landslide during the study time and the results from the C-Core modeling, the FHWA report concluded that the landslide is effectively stable (FHWA, 2006).

Recent deformation

WSDOT South Central Region Maintenance has continued to grade the bump and monitor the condition of the road. Despite the recent paving of W Yakitat Road by county maintenance, abundant tension cracks (Figure 19, Figure 4) are present throughout the length of the road within the slide area. There is also signage warning of several bumps along the road within the slide area as well. A dislocated panel section found along the KID canal (Figure 20) appears to be spatially correlative to the bump found in the eastbound lanes of I-82.

An engineer with KID, in responding to inquiries for this report, explained that KID concluded that movement in the concrete panel sections of the irrigation canal were due to frost heave. The canal was lined at that section and panel joints were sealed in response. No geotechnical investigation was conducted by KID.

Part III: Material Sampling and Characterization

The goal of the following analysis methods is to describe the subsurface of the Prosser Landslide site. Specific interest is placed on measuring the mechanical properties and mineral composition of clay material retrieved during recent drilling. The intention of new drilling was to place a slope inclinometer and vibrating wire piezometer immediately behind the buttress and to collect samples for testing. Borehole logs produced from the most recent drilling then used to create cross sections of the landslide. Clay samples retrieved from the drilling were tested for their plasticity, grain size, and shear strength at the WSDOT Materials Lab, in Tumwater, WA. The intention of this testing is to understand what the material is, how the material behaves under stress, and how that behavior may contribute to movement of the landslide. Finally, because of WSDOT's interest in establishing what minerals constituted the clay material, I analyzed a powdered sample of the same clay sample used in the materials testing using X-ray powder diffraction analysis (XRD). I used the analysis results from this section for the slope stability modeling conducted in Part IV of this report.

Methods

Drilling

Drilling commenced the morning of August 28, 2013 and ended August 29, 2013. A single track-mounted mobile drill was used. Two boreholes were drilled side by side by WSDOT personnel. Borehole H-100si-13 was drilled to a depth of 76 feet. Borehole H-101vwp-13 was drilled to a depth of 35.5 feet. Borings were advanced with wet rotary triple-tube coring in 5 foot intervals. Standard Penetration Tests were conducted in H-101vwp-13, particularly in unconsolidated gravels and silts. Standard Penetration Tests were conducted in accordance with ASTM D 1568 guidelines. Core was logged by a WSDOT drill inspector on site and transported to the WSDOT Materials Lab in Tumwater, WA for review and storage. Two Shelby tubes of clay from H-101vwp-13 were collected at depths of 19 to 20 feet and 24 to 26 feet.

Drillers fitted borehole H-100si-13 with a slope inclinometer and H-101vwp-13 with a vibrating wire piezometer located within a thick clay zone, believed to be the failure zone. The vibrating wire piezometer was grouted at a depth of 25 feet. The bottom of the well was sealed with bentonite chip.

Water level was determined by bailing the well bore of H-100si-13 and allowing it to stabilize overnight.

Drillers had difficulty keeping water in the drill, since there was very little water return while drilling, especially in the gravels and fractured basalt. Drillers reported 100% water loss in H-100si-13.

Plasticity Index, Atterberg Limits, and Soil Classification

Atterberg limits and plasticity indices testing were conducted by WSDOT personnel at the WSDOT Materials Lab. Clay material obtained from a depth of 21 feet from the Shelby tube samples in borehole H-101vwp-13 was sieved in accordance with WSDOT's supplemental to

AASHTO standards T 27 and T 11 (WSDOT, 2013b), and dried in accordance with AASHTO Standard R 58-11. Atterberg limit testing was conducted in accordance with AASHTO standards T 89-10 and T 90-00.

To determine the liquid limit of the sample following Method A of T 89-10, a dry, sieved sample weighing approximately 100 g was placed into a mixing dish and mixed thoroughly with 15 to 20 mL of distilled or demineralized water until the sample has achieve a uniform, stiff consistency. A portion of the sample was placed into the casagrande cup in the liquid limit testing device and leveled to maximum thickness of 10 mm. The leveled sample was then grooved with a grooving tool along the diameter of the sample, aligned with the centerline of the liquid limit device cam follower, and down through the bottom of the sample. Finally, the cup containing the sample was tapped on the rubber of the device by turning the device crank handle at a rate of 2 revolutions per second until the sides of the sample in the bottom of the groove come into contact, and the number of shocks required to do so was recorded. A slice of the material the width of a metal spatula obtained by cutting the sample across the width of the sample in the dish and perpendicular to the groove was then removed and dried to determine moisture content according to AASHTO Standard T 265-11.

Using the number of shocks recorded and the moisture content of the soil (reported as the mass of water over the mass of the oven-dried soil multiplied by 100), a flow curve was constructed by plotting the moisture content on the horizontal axis of a semi-log graph and the number of blows on the y-axis on the logarithmic scale. All trials were plotted and a line is drawn between them. The liquid limit of the material is determined by the moisture content necessary to achieve groove-annealing after 25 shocks according to the flow curve constructed.

The plastic limit was determined in accordance with T 90-00, by taking a 20 g small from the dried material sample material which passing a 0.425-mm sieve (#200) (prepared in accordance with R 58-11) and mixing the dried sample with enough distilled or demineralized water to be easily shaped into a ball. An 8 g portion of the ball was then used for the test. The test was performed simultaneously with the liquid limit test described above.

The sample is then formed into an ellipsoidal mass and rolled into a 3-mm diameter string either using a plastic limit device or by hand at a rate of 80 to 90 strokes per minute. A is counted as the complete motion of the hand forward and back again. After achieving a 3-mm, the string was broken into 6 to 8 pieces. The pieces were then reformed into an ellipsoidal mass and rerolled into a 3-mm string. This process is repeated until the material crumbles and can no longer be formed into a string. The crumbled pieces were then gathered in a covered container and weighed .The moisture content of the crumbled pieces is determined using the methods laid out in T 265-11.

The plastic limit is calculated by dividing the mass of the water in the tested soil by the mass of the oven dried soil and multiplying it by 100. The plasticity index (PI) is determined by subtracting the plastic limit from the liquid limit.

Estimates of the material's residual shear strength were made using the PI and the graph in Figure 5.5 of WSDOT's Geotechnical Design Manual (WSDOT, 2013a) and later supplemented with torsional ring shear testing.

Additionally, clay samples from a depth of 21 in borehole H-101vwp-13 were sieved and weighed to create a grain size distribution curve for the material in accordance with WSDOT's supplemental to AASHTO T 27-11 and T 11 (WSDOT, 2013b).

Ring Shear Testing

WSDOT owns and operates a Wykeham Farrance Torshear Annular Ring Shear testing device. Samuel Wade, a lab technician at WSDOT, conducted the ring shear tests.

Ring shear tests were conducted on clay samples retrieved from the suspected landslide failure zone. The test was performed in general accordance with ASTM D7608-11 (ASTM, 2011b) standards for ring shear testing. In addition to the procedures laid out by ASTM, WSDOT runs additional test using material only sieved to sieve size 40. A suite of tests were conducted at various moisture contents from 103% to 69%% and under a range of confining stresses compatible with the conditions of present at the site.

The sample (Sample D-6) taken a depth of 21 to 23 feet from borehole H-101vwp-13. The sample was chosen by WSDOT personnel. WSDOT personnel chose Sample D-6 for ring shear testing, since there was abundant material for testing. Sample material was dried and prepared in accordance with AASHTO T R 58-11. Remodeled samples were then placed in the ring shear device for initial consolidation. Testing began after the sample had compressed to a point where it was no longer changing volume, and pre-sheared to 90° before testing in order to measure residual shear.

Initial consolidation for samples saturated to 103% moisture content (90% liquid limit) was conducted at normal stresses of 7.3 psi, 14.3 psi, 28.3 psi, and 42.3 psi. The samples were then tested for residual shear at shear stresses of 0.584 psi, 2.100 psi, 2.801 psi, and 6.099 psi respectively.

Consolidation for samples saturated to 92% moisture content (80% liquid limit) was conducted at normal stresses of 6.7 psi, 13.8 psi, 27.8 psi, and 41.8 psi. The samples were then tested for residual shear at shear stresses of 0.550 psi, 1.400 psi, 3.000 psi, and 4.650 psi.

Consolidation for samples saturated to 86% moisture content (75% liquid limit) was conducted at normal stresses of 7.3 psi, 14.3 psi, 28.3 psi, and 42.3 psi. The samples were then tested for residual shear at shear stresses of 0.348 psi, 1.24 psi, 3.260 psi, and 4.930 psi.

Results for samples saturated to 69% moisture content (measured in situ moisture) are pending at the writing of this report.

For each sample run, final moisture content, linear displacement, and angular displacement were recorded by the digital data logger on the ring shear device. Residual shear strengths (φ angle) were calculated automatically the program.

X-Ray Diffraction Mineralogy

Randomly oriented powder XRD analysis functions by the selective diffraction of X-ray radiation though a crystalline substance off crystal planes as the incidence of the X-ray radiation with the substance satisfies the conditions of Bragg's Law. Every crystalline substance produces a unique powder diffraction peak pattern which can be used to identify the substance.

Bragg's Law:

$$n\lambda = 2dsin\theta$$

Where n is an integer, λ is the wavelength of the radiation passing though the material (usually reported in angstroms (Å)), d is the spacing between the crystal lattice planes that the X-ray radiation diffract off (Å), and θ is the angle of diffraction from the crystal planes.

As the sample is rotated in the goniometer (the device which comprises the X-ray emitter, the sample stage, and the detector), X-ray radiation passing through the substance will scatter off of the atoms in the material. If the scattering of the X-ray radiation off of the material is constructive, which is to say that multiple X-ray photons diffract off of the material at the same angle at the same time and are in phase with each other, the X-rays have encountered a crystal plane. When encountering a crystal plane, the angle of incidence of the X-ray radiation satisfies Bragg's Law, and d-spacing can be measured.

Every time Bragg's Law is satisfied during testing, the radiation detected intensifies, forming a peak of intensity when plotted against the 2θ angle of the X-ray beam. The intensity of the X-ray radiation is measured by the detector, usually in detections (counts) per second. The intensity verses 2θ angle plot is the visual output of the XRD analysis process. Intensity peaks from the sample can then be statistically and visually compared to the peak intensity patterns of known materials.

XRD analysis of a randomly oriented powder clay sample was conducted on samples taken from depths of 19 to 21 feet from borehole H-101vwp-13. A Bruker F8 Focus Powder XRD machine owned by the University of Washington Materials Science Engineering lab was used for testing. The Bruker F8 Focus Powder XRD machine emits CuKα X-ray radiation at a wavelength of 1.54 Å, and is filtered for CuKβ radiation using a nickel metal filter on the detector arm.

The randomly oriented powder mount was prepared by heating a 20 g moist sample of clay in an oven at 60º C for 2.5 hours, similar to recommendations made in Moore and Reynolds, 1989. When the clay dried, it was crushed by hand using a mortar and pestle until a fine powder was achieved. The powder was then loaded and formed into an acrylic large well powder stage for analysis.

Analysis was conducted at 40 kV and 40 mA for 50 minutes at 1 second per 0.02 θ step for a total of 2999 steps. The sample was examined at a range between 5º 2θ and 65º 2θ.

Raw XRD data was collected from the testing device using XRD Commander (onboard control software for the Bruker XRD device) and exported to commercial software MDI Jade (Materials Data, Inc., 2013) for processing.

MDI Jade accesses a database of XRD phase data from standardized and tested materials. It can be used to overlay that standardized phase data onto the measured data imported from the XRD device for comparison. It is also possible using MDI Jade to statistically match materials by major element chemistry and stoichiometry. MDI Jade accesses comparison powder diffraction files (PDF) compiled by the International Centre for Diffraction Data (International Centre for Diffraction Data, 2013)

Peak matching between the measured data and database data was done using MDI Jade's onboard match processing with PDF file database entries for the following clay species:

- Montmorillonite: PDF 00-013-0259, PDF 00-029-1498, PDF 00-013-0135, PDF 00-012-0219, PDF 00-029-1499, PDF 00-060-0318
- Saponite: PDF 00-030-0789, PDF 00-013-0086, PDF 00-029-1491
- Nontronite: PDF 00-034-0842, PDF 00-29-1497
- Illite: PDF 00-029-1496, PDF 00-009-0343, PDF 00-031-0968, PDF 00-026-0911, PDF 00-024-0495
- Vermiculite
- Kaolinite
- Mixed layer clays:
    - Illite-montmorillonite: PDF 00-035-0652
    - Kaolinite-montmorillonite: PDF 00-029-1490
    - Rectorite: PDF 00-025-0781

Results for the closest matches were exported from MDI Jade.

Results

Drilling

Drilling at the Prosser Landslide site revealed the presence of a thick clay unit behind the buttress, subrounded to subangular gravels with some amount of matrix, and high material hydraulic conductivity throughout the length of both of the boreholes.

The first hole drilled, H-100si-13, revealed the presence of an olive brown silty clay unit and the gravels with an olive brown clayey matrix beginning at a depth of 9 feet and continuing to a depth of 46 feet. Between a depth of 16 feet and 26.5 feet, the driller noted a continuous length of olive brown silty clay. However, initial efforts to core through the gravel and retrieve the continuous silty clay material with rotatory drilling resulted in the loss of vast majority the matrix. This was noted by the driller and relayed to Tom Badger prior to drilling the second hole. Subsequently, Tom Badger expressed interest in retaining the silty clay material for materials

testing and requested that the driller attempt to sample the silty clay material with a Shelby tube during drilling of the second hole.

At the noted depth from the first hole, the drillers were able to fill two Shelby tubes at 19 feet to 21 feet and at 24 feet to 25 feet in depth in the second hole with the silty clay material for later testing. The contact between the silty clay and the gravel were captured with a split spoon sampler (Figure 21).

At no point during the drilling of either hole did water return exceed 50%. 50% return was reported only when the borehole had intercepted basalt. Groundwater was noted at 66 feet below the surface in H-100si-13 after being left to equilibrate overnight.

Upon extrusion from the Shelby tube, I observed that the clay material captured in the tube was slickensided, polished, and highly disturbed. (Figure 22). The clays were moist upon extrusion of the tube and I could easily pick apart the material by hand, which revealed polished surfaces. The section between 24.5 feet and 25.5 feet in depth was particularly slickensided and polished. Further examination revealed small, white clumps and clasts which do not react with HCl and can be powdered by hand.

There was much disagreement between WSDOT personnel as to the classification of the silty clay either as a low plasticity clay, a low plasticity silt, or as an elastic silt while manual field testing for plasticity. My own manual testing showed that the silty clay material had a moderate dilatancy, moderate toughness, and could be rolled into a 3-mm string several times before crumbling. However, while I had difficulty crushing a dried 1 inch cube of the material, the driller on site had no problem crumbling the cube with moderate pressure.

Plasticity Index, Atterberg Limits, and Soil Classification

Clay samples from the site tested at plasticity indices of 53 and 72, placing the material retrieved in the fat clay range (Figure 23). The following table summarizes the results obtained from the WSDOT Materials Lab. Raw data can be found in Appendix B: Atterberg Limit and Shear Ring Testing Results..

Table 1. Summary results of WSDOT materials testing

Sample Number	Depth (ft.)	Liquid Limit	Plastic Limit	Plasticity Index
D-4	15.5	121	49	72
P-5	19.0	109	56	53
D-6	21.0	115	51	64
P-7	24.0	113	64	49
D-8	26.0	97	42	55

Additionally, a grain size distribution of sample D-6 was constructed (Appendix B). Results from the grain size distribution indicate that it is an elastic silt (MH).

Ring Shear Testing

Initial ring shear testing of sample D-6 produced a very low φ angle value, and therefore additional testing controlling for moisture content was conducted. Results from the test are presented in the following table:

Table 2. Ring shear friction tests of sample D-6.

Sample Number	Moisture Content (%)	Percentage of Liquid Limit (%)	Final Moisture Content (%)	Φ angle
D-6-A	103.0	90.0	80.0	7.4
D-6-A	92.0	80.0	82.0	6.2
D-6-B	86.0	75.0	72.0	6.4
D-6-B	69.0	60.0	76.0	6.0

Sample D-6 was subdivided into samples D-6-A and D-6-B. Each sample was tested twice, each run varying by moisture content. The sample run at 69% moisture content represents in situ moisture conditions as measured by WSDOT. WSDOT Materials Lab results are found in Appendix: B Ring Shear Testing Results.

X-Ray Diffraction Mineralogy

Nine X-ray diffraction peaks were identified by MDI Jade during testing of a randomly oriented powder sample. However, the diffraction peak distribution appears to have more peaks present than the program identified statistically.

Table 3. Summary results of powder XRD statistics

n	d- Spacing (Å)	Angle (2θ)	Intensity
1	14.3878	6.138º	44.8%
2	14.0979	6.264º	56.2%
3	13.6744	6.459º	75.5%
4	13.3008	6.64º	100.0%
5	12.6607	6.976º	68.7%
6	4.4719	19.838º	53.2%
7	4.3756	20.279º	29.5%
8	4.3375	20.459º	23.1%
9	4.0404	21.981º	22.9%

Major peaks from the powder diffraction pattern appear at between 6º and 7º 2θ, 20º 2θ, 35º 2θ, and 62º 2θ (Figure 24).

Of the several clay species compared to the powder diffraction pattern, 4 clay species showed significant matches. Montmorillonite (PDF 00-060-0318), illite-1M (PDF 00-029-1496),

nontronite-15A (PDF 00-029-1497), and saponite-15A (PDF 00-030-0789) all showed significant matches to the peaks in the powder diffraction profile, as statistically analyzed by MDI Jade.

Table 4. Sample peak matches to mineral PDF standards

Peak Number	**Clay Species**			
n	Montmorillonite	Saponite	Nontronite	Illite
1	-	80%	100%	-
2	100%	-	-	-
3	-	-	-	-
4	-	-	-	-
5	-	-	-	-
6	77.20%	100%	-	100%
7	-	-	-	-
8	-	-	-	30%
9	-	-	-	-

Peak number (n) corresponds to the peak numbers in Table 3.

MDI Jade also allows for visual matching of peaks. Visual matches of peaks can be found in Appendix C: X-Ray Diffraction Mineralogy. Closest visual matches appear to be montmorillonite (Figure 25), saponite (Appendix C, Figure C.2), and illite-1M (Appendix C, Figure C.4). Significantly, the upper 2θ angle between the Sample D-6 and montmorillonite (Figure 25) are a close visual match.

Part IV: Slope Stability Modeling

The goal of back analysis modeling in this section is to better understand how the slope responds to changes in material properties (such as φ angle), changes in the construction of the buttress, inhomogeneity of the gravel-with-matrix unit, and the presence of a water table above the silty clay unit.

I developed two different slope failure scenarios based on previous modeling conducted in 1987 and 2004. The first model scenario described in the section is of a large landslide initiating at an elevation of about 900 feet similar to modeling conducted by Doug Anderson, and based on observations of tension cracks observed in 1987 and inclinometer data in the C-Core (2006) report and available from WSDOT. Inclinometer data indicate slope failure upslope of W Yakitat road (Figure 15).

The second model scenario is a small landslide which is local to the shear-key rock buttress, similar to modeling conducted prior to the construction of the buttress in 1987. The ultimate goal of this modeling is to distinguish between which of these two models is the more plausible slope failure scenario, assuming slope failure is possible.

Back Analysis

Back analysis can give insight into the conditions under which a slope of a given geometry and stratigraphy can fail. This can give clues as to the possible causes of real world failure. Back analysis is undertaken by assuming the slope has already failed (a Factor of Safety of a value of less than 1) along a plane in a predefined area, and modeling for conditions which produce Factors of Safety at or below a value of 1.

For the purposes of this modeling, I assumed that the Prosser Landslide is responsible for the deformation and that failure has occurred. By assuming this, I can better characterize the kind of conditions that would enable slope failure, and whether or not they are realistic given on-site observations, borehole data, and typical material characteristics (See WSDOT, 2013a).

Back analysis was chosen as the modeling method to use because of inclinometer data suggesting ongoing failure above and in front of the buttress (See C-Core, 2006 Annex A for inclinometer data).

Stability Modeling Software

Stability modeling was conducted using commercial software by Rocscience called Slide (Rocscience, 2013). Slide is specifically designed to model slope failure through soils and sediments using finite-element modeling. Cross sections can be uploaded, scaled, and digitized using Slide's CAD tools. From there, different material types can be defined and assigned in the model. Water tables, tension, cracks, and slope remediation structures can also be added to the model as well. Finally, the program is able to run a probabilistic analysis of slope failure using chosen slope Factor of Safety calculation methods (Bishop Simplified, GLE-Morgenstern/Price,

Janbu, etc.). The final output is a failure plane through the model with the lowest Factor of Safety as defined by the previous calculation methods.

Relevant to this study, the modeling software can help determine which of the two failure scenarios (large landslide or small landslide) is more likely by seeing how sensitive each scenario is to changes in the slope materials and buttress. Two-dimensional slope stability models determine the balance of forces driving a slope to fail verses those forces that resist failure (Selby, 1993). Inputs to the model include: a geologic cross section, the unit weight of each material used (lbs/ft^3), the φ angle of each material used (degrees), the cohesion of each material (psf), and the number of possible failure planes to model. A water table and windows through which a possible failure plane must intersect can be added using Slide's CAD tools. Outputs include: a failure plane with the lowest factor of safety through the model and the numerical value of that failure plane according to the calculation method used (Bishop, GLE/Morgenstern-Price, Janbu, etc.).

Bishop and GLE/Morgenstern-Price methods were chosen because they are more appropriate modeling methods for translational slope failure scenarios with planar failure zones (Selby, 1993).

Model Inputs and Outputs

In order to create a model for stability analysis, I first constructed cross sections along two section lines chosen by Tom Badger (Figure 26). The location of section A – A' was chosen because it is the steepest downhill gradient, extends through a large portion of the uphill slide mass, and is perpendicular to the buttress. Section A – A' is also the approximate location of the section used in the 2002 modeling by Doug Anderson. Section B – B', while somewhat oblique to the steepest downhill gradient, captures more recently drilled boreholes (including the 2013 drilling), and is situated on the eastern side of the buttress where recent road deformation has occurred. The geologic cross sections I created were drawn at a 1:600 scale (Figure 27, Figure 28). The subsurface geology along the sections was constrained from the following boreholes:

Table 5. Boreholes used for Sections A – A' and B – B'

Section A - A'	Section B - B'
H-8-87	H-8-87
H-2-94	H-2-94
H-7-87	H-7-87
H-3-02	H-1-94
H-6-87	H-100si-13
	H-101vwp-13
	H-5a-02
	H-2-93

Boreholes are indicated on the sections as well (Figures 27, Figure 28).

The buttress and roads were placed onto the cross section by measuring from known points on the aerial photos and using scale designs of the buttress as designed by Todd Harrison of WSDOT in 1987.

Tom Badger chose Section B - B' to use for stability modeling based upon his professional discretion. The intent of using Section B – B' for modeling was to determine if the eastern side of the site is susceptible to slope failure, specifically in the area where recent deformation of the eastbound lanes has occurred.

Within Slide, geomaterial boundaries and properties can be assigned, including material cohesion, unit weight, and shear strength (φ angle). Material properties for gravel units were approximated using WSDOT standard guidelines for similar materials (Table WSDOT, 2013a) and with the guidance of previous modeling efforts from the 1990s and C-Core in 2006. The φ angle for the silty clay unit was assigned based upon the WSDOT materials testing results in Part III.

Six major material units were introduced into the model and are labeled as follows: quarry spalls (buttress material), slide debris, gravels-with-matrix, clean gravels, silty clay, and basalt bedrock. Units were created from WSDOT drill logs.

Slide debris is the upper most unit and consists of basalt fragments in a silty, sandy matrix. The gravels-with-matrix unit consists of subrounded to subangular gravels with a high percentage of fine grained matrix. Frequently, drillers noted that drilling had washed away much of the matrix in these gravels. The silty clay unit represents the material retrieved from the likely failure zone during drilling, and was tested at the WSDOT Materials Lab in the previous section (Part III). The basalt unit is the underlying bedrock unit found at the Prosser Landslide. This unit consists of highly weathered to fresh basalt. The quarry spalls unit is the material which composes the buttress. It consists of basalt rip-rap. Clean gravels are subrounded to subangular gravels without a fine grained matrix. The clean gravels unit was used to test how the stability model would react to heterogeneity within the gravels-with-matrix unit.

The material properties for the 6 units used for modeling are as follows:

Table 6. Material values used for stability modeling

Units	Unit Weight (lbs/ft^3)	Cohesion (psf)	φ
Quarry Spalls (Buttress)	125	0	45º
Slide Debris (Qls)	125	0	20º
Gravels-with-matrix (Qfs)	125	0	25º
Clean Gravels (Qfs)	135	0	30º
Silty Clay (Qfs)	115	0	7º
Basalt (Mvem)	175	1000	45º

No cohesion was assign to granular materials such as gravel and quarry spalls that lacked abundant fine-grained matrix. The clay layer, believed to be the primary failure zone of the landslide, was assumed be at residual strength, due to the extensive, long-term deformation of

the landslide. Its strength was assigned based primarily on ring shear test results and subsequently confirmed through back-analyses. Evidence of deformation could be seen in the disturbed state of the clay material retrieved from the Shelby tubes, indicating the clay material is likely only as strong as its residual shear strength (Holtz, Kovacs, and Sheehan, 2012).

The depth of the buttress key was modeled at the full designed depth below the clay unit (full key), above designed depth seated within the middle of the clay unit (partial key), and above the designed depth seated on top of the clay unit (absent key). These scenarios are intended to simulate the possibility that the buttress was not constructed as it was designed, and how much these design scenarios affect the ability of the slide to move.

Stratigraphy within the gravel with matrix unit was simulated as both a homogenous unit and as a stratified unit with 2 clean gravel lenses. The clean gravel lenses were placed within the unit in accordance with the drill logs which indicated the likely presence of gravels without matrix. The intention of adding clean gravel lenses was to see how sensitive the two modeling scenarios are to likely inhomogeneity of the gravel-with-matrix unit.

Failure analysis was completed assuming a non-circular failure plane. Factor of Safety for modeling scenarios was calculated using Bishop Simplified (Bishop, 1955) and GLE/Morgenstern-Price (Morgenstern and Price, 1965) methods. A block search was conducted by modeling 5000 possible failure planes through pre-defined windows corresponding to failure surfaces identified in inclinometer data. The angle through which the failure plane could enter and exit the slide mass were adjusted to 45° for entry and between 15° and 75° for the exit. The reason that the headscarp initiation point was assigned a value of 45° is that headscarps are initiated by tensional stresses and are typically steep (Selby, 1993).

Stability Modeling Results

Stability modeling results for the large landslide scenario show that failure is most sensitive to changes in the material properties of the gravel-with-matrix layer. The condition of the buttress did not have a large effect on the Factor of Safety in a landslide modeled at this scale.

However, the smaller landslide was very sensitive to buttress construction and much less sensitive to the material properties of the gravels-with-matrix unit than the large landslide scenario.

Tables containing the output Factors of Safety for model runs can be found in Appendix D: Stability Modeling Results.

<u>Large Landslide</u>

In cases where the Factor of Safety is below 1 and the buttress has a full key, the modeled slide plane avoids the buttress from underneath (Figure 29). In cases where the buttress is partially keyed or the key is absent, the modeled slide plane preferentially follows the clay unit. However, in nearly all scenarios, there did not appear to be a significant distinction between runs where the buttress was fully keyed and where the buttress was not.

Modeling of the large landslide with the initial conditions listed in Table 6 produced the following Factors of Safety:

Table 7. Factors of Safety for initial conditions of the large landslide scenario:

	Bishop Simplified	GLE/Morgenstern-Price
Full Key	2.230	2.212
Partial Key	2.157	2.138
Absent Key	2.157	2.140

However, modeling this scenario in the complete absence of the buttress did not produce a Factor of Safety lower than 1, indicating that under those conditions the hillslope would not fail at all. Therefore, in order to produce a state where the landslide would be at or near failure, the φ angle for the gravels-with-matrix unit were reduced to 10º for the majority of the modeling. The reason the φ angle in the gravels-with-matrix unit was reduced is that the φ angle of that particular unit is likely highly variable and largely determined by the φ angle of the clay material within it (See my discussion of the gravel matrix in Part V). Reducing the φ angle to this value produced Factors of Safety at the slide of around 1, which indicate marginal stability. Since the 10º φ angle satisfies the conditions for back analysis of slope failure (marginal stability).

Sensitivity to material properties

Modeling with changes in the φ angle of gravels-with matrix unit showed that the large landslide scenario was particularly sensitive to this variable.

Lowering the φ angle to 10º produces Factors of Safety which would indicate marginally unstable conditions (Appendix D: Table D.1). Increasing the φ angle of the silty clay unit to 10º, the same as the Gravels-with-matrix unit produces Factors of Safety near 1, indicating marginally stable conditions (Appendix D: Table D.2). In this scenario, the slide plane does not preferentially follow the clay unit. This scenario is meant to test how sensitive the model is to the absence of a very weak clay unit near the buttress, which may shed insight into the real life importance of the silty clay unit found near the buttress.

Heterogeneous Stratigraphy

Adding lenses of the Clean Gravels unit into the stratigraphy produced Factors of Safety slightly above 1, indicating marginally stable conditions (Appendix D: Table D.3). The goal of this exercise is to model the effects of heterogeneous stratigraphy within the gravels-with-matrix unit with the inclusion of gravel without any matrix present. Drill logs indicate heterogeneity within the gravels-with-matrix unit, but it was very difficult for me to separate the changes in material into individual units.

Perched Water Table

A small perched water table was modeled above the clay unit. This scenario produced Factors of Safety slightly below 1, indicating marginally unstable conditions (Appendix D: Table D.4).

I created this scenario to address previous attention and concern over water pooling in and around the buttress and the silty clay unit by Arnie Korynta in the 1993-1995 geotechnical study was that the buttress key was acting as a reservoir for rainwater as it infiltrated the site.

Since the water table at the site appears to be developed within the basalt, water table was modeled in the basalt unit in the model. However, the presence or absence of a water table in basalt did not affect the Factor of Safety in any scenario.

Small Landslide

The small landslide models a scenario similar to that modeled in 1987, where it was assumed that the landslide was localized to the buttress and roadway. The scenario produces a headscarp near the headscarp identified in 1987.

In scenarios where there is a partial or absent buttress key and the Factor of Safety is below 1, the failure plane created by the model (Figure 30) is plotted through where the buttress would be, following along the clay layer. In scenarios where there is a full buttress key and Factor of Safety is below 1, the slide plane circumvents the buttress from underneath. In all scenarios, the slide toe emerges in the eastbound lanes of I-82. In none of the scenarios modeled was it possible to fail the slide through the buttress or produce a toe in the median or the westbound lane.

Heterogeneous stratigraphy did not affect Factors of Safety in any model run for the small landslide scenario.

Initial conditions for the scenario produced the following Factors of Safety:

Table 8. Initial Factor of Safety conditions for the small landslide scenario:

	Bishop Simplified	GLE/Morgenstern-Price
Full Key	1.217	1.284
Partial Key	0.866	0.875
Absent Key	0.866	0.874

The full key scenario above produces a Factor of Safety close to the original Factor of Safety (FS=1.25) that the buttress was designed to produce by stabilizing the landslide. Factors of Safety for partial and absent key scenarios indicate moderate to high slope instability.

Sensitivity to material properties

Increasing the φ angle of the Gravels-with-matrix to 35º produced a Factor of Safety significantly above 1 for a fully keyed buttress, and Factors of Safety below 1 for a partial and absent key (Appendix D: Table D.5) . A fully keyed buttress in this scenario would be effectively stable while partial and absent key situations would be marginally unstable. The reason for testing this particular set of conditions is to see how sensitive the small landslide is to the φ angle of the gravels-with-matrix unit. Having a higher φ angle in the gravel is more representative of standard assumed φ angles for gravels (WSDOT, 2013a).

Decreasing the φ angle of the gravels-with-matrix to 15º produces a Factor of Safety significantly above 1 for a fully keyed buttress, and Factors of Safety significantly below 1 for a partial or absent buttress (Appendix D: Table D.6). A fully keyed buttress would be effectively stable in this scenario while a partial or absent buttress key would be significantly unstable. The φ angle assumed in this scenario for the Gravels-with-matrix unit is similar to the assumptions for this unit used in both the 1987 modeling and that of 2004. Factors of Safety in this scenario indicate high instability should the buttress not be built as it was designed. High instability has not been observed at the Prosser Landslide since prior to the construction of the buttress.

Decreasing the φ angle of the gravels-with-matrix even further to 10º produces Factors of Safety below 1 for all conditions of the buttress key (Appendix D: Table D.7). The high instability indicated in this scenario is not what has been observed presently at the Prosser Landslide. The reasons for modeling this instance are similar to the reasons used previously for the 10º φ angle in the large landslide scenario.

Perched Water Table

Modeling a perched water table above the clay unit produces a Factor of Safety significantly above 1 for a fully keyed buttress and Factors of Safety significantly below 1 for a buttress with a partial or absent key (Appendix D: Table D.8). Again, the absence or partial absence of a buttress key produces Factors of Safety which would indicate high instability of the slide mass.

Part V: Discussion and Conclusion

The original geotechnical investigation of the 1980s identified the silty clay at the base of the I-82 cutslope as the geologic unit responsible for the significant slope failure which initiated during highway realignment.

Geology and Origin of the Silty Clay and Gravel Units

The Prosser Landslide is situated at the confluence of the lower end of the Yakima Valley and the Pasco basin, both of which have distinct depositional histories within the larger context of the Columbia Basin and the YFTB. Much work in the Pasco Basin specifically has been done to characterize the suprabasalt sediments in an effort to further aid in the remediation of the Hanford Site, and therefore the stratigraphy and depositional history of the Pasco Basin has been heavily scrutinized and documented. Conversely, while there has been interest in the Yakima Valley related to the Ellensburg Formation sediments, resources and attention have not been as abundant as in the Pasco Basin. However, between Smith (1988) and the abundance of DOE-funded studies, it is possible to put together an origin for the silty clay unit despite the prevalence of fluvial-dominated activity in the early Quaternary.

Previous mapping efforts in the area by Reidel and Fecht, 1994 and Hagood, 1986 have identified numerous outcrops of Elephant Mountain Member basalts at the elevation of the basalt knob across the road from the buttress; therefore, it is likely safe to correlate the basalt found immediately under the unconsolidated material of the Prosser Landslide with the Elephant Mountain Member basalt. Sedimentary units lying above the basalt are limited to either upper Ellensburg Formation units which have not been identified (Hagood 1986; Smith, 1988), unmapped Ringold Formation sediments (Lindsey and Gaylord, 1990), or slackwater deposits from within the Hanford Formation flood deposits (Reidel and Fecht, 1994). Flood waters may also be responsible for scouring of previous sediments from ancestral Columbia River or Yakima River systems (DOE, 2009; DOE, 2002; Smith 1998), increasing the difficulty of identifying the sediments.

Smith (1988) mentions that the Cascade Range in the Late Miocene input copious quantities of pyroclastic and ash fall deposits into the upper Yakima Valley. These volcanic sediments are well recorded in the Ellensburg Formation sediments of that time period (Smith, 1988). At the same time, the development of the YFTB folds appears to fix the Yakima River within what is now the Yakima Valley (Smith, 1988). Deposition of upper Ellensburg Formation sediments has been noted along the valley (Smith, 1988). Of specific interest in these upper Ellensburg Formation Sediments are the lake bed sediments which formed in the southeast portions of the basin (Smith 1988, Figure 2). At the same time, regional lakes began to form within the Pasco Basin, depositing laminated silts and clays (Ringold Formation) (Lindsay and Gaylord, 1990). Hagood, 1986 also notes the presence of an undifferentiated Ellensburg clay unit along the Horse Heaven Hills several miles away from the Prosser Landslide. It is possible that the clay found at Prosser Landslide correlates to Hagood's undifferentiated Ellensburg Formation sediments. However, the area was mapped previously as being part of the Hanford Formation Touchet beds (USGS, 1977), but it is possible that the deposits belong to a Ringold-equivalent unit of the Ellensburg Formation instead.

Influx of fluvial sediments bearing pyroclastic and ash fall sediments into the regional lake in the Pasco Basin may be responsible for the content of the clay found at the site as well. If indeed ash fall and pyroclastic sediments were able to migrate down the Yakima Valley since the Late Miocene into the Prosser Landslide vicinity and were incorporated into the lake deposits at the southeast end of the Yakima Valley, decomposition of those ash could produce the smectite-group clay minerals (Selley, Cocks, and Pliner, 2005; Bain, 1971) that are responsible for the swelling properties and characteristically low shear strength of the silty clay material found in the locality of the shear key rock buttress.

Gravels lying above the clay units are likely part of the Hanford Formation (or Hanford-Formation equivalent) gravels deposited during the Missoula Floods (USGS, 1977; Reidel and Fecht, 1994).

Material Properties

Both the plasticity index testing and the ring shear testing revealed surprising material properties for the silty clay unit. Previous studies dated to the 1993 geotechnical investigation revealed high plasticity indices for what appears to be the same silty clay material as that material tested for this investigation, which had high plasticity indices as well.

While high plasticity index is correlated with a low angle of internal friction, recent ring shear testing assigned a much lower φ angle than originally anticipated. Preliminary results from the ring shear testing were initially thought to be erroneous because the value of the φ angle was half of what was originally estimated using established correlation methods (See WSDOT 2013a, Chapter 5). However, ring shear results may not seem so surprising in light of updated empirical correlations between liquid limit and residual shear strength made in Stark and Hussain (2013). Figure 2 of Stark and Hussain (2013) illustrates the updated correlation between liquid limit and residual shear strength, showing that soils with liquid limits of near 100 would likely have residual shear strengths between 12º and 6º with a given confining pressure. In this context, the residual shear strength of the silty clay material retained from the Prosser Landslide is within the range of expected values.

During ring shear testing, it became apparent that the residual shear strength of the silty clay is not dependent on moisture content It is likely that because it displays low shear strength even when not saturated, that the landslide might be mobile under non-saturated conditions. This is to say, this implies that the Prosser Landslide might be an essentially dry landslide.

It is also curious that the grain size distribution indicates that it is an elastic silt rather than a fat clay, as was assumed in previous studies. Given its previously established expansiveness and low φ angle, it might be reasonable to assume that despite the silt-sized particles, the physical properties of the clay fraction are the controlling factor on the material's overall mechanical properties.

The same can be said about the gravels as well. As noticed by the drillers, the gravels contained a significant amount of matrix in them. However, conventional drilling methods, like the wet

rotary drilling used, will wash the matrix from the gravel, especially if the gravel blocks the tube during drilling. During the recent drilling, drillers noticed that the gravel matrix was being washed from the tube into the return water. They therefore could not quantify the amount of matrix present in the gravel layers. Previous drilling likely encountered similar difficulties as well, since they all appear to have used wet rotary coring methods. If this is the case, what has been identified as a clayey gravel or a silty gravel may in fact be a gravelly silty clay.

Even if this is not the exactly the case, it has been established that given a high enough proportion of matrix to gravel, the physical properties of a material are dominated by the matrix (Holtz, Kovacs, and Sheehan, 2012). Given this and the material properties of the silty clay found at the site, the low φ angles for gravel evaluated in in some of the stability modeling scenarios may be reasonable.

XRD Mineralogy and Likely Clay Composition

XRD results from untreated clay samples can be difficult to discern because of the presence of organic material, calcium carbonate, or mixed clay mineralogies. In the case of typical swelling clays, such as smectite-group clays, octahedral layers from other clay types such as illite may substitute into the lattice as the clay decomposes from a smectite to illite (Eberl, 1984; Selley, Cocks, and Pliner, 2005; Moore and Reynolds, 1989). The ordering of the smectite-illite layers, either ordered or disordered, can affect diffraction patterns (Moore and Reynolds, 1989). Essentially, clay identification with XRD analysis requires not only a diffraction pattern but also qualitative knowledge of how clay diffraction patterns can be affected by changes in crystal structure due to conditions present at the site.

In the case of clay minerals, almost all of them have a strong peak at around 20 2θ (Moore and Reynolds, 1989). Smectite group clays have a strong peak at between 6.5 and 7 2θ, and several smaller, but strong peaks around 35 2θ, and only strong high angle peak at near 62 2θ. Mixed layer clay species, such as illite-montmorillonite, kaolinite-montmorillonite, and rectorite show higher 2θ strong low angle peaks than more pure smectite samples. Additionally, the strong 20 2θ peak present in all common smectites and illite is either reduced or shifted to a higher 2θ. Some additional strong peaks around 20 2θ may also be present in mixed layer clays. (See Appendix C for examples)

Upon visual inspection, the powder diffraction sample taken from the Prosser Landslide shows several strong peaks that are correlative to smectite-group clays (Figure 24). A strong visual correlation between the measured sample and illite-1M, saponite, nontronite, and montmorillonite can be seen in the sample. Given that smectite-species clays and illite are related (Moore and Reynolds, 1989; Selley, Cocks, and Pliner, 2005), this perhaps is not surprising. Of the 4 clay minerals mentioned, illite and montmorillonite had the strongest matches for major peaks, especially the high 2θ peak at 62 2θ.

Additional sample treatment, such as an ethylene glycol solvated sample, could better resolve the identity of the clay species present at the Prosser Landslide. However, between illite and montmorillonite, there exists an important macro-scale difference between the two clays: montmorillonite is a swelling clay, arguably one of the most expansive of the swelling clays (Bain, 1971), illite is not. Since the material does not appear to show the 2 low 2θ high intensity

peaks or the high intensity peak at 26 2θ like a mixed layer illite-montmorillonite clay, it is likely a montmorillonite-dominated clay. Given its high plasticity index (Bain, 1971), much higher than that of an illite-dominated clay, this is likely the case.

Construction History

Throughout the length of the several investigations launched to identify the cause of the deformation of the eastbound lanes of I-82, several hypotheses have been pursued by WSDOT personnel as an explanation. The 1990s saw the introduction of the swelling clay hypothesis by Arnie Korynta as an alternative to the landslide being the culprit. C-Core in 2006 hypothesized that frost heave could be also be responsible for the deformation of the eastbound lanes. Both of these explanations have their flaws.

The swelling clay hypothesis supposes that the key of the buttress acts as a reservoir for water or that water is contributed to the site from the KID canal nearby which then hydrates the silty clay unit, causing it to expand and resulting in vertical displacement of the road. However, C-Core's calculations of the expansion potential of the silty clay indicates that it would not be able to produce the magnitude of displacement observed at the site.

Even if the clays were able to swell and cause heave in the road, it appears unlikely that the shear key could act as a reservoir. The quarry spalls from which the buttress is made has a high porosity, as it is basalt rip rap. That porosity could provide space where water could pool. However, this would require that the water be able to stay within the key. This appears unlikely given the several drillers' accounts of being unable to keep water in the drill throughout drilling through the gravels at the site (Appendix: A). Drillers noted a water level at a depth 66 feet in H-101vwp-13. In 2002, drillers noted a water level of 24 feet in borehole H-5b-02 (same location as H-5b-02) which was drilled at the same elevation as the road surface of I-82 at the bottom of the shear key buttress. Silty clay in the same area below the road is seen from approximately 5 to 10 feet below the roadbed for about 5 feet (C-Core, 2006 Annex A) (Figure 13). Assuming some connection between the standing water elevations of H-101vwp-13 and H-5b-02, any saturated material is below the buttress key in the fractured basalt (Figure 27). Therefore, pooling in the buttress key seems unlikely.

Input of water from the KID canal nearby seems unlikely as well. In the 2004 Anderson and Allen memo to Mr. Yates, they note that deformation observed in the slope inclinometers above and in front of the buttress is larger in the winter months than in the summer months. During the summer months, as they state, KID increases the flow through the irrigation canals. If the irrigation canals were contributing water to the silty clay, there might be an accompanying increase in deformation seen in the slope inclinometers. However, as they conclude, this is not the case.

The C-Core's frost heave hypothesis is similar to the assessment made by KID of the cause of the displacement in the irrigation canal.. However, in neither of these hypotheses appear to have lab testing to substantiate the claim. Furthermore, the C-Core report undermines the frost heave hypothesis by concluding that the development of a frost front would only penetrate 8 inches below the subgrade and displace the road surface only 0.3 inches over the entire season, which is

not enough to count for the bump which has repeatedly formed. C-Core's analysis however, was only a desk study using a 1-dimensional thermal model which links thermal changes to water phase changes. Finally, Region Maintenance of the South Central region has previously reported in the 1990s studies that the formation of the bump does not appear to correlate with seasonal changes in precipitation or temperature. The 2004 Anderson and Allen memo supports this observation.

The landslide hypothesis has been revisited each time the site has been investigated since the 1990s. Arnie Korynta disregarded it as an option on the assumption that the buttress was keyed to specifications and that it would arrest further slope failure. However, at the time, there were conflicting accounts over whether the buttress was not in fact built as it was designed. Further, the buttress as it was designed was only supposed to remediate a slide localized to buttress and W Yakitat Road.

However, photos and WSDOT engineering geologists' accounts dated to during the buttress construction appear to indicate that the buttress, at least on the eastern half, is not built to designed specifications. Photos and descriptions from the 1987 memo from Dave Jenkins and Steve Lowell indicate that the buttress is not keyed below the silty clay unit it was designed to intercept. If this is in fact the case, movement after the construction of the buttress is could be due to slope failure rather than swelling or heaving of the road subgrade, since the buttress is not intercepting the slide plane along the silty clay unit as designed and therefor arresting slope failure.

Stability Modeling

Stability modeling has been conducted several times over since the initiation of sliding at the Prosser Landslide since the 1980s. Original modeling efforts modeled a landslide which was localized to immediately above W Yakitat Road and the new I-82 road bed. Similarly, the buttress was designed only for a smaller slide. However, the modeling in the 1990 by Doug Anderson and the C-Core report both model slides of much larger extents. For the purposes of this study, both of those scenarios have been recreated to evaluate the merits of both of these models.

Small Landslide

In the case of the small slide scenario, the Factor of Safety is sensitive to changes in buttress construction. What was surprising was that the Factor of Safety was effectively the same between the partial and absent buttress scenarios, which may indicate that the stability of the small slide is entirely dependent on whether or not the silty clay unit has been intercepted by the buttress key.

For the majority of the scenarios, the slide plane predicted by the model is through the buttress unless the surrounding Gravels-with-matrix unit is sufficiently weak. Higher φ angles in the Gravels-with-matrix appear to force any viable slide plane along the silty clay unit, since it is the weakest portion of the model. If this is the case, then this would indicate that interrupting the silty clay unit is paramount to the stability of the slide.

If the buttress key is partially or completely removed, the model predicts that the landslide is unstable at standard φ angles in the Gravels-with-matrix unit (25º to 35º). Should those gravels have a much higher proportion of matrix in them than originally thought and as such have a 10º φ angle, it is possible to get failure underneath the buttress even if it is fully keyed.

The advantage to the small landslide model is that it accounts for the continued movement of W Yakitat Road above the buttress as well as the shearing of the H-1-94 inclinometer at a shallow depth (C-Core, 2006 Annex A). Should the buttress key not be built to its original specifications, reasonable φ angles in the Gravels-with-matrix unit can still result in slope failure. Finally, the model predicts headscarp development in a similar location to that seen in the 1980s near the buttress. However, the model does not account for movement seen further up hill, as seen in the up-slope inclinometers and as noted in the 1980s accounts of the initial failure. Also, in the event of low material strength in the Gravel with Matrix, the model indicates that there should be high instability within the slope, which is not what is seen at the site.

Large Landslide

The larger landslide hypothesis overall is most sensitive to changes in the material properties of the Gravels-with-matrix unit. Modeling by Doug Anderson and C-Core placed the φ angle of this material at near 16º. However, if the material is dominated by the silty clay matrix composed of primarily of montmorillonite clays, the φ angle may be considerably lower. Because of the larger influence that the Gravels-with-matrix has on the modeled behavior of the slide, it became apparent that in this scenario, the buttress as it is built is less of a factor in the stability of the slope. This renders the controversy over whether or not the buttress is keyed irrelevant.

In the majority of the scenarios modeled, even with a full buttress key, a viable slide plane can fail beneath the buttress and daylight in the eastbound lanes. This would indicate that the model predicts that the slide mass is likely to be large enough to render the effects of the buttress minimal, since it is possible for a viable plane to circumvent it even with a full key.

Extension of the clay unit further back into the hillside produces failure through the buttress itself. Given that there has been no evidence of movement or deformation of the buttress, it this is likely not a plausible scenario and that the weakest clay portions are localized to the buttress area only.

The introduction of clean, high φ angle, gravel lenses into the large slide scenario raised the Factor of Safety in all scenarios. It would appear that the interruption of low strength materials makes it more difficult for a slide plane to be viable. However, still with a low enough φ strength within the gravels, a marginally stable (FS = ~1) slide plane is able to fail underneath a fully keyed buttress. This means that the actual slide likely is sensitive to variations in the stratigraphy at the site.

Increasing the clay unit's φ angle to 10º produced a situation where the landslide is marginally stable with a fully keyed buttress. This likely demonstrates that the instability of the slide is not completely dependent on an extremely weak clay layer at the base of the hill.

The advantages of the large landslide scenario include taking into account measured movement in the inclinometers further up the hillslope, accounting for tension crack and scarp development seen further up the hillslope as noted in the initial 1980s investigation, and not being dependent upon the presence of state of the buttress key to slide. Unfortunately, this scenario relies upon very low shear strength in the Gravels-with-matrix unit exclusively.

General Discussion

In all modeling scenarios, the model predicts that the toe will appear only in the eastbound lanes. This appears to indicate that despite the size of the landslide, it is only capable of deforming the eastbound lanes. This might have more to do with the geometry of the site, such as the gradual decrease in the thickness of the unconsolidated sedimentary cover against the basalt and reduced confining stress on the modeled failure surface, rather than the size of the slide.

Given the results of the ring shear testing, a perched water table over the silty clay unit may not have as much of an impact on the slope stability as would otherwise be assumed. Modeling scenarios using both the large and the small slide geometries show a decrease in the Factor of Safety with the addition of a perched water table, however if the silty clay is not responsive to saturation, then these scenarios may be irrelevant.

Between the large landslide and small landslide scenarios, the larger landslide scenario has the advantages of not relying on buttress construction, which cannot be verified without dismantling the buttress, and taking into account much larger evidence of mass movement. The smaller slide has the advantage of having more typical material strengths. Should the key be partial or absent in cases where the material strength of the gravel is below 35º, however, the model indicates that such a situation would precipitate rapid failure, which is not what is seen at the site. The marginal stability or slight instability of the larger slide scenarios appears to be the more plausible situation.

Tom Badger briefly floated the idea of a retrogressive landslide, where a smaller block failure near the base of the landslide allows for a larger block upslope to move. This would require the assumption that the upper portions of the site are absolutely stable and that it would not move unless de-buttressed by movement of the material in the landslide toe. Given that the low strength within Gravel with Matrix unit is plausible, this hypothesis may not be required, since the larger slide is potentially viable without removing a portion of the toe.

Conclusions

Material strength of the gravels and clays, and continuity of these units, at the Prosser Landslide appears to be the determining factor in the movement of the larger slope. Silty clay samples from the site show residual strengths which are lower than what previous investigators considered. Observations during drilling suggest the widespread gravel-with-matrix unit may have significantly more matrix than has been captured by sampling. Previous studies have shown the unlikelihood of swelling clays being physically able to deform the road surface to the extent that it becomes a hazard to the traveling public. Similarly, frost heave has been shown to be equally unlikely.

Given the likelihood of there being continuous low material strengths within the slide mass and the very real possibility that the buttress is not keyed below the silty clay, it is likely that deformation in the eastbound lanes is caused by movement of the landslide underneath the buttress on the east end. Furthermore, of the two plausible landslide geometries, it would appear that the larger landslide geometry is the one which is most likely responsible for the deformation observed in the eastbound lanes.

Acknowledgments

I would like to thank Tom Badger and WSDOT for their generosity in offering this project as an internship. Tom Badger's mentorship and guidance have been essential for the completion of this project.

I would like to thank my advisor, Juliet Crider, for her patience, guidance, and time during the writing of this report. I would also like to thank Kathy Troost for facilitating the XRD analysis with the UW Materials Science and Engineering Department. In addition, I would like to express my sincere gratitude to both Kathy and Juliet for establishing the MESSAGe Program, and for taking me on as one of the inaugural group of MESSAGe students.

Also, I am very grateful for and humbled by the support given to me by my family and friends over the course of this program. Especially, I would like to thank my friend, Amanda Bartoy, for encouraging me to pursue graduate school and for motivating me to seek enrollment in the MESSAGe Program.

References

American Association of State Highway and Transportation Officials (AASHTO). 2011. Dry Preparation of Disturbed Soil and Soil-Aggregate Samples for Test: AASHTO Standard R 58-11. Washington, DC.

American Association of State Highway and Transportation Officials (AASHTO). 2012. Standard Method of Test for Determining the Liquid Limit of Soils: AASHTO Standard T 89-10. Washington, DC.

American Association of State Highway and Transportation Officials (AASHTO). 2008. Determining the Plastic Limit and Plasticity Index of Soils: AASHTO Standard T 90-00. Washington, DC.

American Association of State Highway and Transportation Officials (AASHTO). 2012. Standard Method of Test for Laboratory Determination of Moisture Content of Soils: AASHTO Standard T 265-12. Washington, DC.

American Society for Testing and Materials (ASTM). 2011a. Standard Practice for Classification of Soils for Engineering Purposes (Unified Soil Classification System). Designation: ASTM D2487 – 11

American Society for Testing and Materials (ASTM). 2011b. Standard Test Method for Torsional Ring Shear Test to Determine Drained Fully Softened Shear Strength and Nonlinear Strength Envelope of Cohesive Soils (Using Normally Consolidated Specimen) for Slopes with No Preexisting Shear Surfaces. Designation: D7608 – 10.

Bain, J. A. 1971. A plasticity chart as an aid to the identification and assessment of industrial clays. *Clay Minerals*, vol. 9.

Bishop, A. W. 1955. The use of the slip circle in the stability analysis of slopes. *Geotechnique*, vol. 5, pp. 7 - 17

Selley, R. C. (ed.), Cocks, L. R. M. (ed.), Pliner, I. R. (ed.). 2005. Encyclopedia of Geology [First Ed.]. Elsevier Academic Press Vol. 1 – 5, pp. 65 and pp. 362

C-Core. 2006. Geotechnical considerations of the Prosser slide site. C-CORE Report Number: R-05-053-260v1.0. St. John's, Newfoundland, Canada.

Eberl, D. D. 1984. Clay mineral formation and transformation in rocks and soils. *Philosophical Transactions of the Royal Society of London A*, vol. 311, pp. 241 - 257

Esri. 2013. ArcGIS (v. 10.2) [Software]. California: Redlands.

Federal Highway Administration (FHWA). 2006. InSAR Applications for Highway Transportation Projects. Publication Number FHWA-CFL/TD-06-00x. Central Federal Lands Highway Division. Lakewood, CO.

Google, Inc. 2013. Google Earth (v. 7.0.3.8542) [Software]. California: Mountain View.

Hagood, M. C. 1986. Structure and evolution of the Horse Heaven Hills in south-central Washington. [US Department of Energy Contract No. DE-AC06-77RL01030]. Rockwell International: Richland, WA

Harris, C. F. T, and Schuster, E. J. compliers. 2000. 1:100,000-Scale Digital Geology of Washington State [vector dataset]. Department of Geology and Earth Resources, Olympia, WA. Retrieved from: http://www.dnr.wa.gov/ResearchScience/Topics/GeosciencesData/Pages/gis_data.aspx

Holtz, R. D, Kovacs, W. D., and Sheehan, T. C. 2012. An Introduction to Geotechnical Engineering [First Ed.]. Prentice Hall, USA.

International Centre for Diffraction Data. 2013. PDF-4/Minerals [Powder Diffraction File Database]. Newton Square, PA.

Janbu, N., Bjerrum, L., and Kjaernsli, B. 1956. Stabilitetsberegning for fyllinger skjaeringer og naturlige skraninger [Translation: "Stability Calculation of fillings cuts and natural slopes"]. *Norwegian Geotechnical Publication* No. 16. Oslo, Norway

Lindsey, K. A., Gaylord, D. R. 1990. Lithofacies and sedimentology of the Miocene-Pliocene Ringold Formation, Hanford Site, south-central Washington. *Northwest Science*: vol. 64, no. 3, pp. 165 – 180.

Materials Data, Inc. 2013. MDI Jade (v. 9.5.0) [Software]. California: Livermore

Morgenstern, N. R. and Price, V. E. 1965. The analysis of the stability of general slip surfaces. *Geotechnique*, vol. 15, pp. 70 – 93.

Moore, D., and Reynolds, R. 1989. X-Ray Diffraction and the Identification and Analysis of Clay. Oxford University Press, New York, New York.

Power, D., Youden, J., English, J., Russell, Churchill, S., Anderson, S.A., Surdahl, R., Blair, A., Lofgren, D.C., Anderson, D.A. 2006. InSAR evaluation of landslides in support of roadway design and realignment. *2006 IEEE International Geosciences and Remote Sensing Symposium*. Denver, CO.

Reidel, S. P. 1984. The Saddle Mountains: the evolution of an anticline in the Yakima fold belt. *American Journal of Science*, Vol. 284, pp. 942 - 978

Reidel, S. P.; Fecht, K. R., compilers. 1994. Geologic map of the Richland 1:100,000 quadrangle, Washington: Washington Division of Geology and Earth Resources Open File Report 94-8, 21 p., 1 plate. Olympia, WA. Retrieved from: http://www.dnr.wa.gov/Publications/ger_ofr94-8_geol_map_richland_100k.zip

Repasky, T. R., Hyde, E. R., Link, C.A., Speece, M.A.. 2009. Landstreamer/gimbaled geophone acquisition of high‐resolution seismic reflection data north of the 200 Areas, Hanford Site, Rep. SGW–43746, 78 pp., U.S. Dep. of Energy, Washington, D. C.

Rocscience Inc. 2013. Slide (v. 6.025) [Software]. Ontario: Toronto.

Selby, M. J. 1993. Hillslope Materials and Processes [Second Ed.]. Oxford University Press, USA.

Smith, G. A. 1988. Neogene synvolcanic and syntectonic sedimentation in central Washington. *Geological Society of America Bulletin* 1988, vol. 100, no. 9, pp. 1479-1492. doi: 10.1130/0016-7606(1988)100<1479:NSASSI>2.3.CO;2

Stark, T. D., Hussain, H. 2013. Empirical correlations; drained shear strength for slope stability analysis. Journal of Geotechnical and Geoenvironmental Engineering, vol. 139, no. 6, pp 853 - 862

U.S. Department of Energy (DOE). 2002. Standardized stratigraphic nomenclature for post-Ringold-Formation sediments within the central Pasco Basin [Document No. DOE/RL-2002-39]. Washington: Richland

U.S. Department of Energy (DOE). 2009. Hanford Site groundwater monitoring and performance report. Vol. 1, Chapter 3, pp. 1 – 17. Washington: Richland

United States Geologic Survey (USGS). 1977. Corral Canyon 15’ quadrangle. (1:24,000 scale) [Map]. United States Geologic Survery: Denver, CO.

United States Geological Survey (USGS). 1998. USGS 10-meter DEM (Corral Canyon Quad). (10 meter resolution) [Digital Elevation Model]. Retrieved from: Washington Geospatial Data Archive http://gis.ess.washington.edu/data/raster/tenmeter/byquad/yakima/index.html

Washington State Department of Transportation (WSDOT). 2013a. WSDOT Geotechnical Design Manual [Document Number M 46-03.08]. Olympia, WA. Retrieved from http://www.wsdot.wa.gov/publications/manuals/fulltext/M46-03/M46-03.08Revision.pdf

Washington State Department of Transportation (WSDOT). 2013b. WSDOT FOP for WAQTC/AASHTO T 27/T 11: Sieve Analysis of Fine and Coarse Aggregates. WSDOT Materials Manual. Olympia, WA.

Figure Index

Figure 1a: The Prosser Landslide is located in South Central Washington in the Columbia Basin, west of Tri-Cities. Image from Google Earth.

Figure 1b: The Prosser Landslide, seen here at the northern most portion of the Horse Heaven Hills, lies between the towns of Prosser and Benton City. Image modified from Google Earth satellite imagery.

Figure 2: The KID Canal north of I-82 and the buttress. Cars on I-82 can be seen in the upper left of the photo. The shear-key buttress can be seen in the upper right with the WSDOT drilling crew during August 2013.

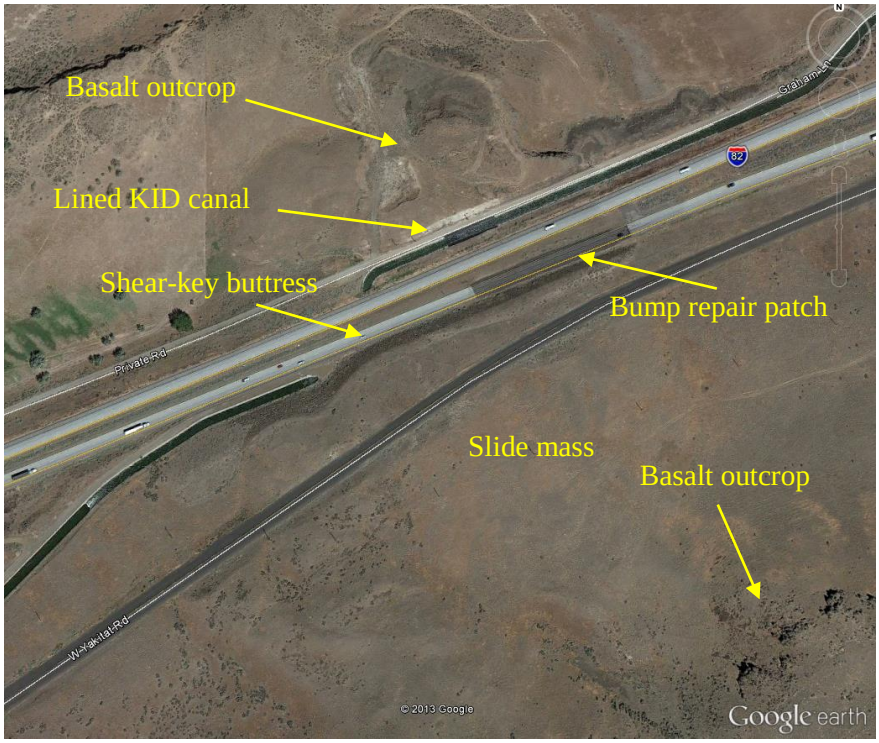

Figure 3: A satellite imagery of the Prosser Landslide site, I-82, and the shear-key buttress. The bump repair patch consists of darker asphaltic concrete pavement. Image modified from Google Earth satellite imagery.

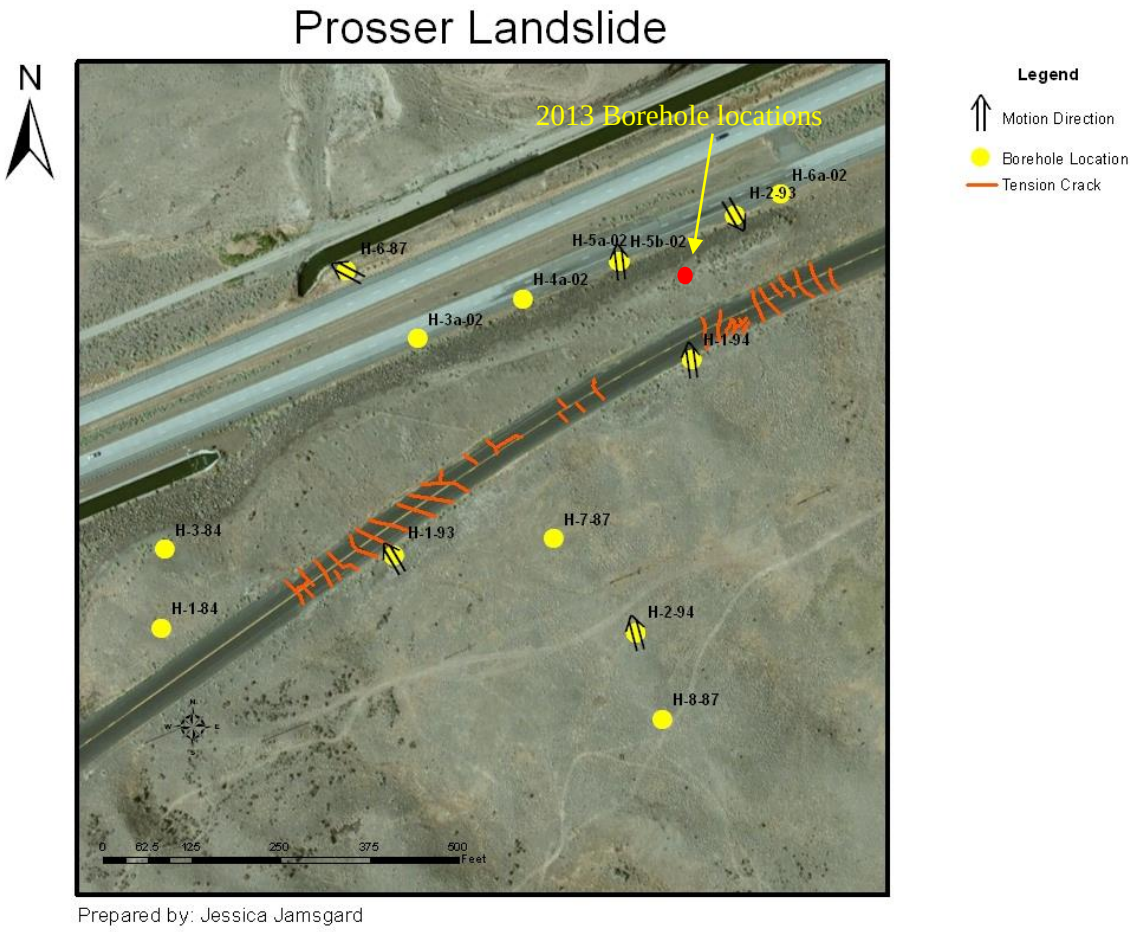

Figure 4: Locations of instrumented boreholes at the Prosser Landslide. This map is not a complete map of all the boreholes ever drilled at the site. Coordinates for many boreholes appear to have been lost. This map also shows the direction of slope movement as recorded by each inclinometer (See C-Core, 2006 Annex A for processed data). I have also added the relative locations and orientations of tension cracks I observed in W Yakitat Road during my site visit in August of 2013. This image was made using Esri ArcGIS with Ersi's basemap satellite imagery.

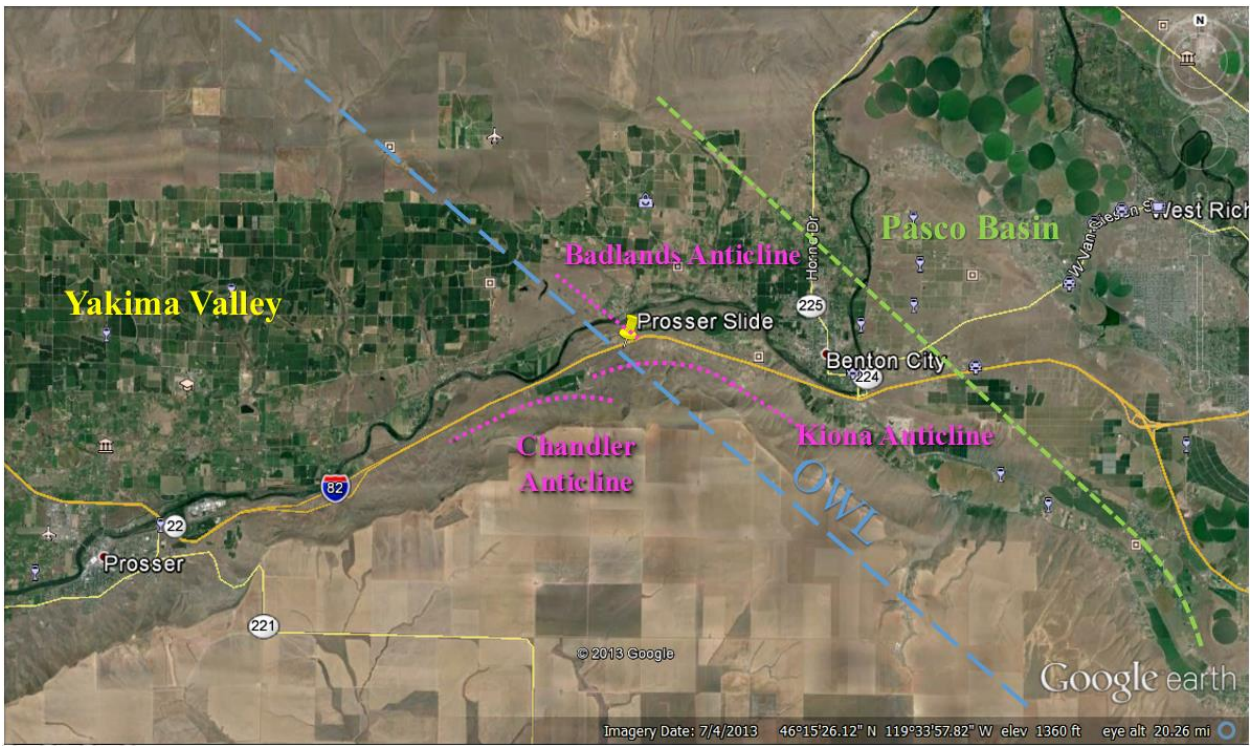

Figure 5: A map of the major structural elements around the Prosser Landslide Area, including the approximate western limit of the Pasco Basin (green), the Yakima Valley, the approximate western limit of the Olympic-Wallowa Lineament (OWL) (blue), and major anticlines (Chandler, Kiona, and Badlands) (magenta). Locations from Hagood (1986) and DOE (2009). Image modified from Google Earth satellite imagery.

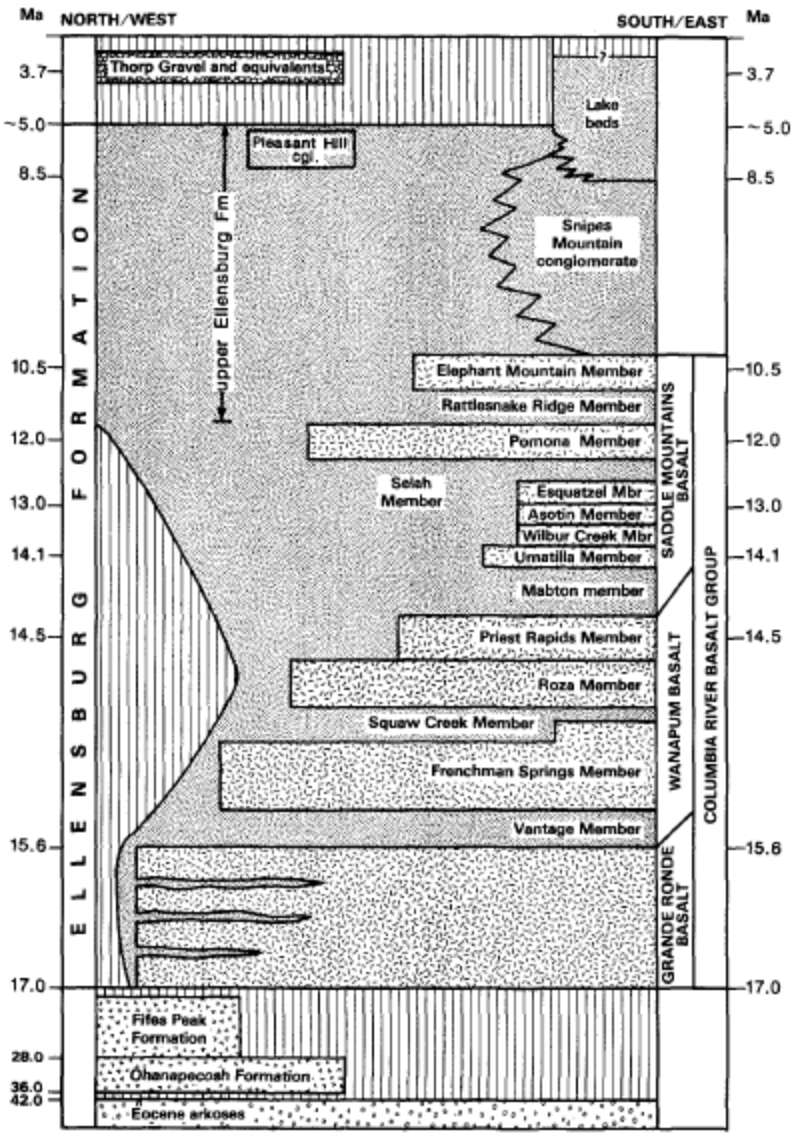

Figure 6: Here Smith (1988) shows the stratigraphic relations between the Columbia River Basalt members and the Ellensburg Formation along the Yakima Valley between the Eocene and Quaternary. The stratigraphy on the right side of the figure, specifically the upper portions, is likely representative of the stratigraphy seen at the Prosser Landslide. From Smith (1988) Figure 2

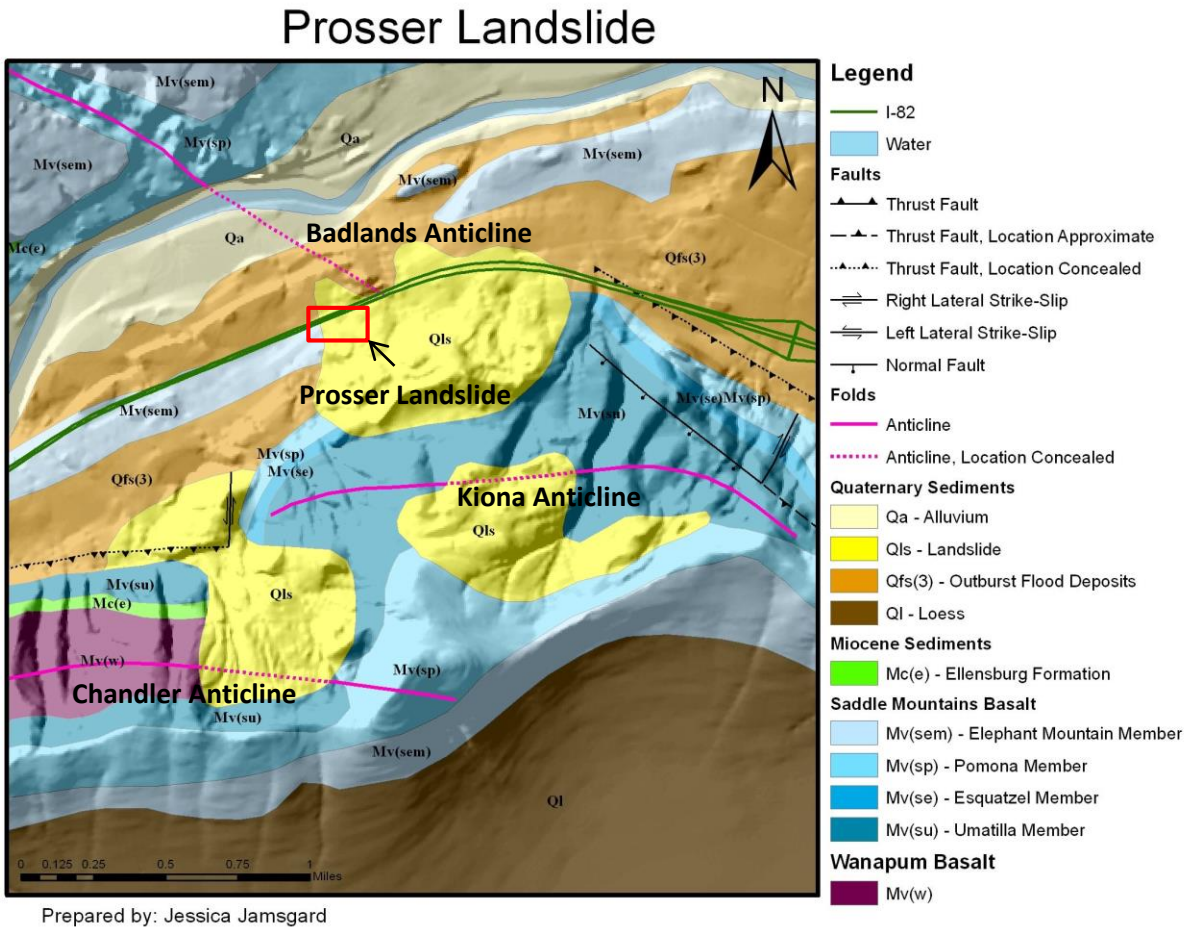

Figure 7: A map of the geology near the Prosser Landslide at the 1:100,000 scale (Harris and Schuster, 2000). Shaded relief has been added to the figure for referece. The oldest units in the area are the Miocene Wanapum Basalt (Mv(w)) which is the royal purple unit to the in the southwest of the figure. Above that is the Saddle Mountains Basalt (Mv(su), Mv(se), Mv(se), Mv(sem)), which can be seen as the brown throughout the central portions of the figure in blue. The Ellensburg Formation (Mc(e)) can be seen in green on the left side near the center of the sides. The Quaternary Flood Sediments (Qfs), which has incorporated the Hanford Formation, can be throughout the as the orange unit in the upper portions of the figure. Quaternary Loess (Ql) is the dark brown unit in the bottom of the figure and covers the top of the Horse Heaven Hills. Quaternary alluvium (Qa), can be seen around the banks of the Yakima River near the very top of the figure. Finally, Quaternary Landslide (Qls), in yellow can be seen on the steep northern limit of the Horse Heaven Hills. The Prosser Landslide makes up a tiny portion of the larger, older landslide.

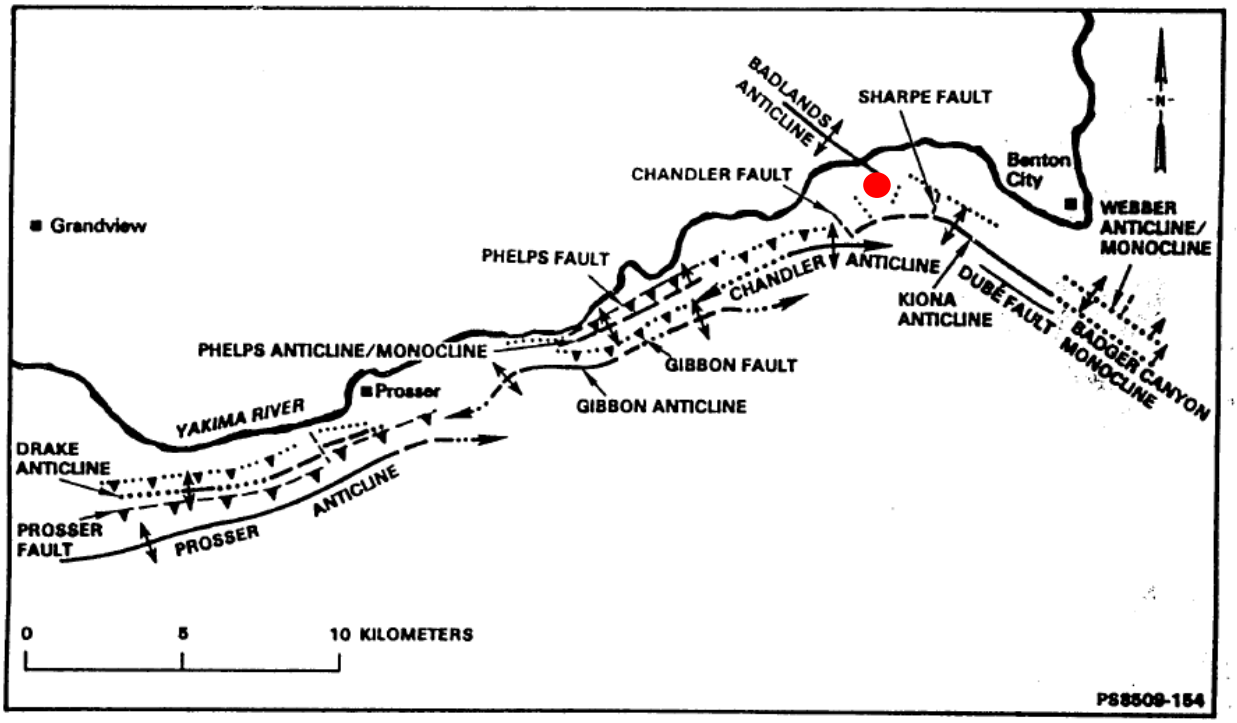

Figure 8: A map of the YFTB structures in and around the Yakima Valley and the Horse Heaven Hills. The Prosser Landslide is located at the red dot. Modified from Hagood (1986) Figure 14.

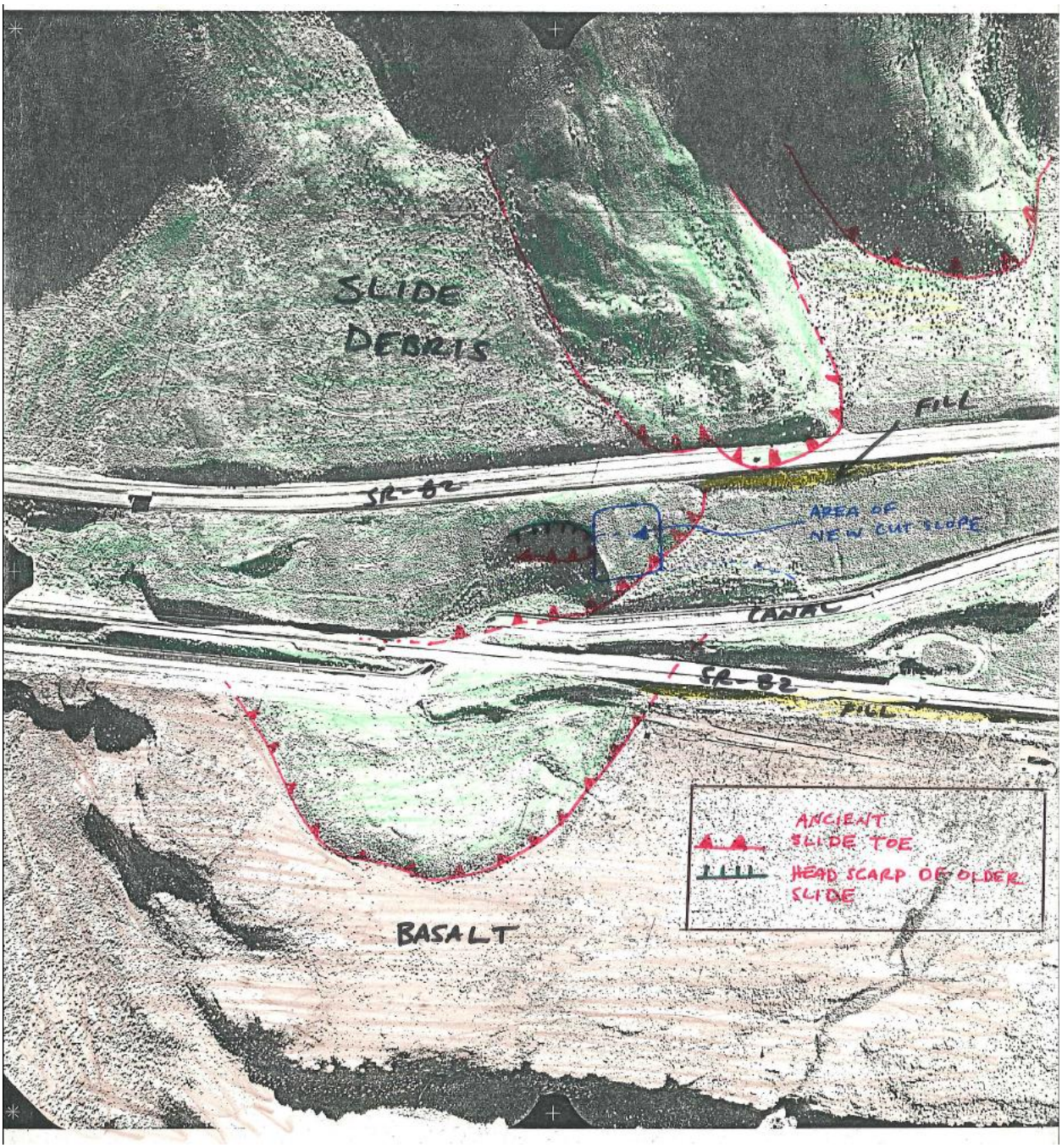

Figure 9: Annotated aerial imagery taken prior to the realignment of I-82 in 1987. Several modern features of the landslide site are missing in this photo, including the shear-key buttress and the modern eastbound lanes of I-82. The upper roadway indicated on the photo as I-82 is now W Yakitat Road. Green indicates landslide debris. Red indicates basalt. Yellow indicates artificial fill. Small landslide toes are indicated with the red lines, while an older headscarp is indicated in black near the center. North is to the bottom. Photo courtesy of WSDOT via the Washington State Archives.

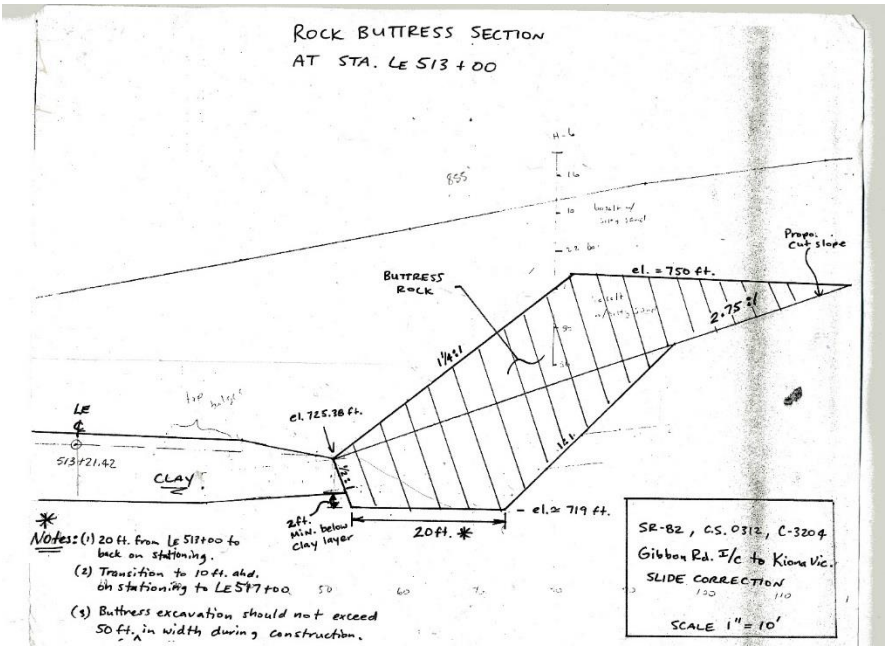

Figure 10: A scale drawing (originally 1 inch to 10 feet) of the buttress as it was meant to be built on the west side of the project area. The clay unit depicted in the drawing was meant to be intercepted by the buttress key in order to arrest slope failure. The buttress was designed by Todd Harrison of WSDOT. Image courtesy of WSDOT via the Washington State Archives.

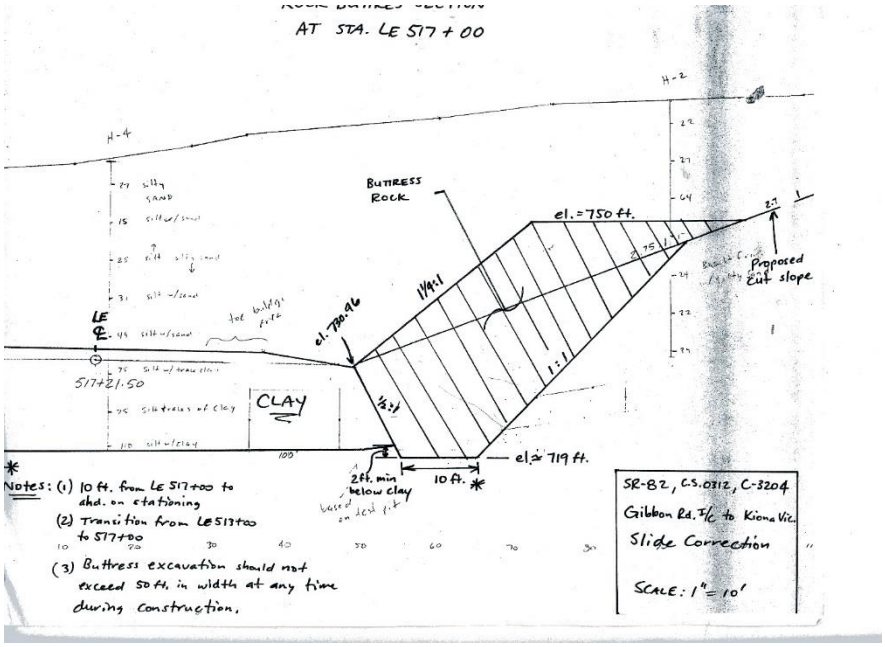

Figure 11: A scale drawing (originally 1 inch to 10 feet) of the buttress as it was meant to be built on the east side of the project area. The clay unit depicted in the drawing was meant to be intercepted by the buttress key in order to arrest slope failure. The buttress was designed by Todd Harrison of WSDOT. Image courtesy of WSDOT via the Washington State Archives.

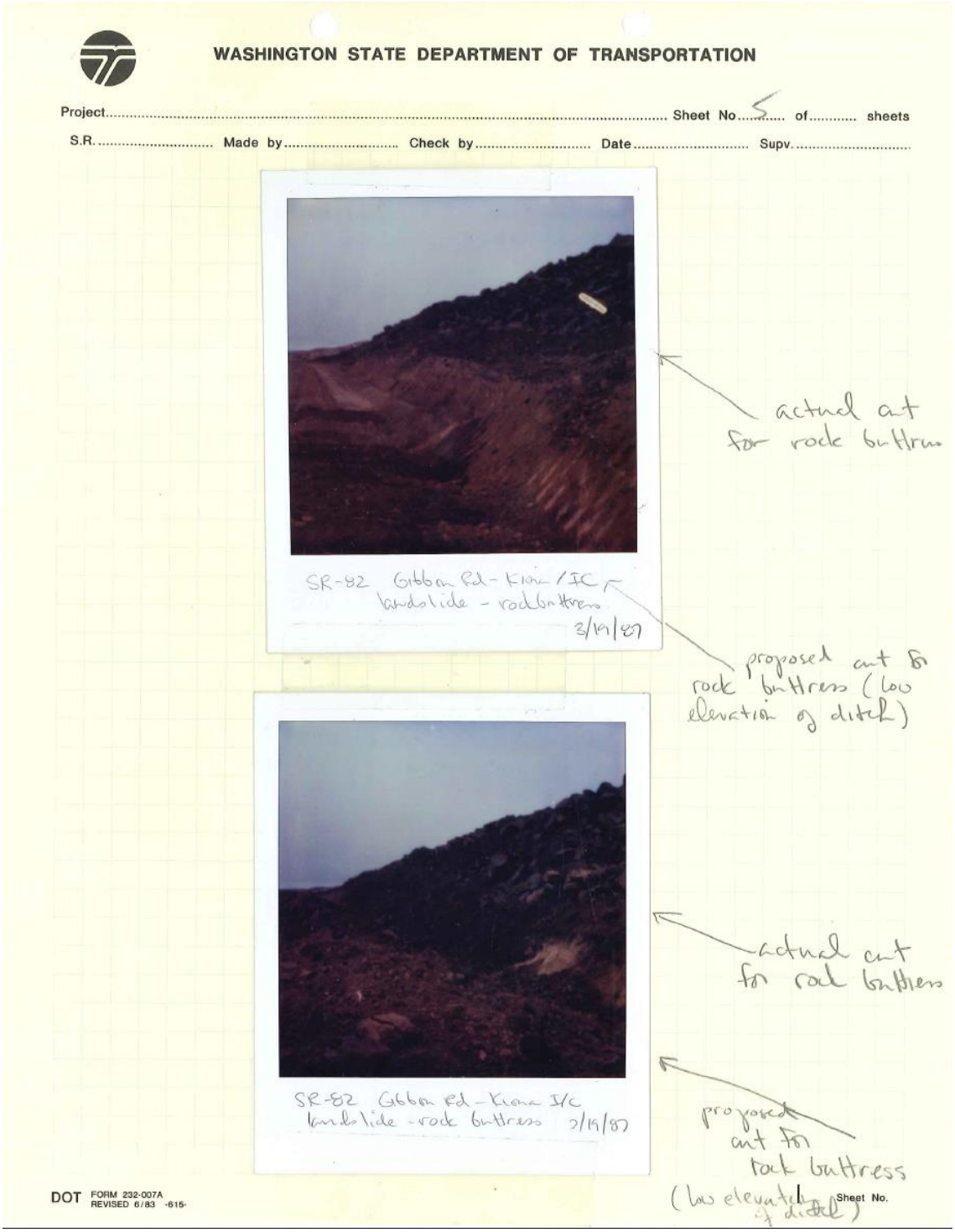

Figure 12: The second page of the March 20, 1987 Jenkins and Lowell memo showing annotated Polaroid photos of the shear-key buttress as it was being constructed. They argue that the buttress was not constructed to the specifications laid out by Todd Harrison. Specifically, in the photos they show that the buttress key is constructed above the planned grade. The buttress was not seated in the cut (ditch) at the bottom of the photos. Image courtesy of WSDOT via the Washington State Archives.

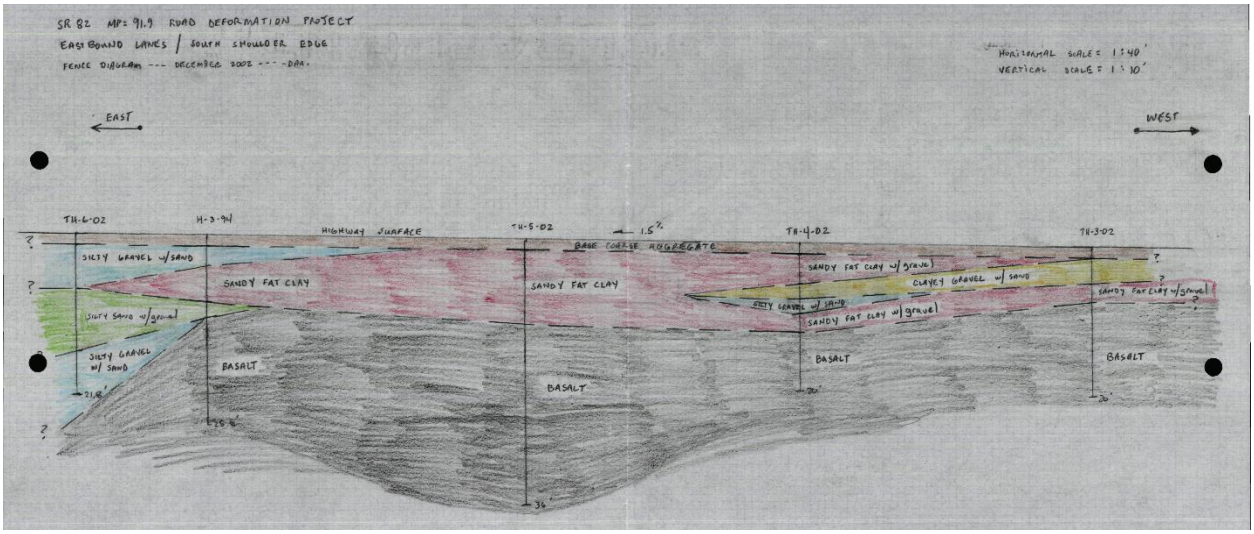

Figure 13: A fence diagram (cross section) of the subsurface of the I-82 eastbound lanes. The fat clay (red) in the middle of the diagram is the unit that has been cause for concern since the 1987 construction. This is the unit that the buttress key is intended to disrupt. The diagram runs longitudinally along I-82. The diagram was created by Doug Anderson in December of 2002. Image courtesy of WSDOT via the Washington State Archives.

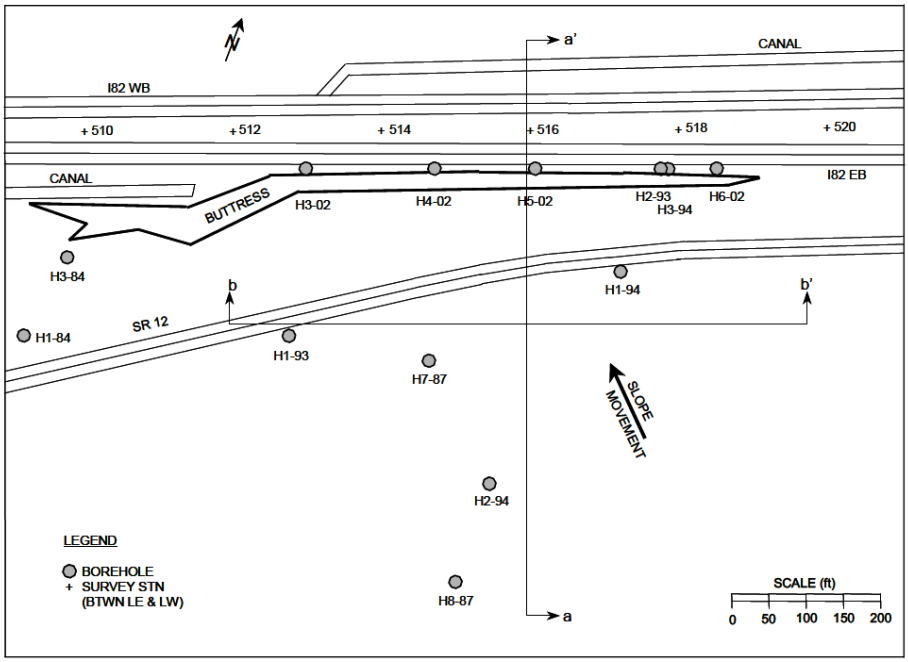

Figure 14: A map of existing boreholes with C-Core's section lines plotted. C-Core has also given a vector direction of mean slope movement. From C-Core (2006) Figure 1.

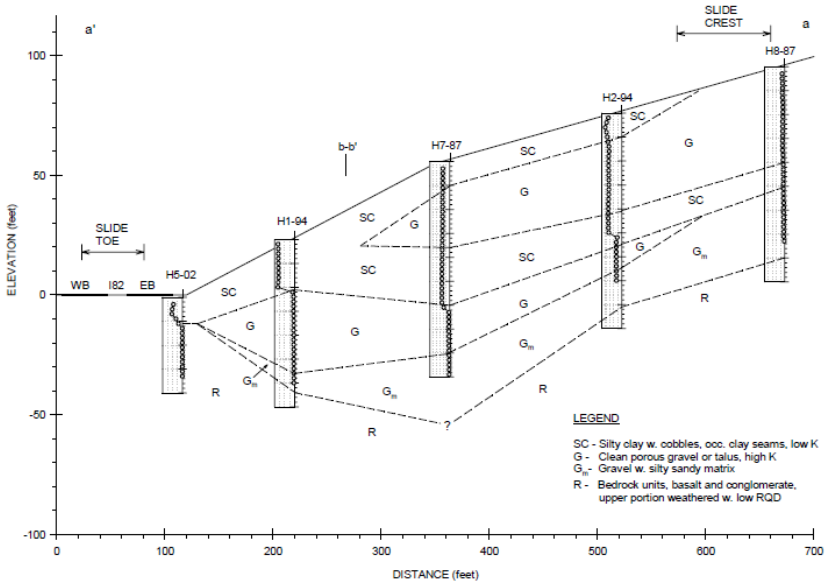

Figure 15: C-Core's cross section which was eventually used in both their limit equilibrium modeling and the finite element modeling. Absolute elevations are not given by C-Core and the buttress has not been incorporated into their model. Slope inclinometer data is superimposed on each borehole. There is a 2:1 vertical exaggeration of the image. From C-Core 2006 Figure 2.

$\bar{B}_{sc}$	Safety Factors			
	Ordinary	Bishop	Janbu	GLE
0	1.361	2.655	2.126	2.212
0.25	0.998	1.993	1.604	1.665
0.50	0.635	1.329	1.078	1.117
0.60	0.490	1.063	0.866	0.897

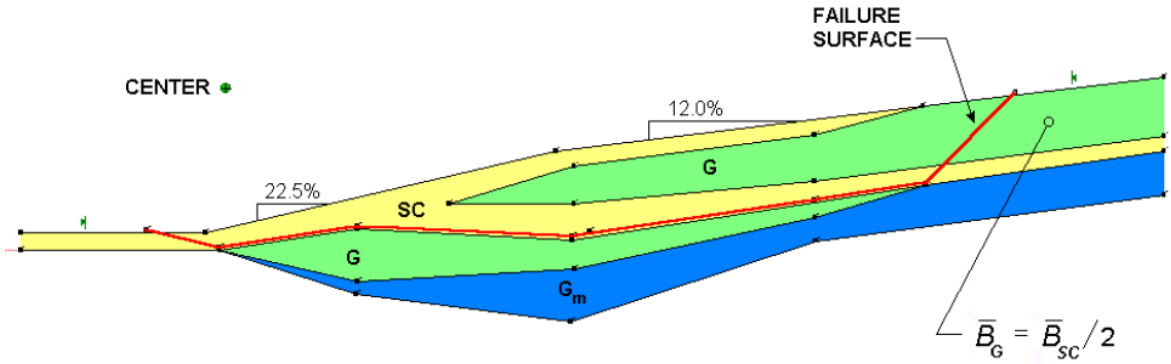

Figure 16: C-Core here hypothesizes that the failure surface follows the interface between the silty clay unit and the lower gravel contact. Gravels (G), silty clays (SC), and gravels-with-matrix (G_m) are modeled). Again, the buttress is not included in the model. No scale is given. From C-Core (2006) Appendix B Figure 2.

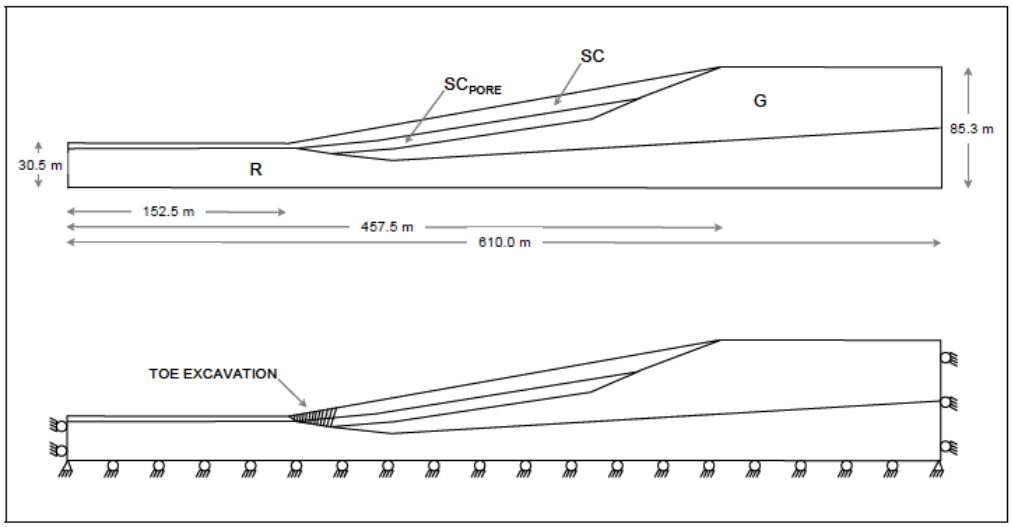

Figure 17: An illistration of the FEM model geometry and limits. The only units modeled are a silty clay unit (SC), a silty clay unit with pore space (SC_{pore}), and gravels (G). From C-Core Appendix B Figure 3.

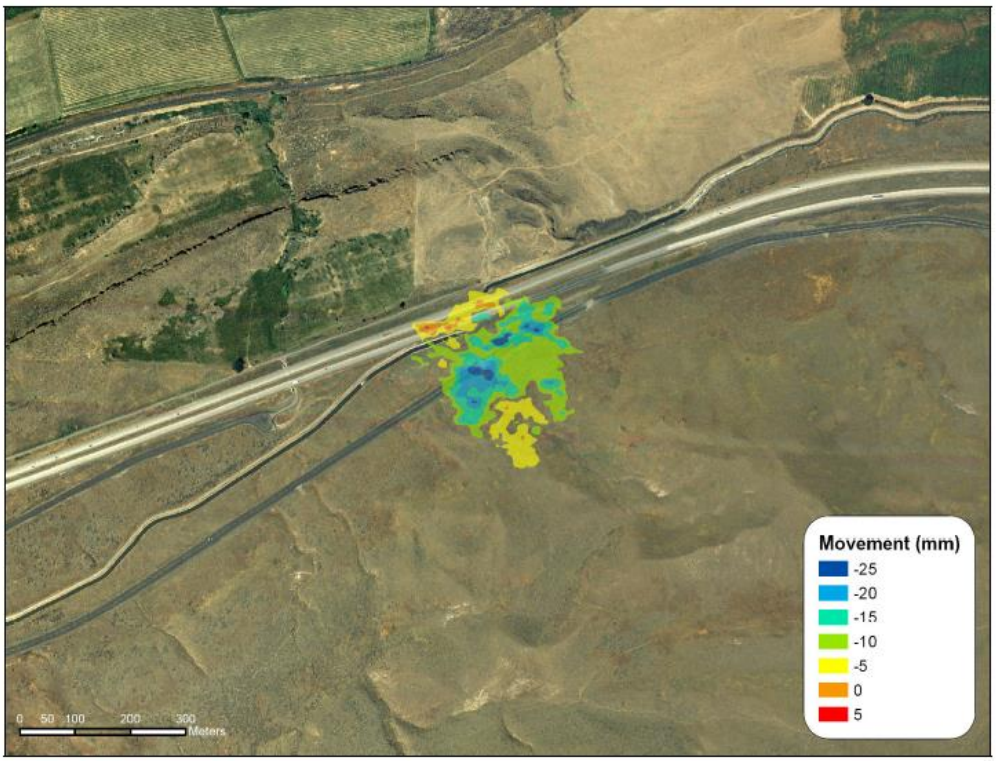

Figure 18: A composite image of the ground movement reported in FHWA (2006). The figure generally shows subsidence in the hillside (blue to yellow) and heave in the roadbed (red). However, the magnitude of the deformation of the roadway this figure is within the 10 mm of error reported in the original FHWA (2006) report. From C-Core (2006) Figure 21.

Figure 19: A photo of the surface of W Yakitat Road showing an open tension crack in the asphaltic concrete pavement. The road was recently (prior to my August 2013 visits) paved with chip seal, seen as the black gravel on top of asphaltic concrete pavement and in the tension crack. This particular crack is located on the edge of the northern shoulder of the westbound lane uphill of the buttress. Scale arrow faces north. The black fields on the scale measure 1.96 inches (5 cm). Photo was taken August 2013.

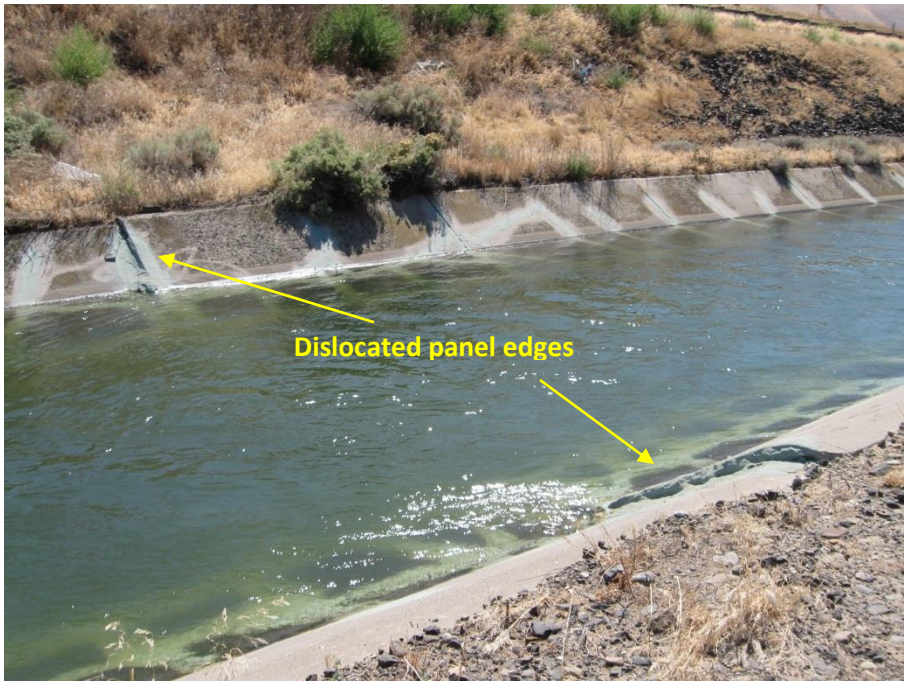

Figure 20: A photo of the KID canal taken during August 2013 showing an unlined section. The panel at the center of the photo has been dislocated from its original position. The KID reported that this was due to frost heave. Canal joints have been sealed with a green substance.

Figure 21: A photo of the silty clay and gravel with matrix contact taken immediately after the split spoon sampler was opened. Sample is D-8 and was taken at a depth of 28 feet from borehole H-101vwp-13.

Figure 22: The contents of the Shelby tube taken at a depth of between 24 feet and 26 feet from borehole H-101vwp-13. I observed as I picked apart the silty clay the material could be easily separated by hand along abundant polished surfaces, especially in material from a depth of around 25 feet. Small metal spatula and Sharpie marker for scale.

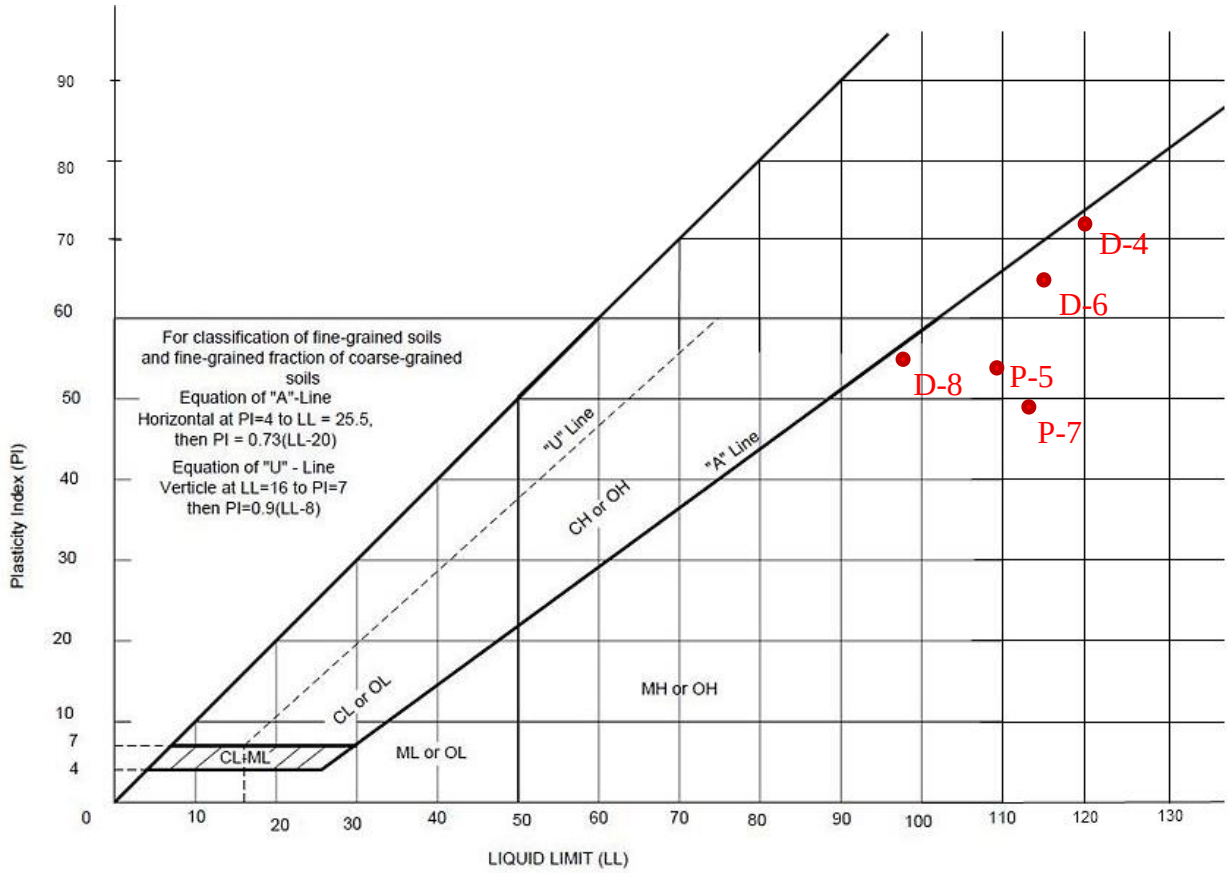

Figure 23: A modified Atterberg limits chart from ASTM D2487 – 11 showing recent materials testing results of samples retrieved from the Prosser Landslide in 2013 by WSDOT. The limits of the chart have been extended to accommodate the high liquid limits and plasticity indices of the sample. Despite having very high liquid limits, the soils fall into the elastic silt (MH) field. Sample labels correspond to samples reported in Appendix B.

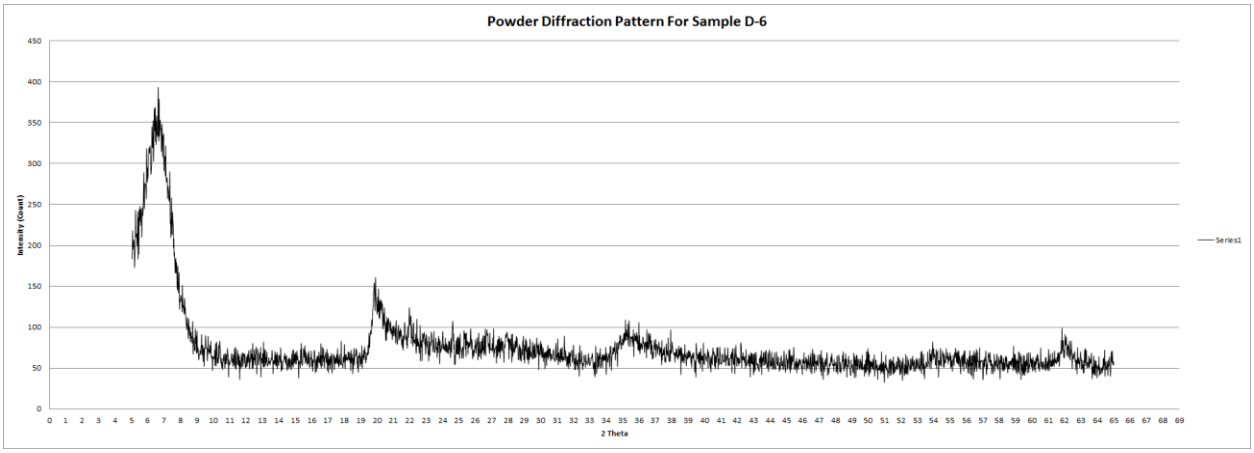

Figure 24: The powder XRD peak distribution pattern for the D-6 sample taken from borehole H-101vwp-13. The first low angle peak is between 6º and 7º 2θ, followed by peaks at 20º 2θ and 35º 2θ. Finally, there is a high angle peak at 62º 2θ.

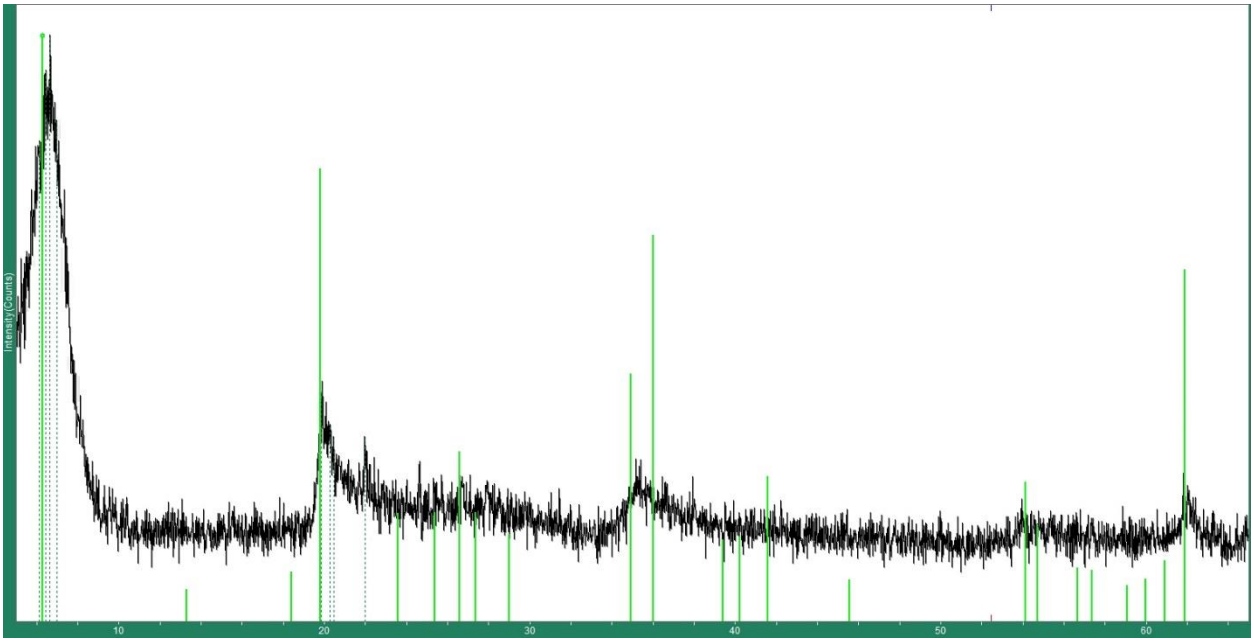

Figure 25: Major and minor peaks from Montmorillonite PDF 00-060-0318 are superimposed on the powder sample peak pattern. Matches with major peaks, such as the low angle 2θ peak can be made. Image exported from MDI Jade.

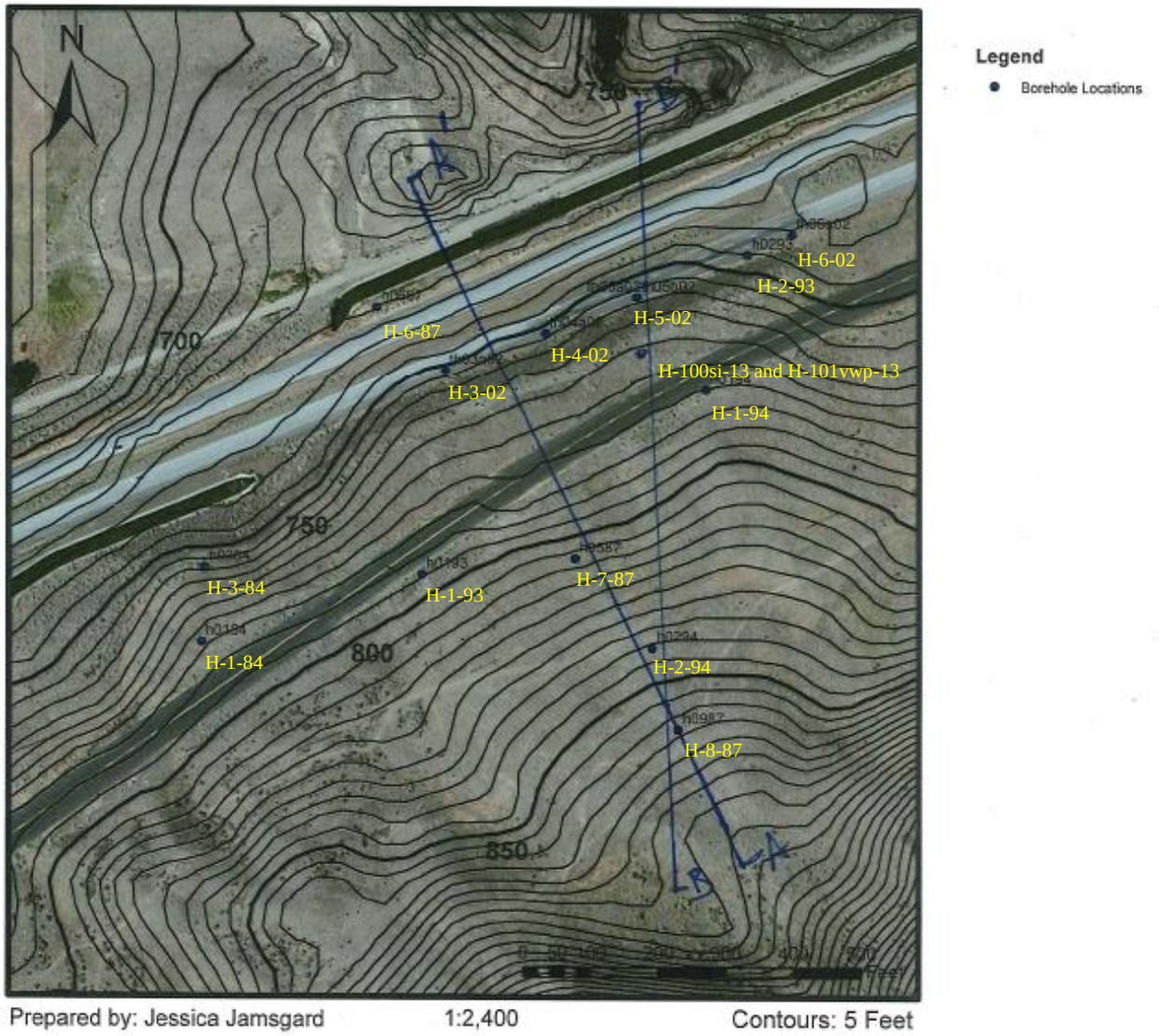

Figure 26: A map of the Prosser Landslide with section lines. Topographic contours are in 5-foot intervals. Index contours are given every 50 feet. Borehole locations are represented with blue dots. Section lines were drawn by Tom Badger based upon his professional discretion. The location of Section A – A' was chosen because it is the steepest downhill gradient, extends through a large portion of the uphill slide mass, and is perpendicular to the buttress. The location of Section B – B' was chosen because it intersects new drilling while capturing the upslope boreholes, and intersects the eastern side of the buttress where deformation of the road is occurring. Topographic contours were made by processing a USGS 10-meter DEM for the Corral Canyon Quadrangle (USGS, 1998). I processed the DEM data in Esri ArcGIS (Esri, 2013). This image was made using Esri ArcGIS with Ersi's basemap satellite imagery.

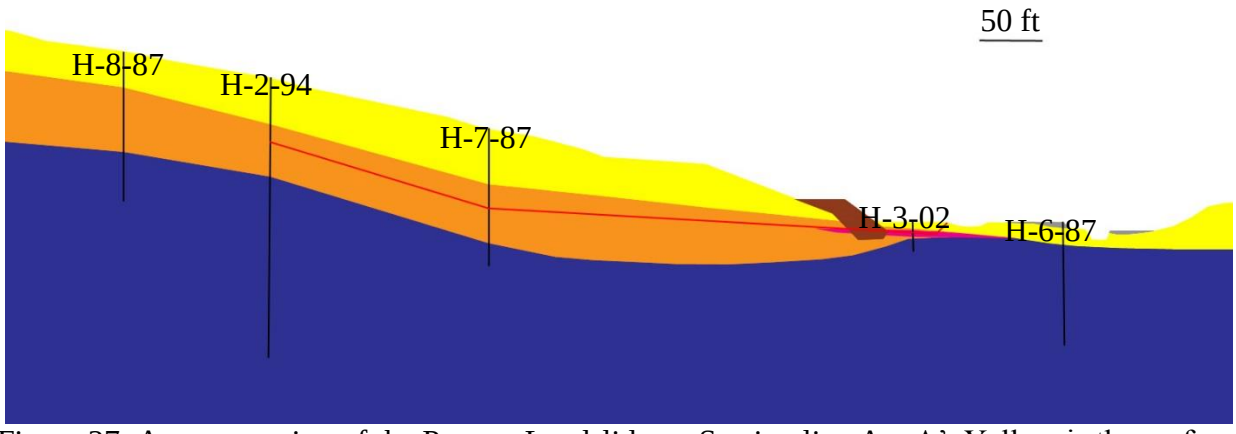

Figure 27: A cross section of the Prosser Landslide on Section line A – A'. Yellow is the surface landslide debris. This cross section was made by interpolating between boreholes located near the section lines drawn in Figure 26. Orange is the gravels-with-matrix unit. Pink is the weak silty clay. Blue is basalt. Reddish brown is the buttress. Gray is artificial fill. Black vertical lines are boreholes. A red line defines a possible failure plane based on inclinometer data. Notice that the silty clay unit is likely quite small. No vertical exaggeration. I drew the original sections by hand then digitized them for clarity.

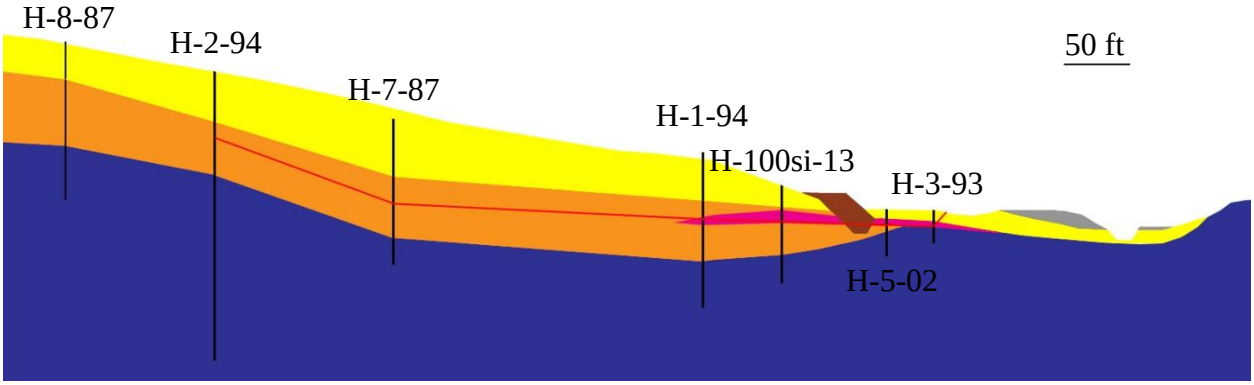

Figure 28: A cross section of the Prosser Landslide on Section line B – B'. This cross section was made by interpolating between boreholes located near the section lines drawn in Figure 26. Yellow is the surface landslide debris. Orange is the gravels-with-matrix unit. Pink is the weak silty clay. Blue is basalt. Reddish brown is the buttress. Gray is artificial fill. Black vertical lines are boreholes. A red line defines a possible failure plane based on inclinometer data. Notice that the silty clay is much larger in this section than A – A'. No vertical exaggeration. I drew the original sections by hand then digitized them for clarity.

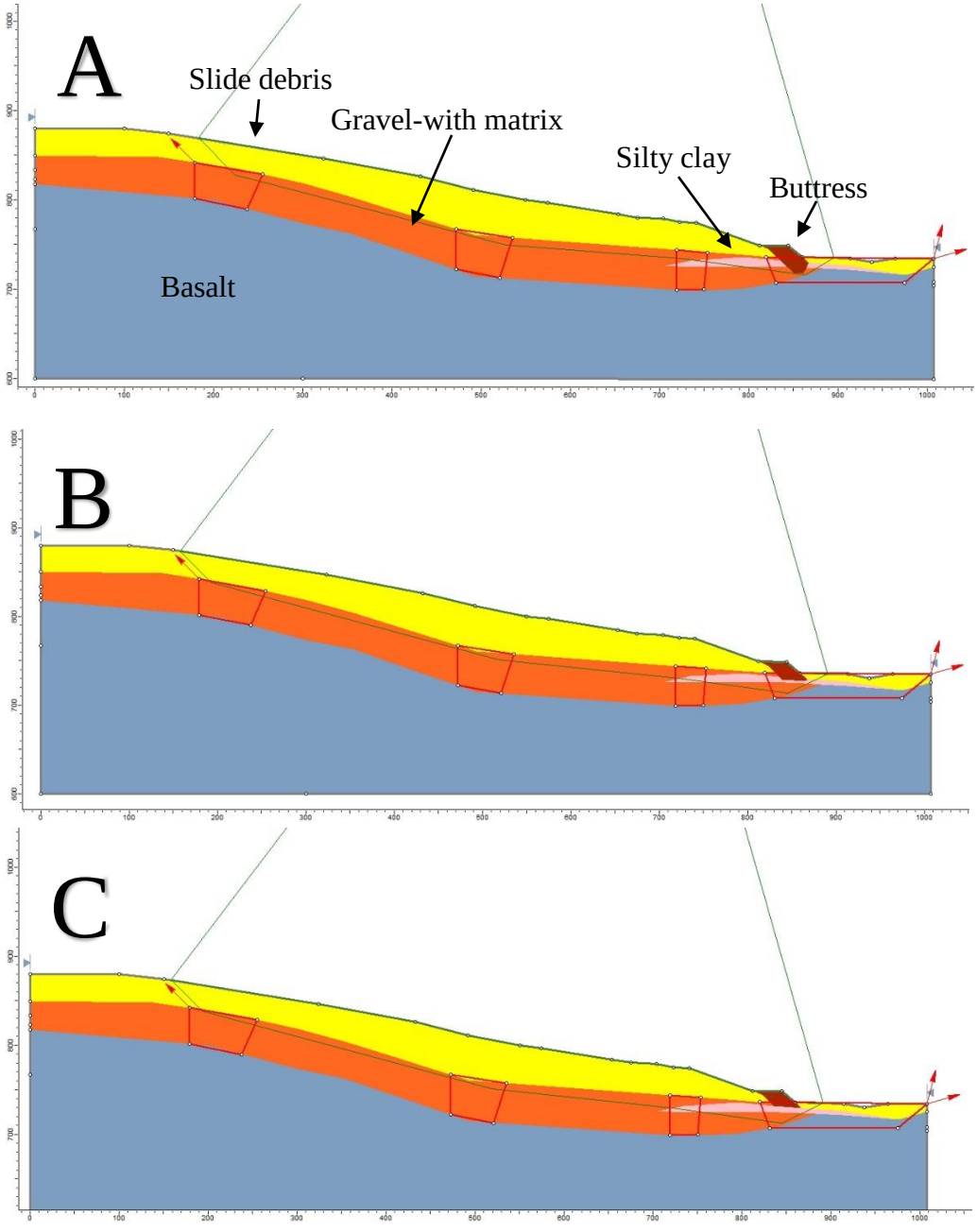

Figure 29: Three images exported from Rocscience Slide showing the modeled failure plane (green line) for the large landslide scenario. The green lines ascending from the cross section point to the Factor of Safety associated with the modeled failure plane. The upper cloud of Factor of Safety points the lines point into has been cut off in order to show the cross section with better clarity. Yellow is the surface landslide debris. Orange is the gravels-with-matrix unit. Pink is the weak silty clay. Blue is basalt. Reddish brown is the buttress. The red boxes are the windows through which the software searches to find a viable failure plane. "A" depicts the large landslide with a fully keyed buttress. "B" depicts a buttress which is keyed halfway into the silty clay unit. "C" Depicts a buttress where the buttress key is absent and the buttress simply rests on top of the clay. The material properties for the units depicted here are the same as in the model run described by Appendix D: Table 1.

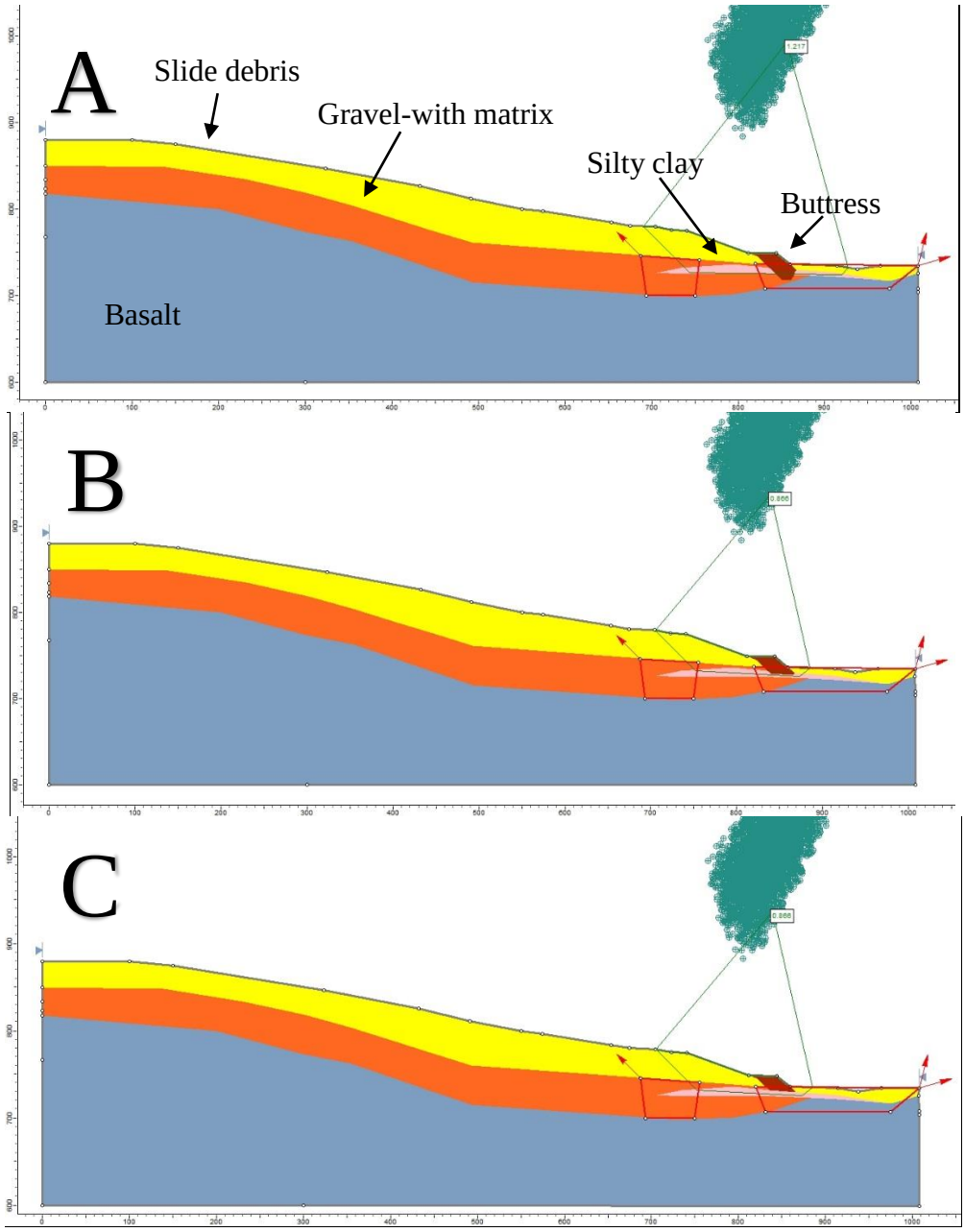

Figure 30: Three images exported from Rocscience Slide showing the modeled failure plane (green line) for the small landslide scenario. The green lines ascending from the cross section point to the Factor of Safety associated with the modeled failure plane. The cloud of points is the Factors of Safety for the 5000 modeled failure planes. The upper cloud of Factor of Safety points the lines point into has been cut off in order to show the cross section with better clarity. Yellow is the surface landslide debris. Orange is the gravels-with-matrix unit. Pink is the weak silty clay. Blue is basalt. Reddish brown is the buttress. The red boxes are the windows through which the software searches to find a viable failure plane. "A" depicts the large landslide with a fully keyed buttress. "B" depicts a buttress which is keyed halfway into the silty clay unit. "C" Depicts a buttress where the buttress key is absent and the buttress simply rests on top of the clay. The material properties for the units depicted here are the same as in the model run described by Appendix D: Table 8.

Appendix A
Drill Logs

Drill logs in this section were produced by WSDOT after drilling was completed during the summer of 2013. The logs are drafts only. WSDOT has not published official drill logs at this writing. Historic drill logs can be obtained by request from WSDOT or found within Annex A of C-Core (2006).

Washington State Department of Transportation

LOG OF TEST BORING

Start Card RE-08861
HOLE No. H-100si-13
Sheet 1 of 4

Job No. MT-0472 gp07 SR 082 Elevation No data

Project I-82 Prosser Landslide Area Vic. MP92 Driller Shepherd, Robert Lic# 2710

Component Inspector Fetterly, Jamie #2507

Start August 20, 2013 Completion August 21, 2013 Well ID# BHM-880 Equipment CME 850 (9C2-3)

Station Offset Hole Dia (inches) 6 Historical SPT Efficiency Past Rig Efficiency 86.9%

Northing Easting Collected by HQ Geotech Office Method Wet Rotary

Lat Long Datum NAD 83/91 HARN, NAVD88, SPS (ft) Drill Fluid Polymer

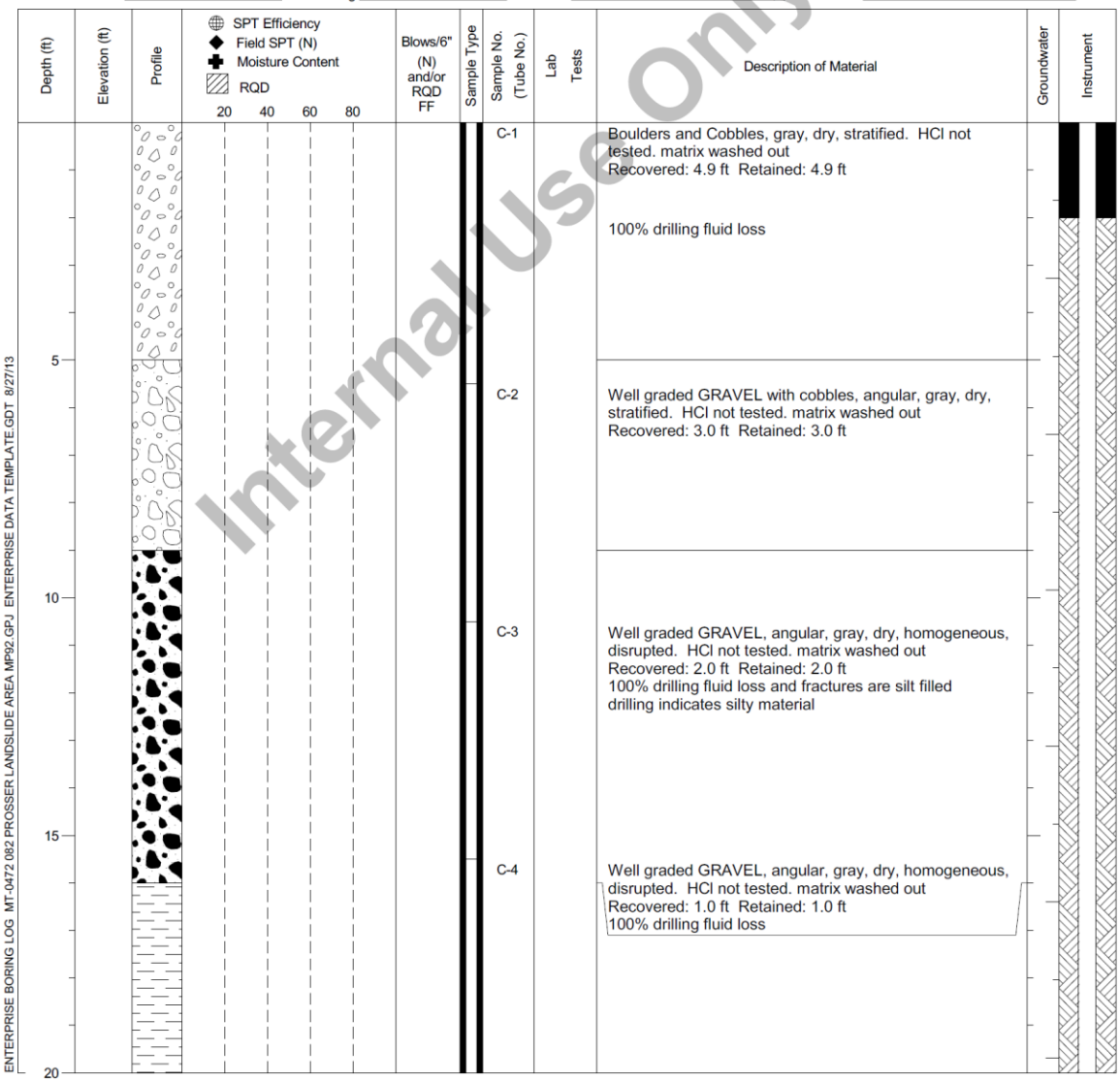

ENTERPRISE BORING LOG MT-0472 082 PROSSER LANDSLIDE AREA MP92.GPJ ENTERPRISE DATA TEMPLATE.GDT 8/27/13

Washington State Department of Transportation

LOG OF TEST BORING

Job No. MT-0472 gp07 SR 082 Elevation No data HOLE No. H-100si-13

Sheet 2 of 4

Project I-82 Prosser Landslide Area Vic. MP92 Driller Shepherd, Robert

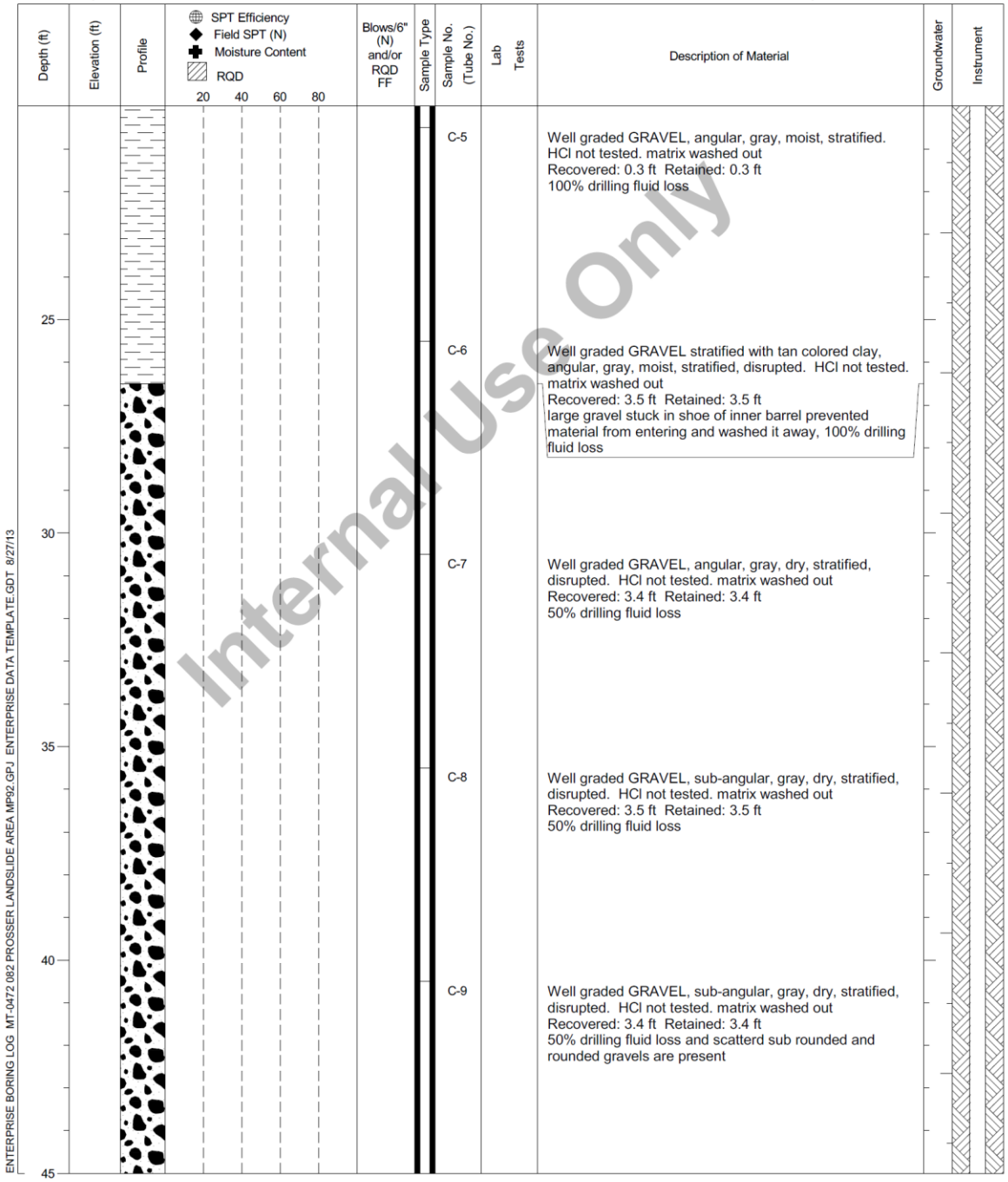

ENTERPRISE BORING LOG MT-0472 082 PROSSER LANDSLIDE AREA MP92.GPJ ENTERPRISE DATA TEMPLATE.GDT 8/27/13

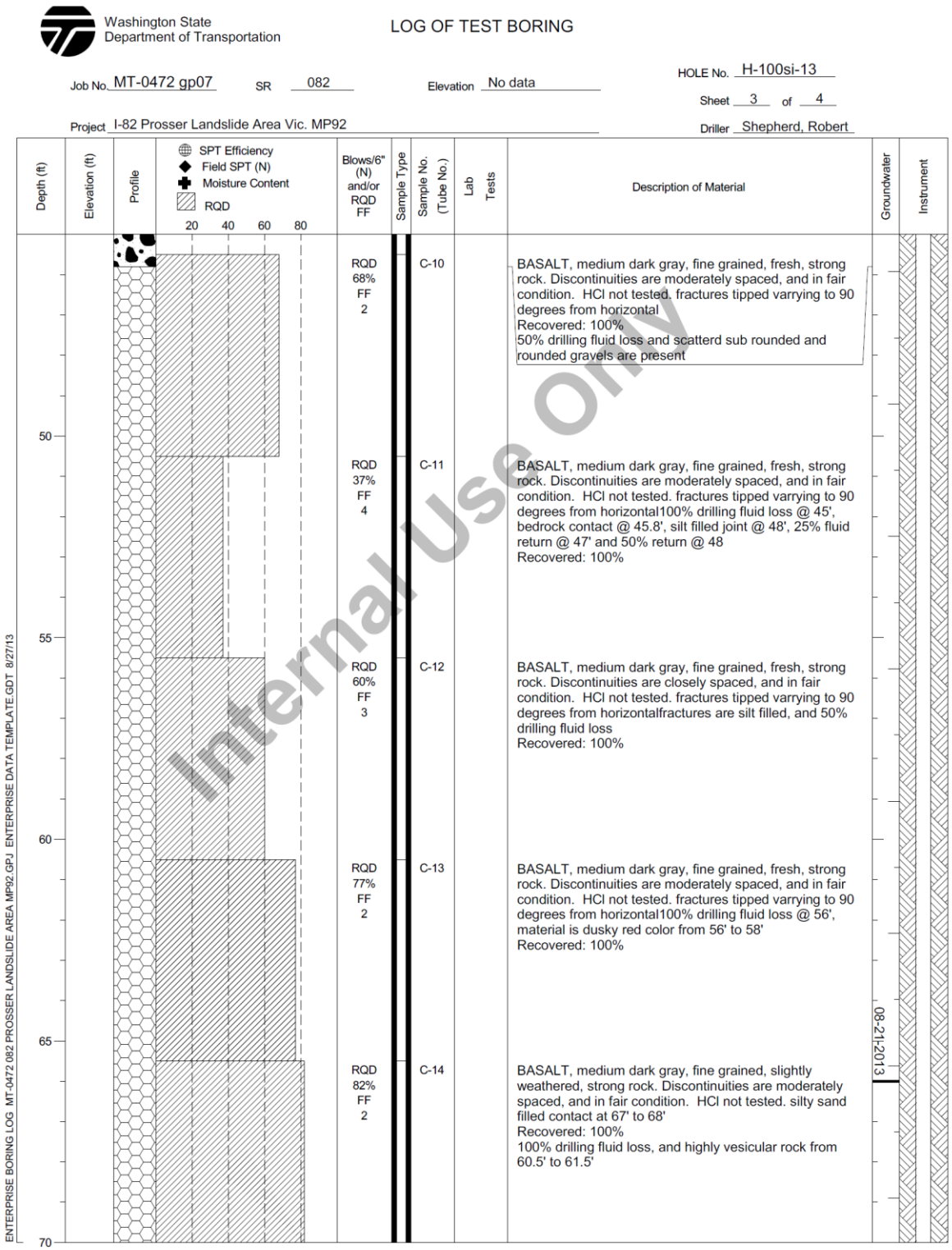
Washington State
Department of Transportation
LOG OF TEST BORING
Job No. MT-0472 gp07
SR 082
Elevation No data
HOLE No. H-100si-13
Sheet 3 of 4
Project I-82 Prosser Landslide Area Vic. MP92
Driller Shepherd, Robert
Depth (ft)
Elevation (ft)
Profile
SPT Efficiency
Field SPT (N)
Moisture Content
RQD
20 40 60 80
Blows/6" (N) and/or RQD FF
Sample Type
Sample No. (Tube No.)
Lab Tests
Description of Material
Groundwater
Instrument
RQD 68% FF 2
C-10
BASALT, medium dark gray, fine grained, fresh, strong rock. Discontinuities are moderately spaced, and in fair condition. HCl not tested. fractures tipped varrying to 90 degrees from horizontal
Recovered: 100%
50% drilling fluid loss and scatterd sub rounded and rounded gravels are present
50
RQD 37% FF 4
C-11
BASALT, medium dark gray, fine grained, fresh, strong rock. Discontinuities are moderately spaced, and in fair condition. HCl not tested. fractures tipped varrying to 90 degrees from horizontal100% drilling fluid loss @ 45', bedrock contact @ 45.8', silt filled joint @ 48', 25% fluid return @ 47' and 50% return @ 48
Recovered: 100%
55
RQD 60% FF 3
C-12
BASALT, medium dark gray, fine grained, fresh, strong rock. Discontinuities are closely spaced, and in fair condition. HCl not tested. fractures tipped varrying to 90 degrees from horizontalfractures are silt filled, and 50% drilling fluid loss
Recovered: 100%
60
RQD 77% FF 2
C-13
BASALT, medium dark gray, fine grained, fresh, strong rock. Discontinuities are moderately spaced, and in fair condition. HCl not tested. fractures tipped varrying to 90 degrees from horizontal100% drilling fluid loss @ 56', material is dusky red color from 56' to 58'
Recovered: 100%
65
08-21-2013
RQD 82% FF 2
C-14
BASALT, medium dark gray, fine grained, slightly weathered, strong rock. Discontinuities are moderately spaced, and in fair condition. HCl not tested. silty sand filled contact at 67' to 68'
Recovered: 100%
100% drilling fluid loss, and highly vesicular rock from 60.5' to 61.5'
70
ENTERPRISE BORING LOG MT-0472 082 PROSSER LANDSLIDE AREA MP92.GPJ ENTERPRISE DATA TEMPLATE.GDT 8/27/13
Internal Use Only

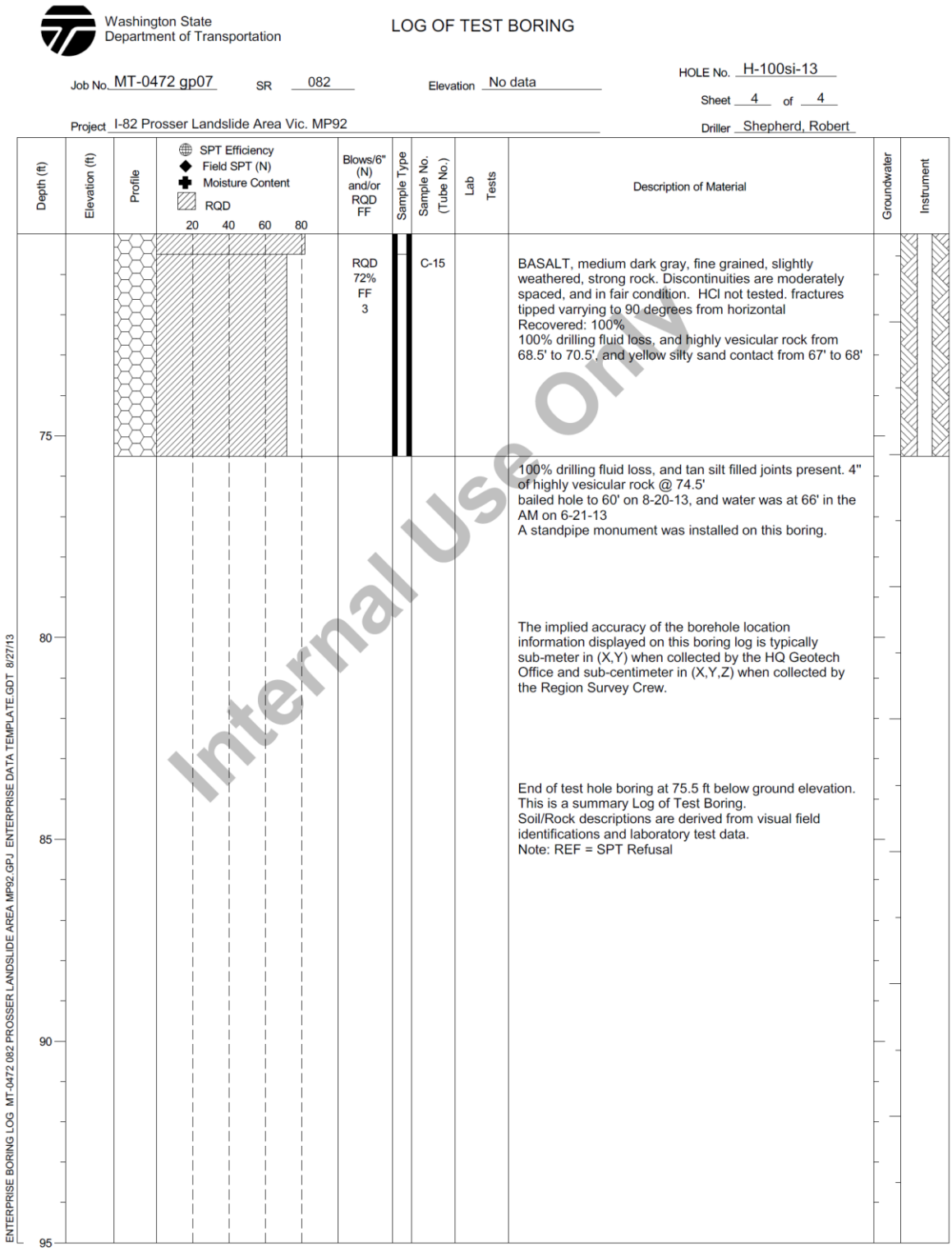
Washington State
Department of Transportation
LOG OF TEST BORING
Job No. MT-0472 gp07
SR 082
Elevation No data
HOLE No. H-100si-13
Sheet 4 of 4
Project I-82 Prosser Landslide Area Vic. MP92
Driller Shepherd, Robert
Depth (ft)
Elevation (ft)
Profile
SPT Efficiency
Field SPT (N)
Moisture Content
RQD
20 40 60 80
Blows/6" (N) and/or RQD FF
Sample Type
Sample No. (Tube No.)
Lab Tests
Description of Material
Groundwater
Instrument
RQD
72%
FF
3
C-15
BASALT, medium dark gray, fine grained, slightly weathered, strong rock. Discontinuities are moderately spaced, and in fair condition. HCl not tested. fractures tipped varrying to 90 degrees from horizontal
Recovered: 100%
100% drilling fluid loss, and highly vesicular rock from 68.5' to 70.5', and yellow silty sand contact from 67' to 68'
100% drilling fluid loss, and tan silt filled joints present. 4" of highly vesicular rock @ 74.5'
bailed hole to 60' on 8-20-13, and water was at 66' in the AM on 6-21-13
A standpipe monument was installed on this boring.
The implied accuracy of the borehole location information displayed on this boring log is typically sub-meter in (X,Y) when collected by the HQ Geotech Office and sub-centimeter in (X,Y,Z) when collected by the Region Survey Crew.
End of test hole boring at 75.5 ft below ground elevation.
This is a summary Log of Test Boring.
Soil/Rock descriptions are derived from visual field identifications and laboratory test data.
Note: REF = SPT Refusal
75
80
85
90
95
ENTERPRISE BORING LOG MT-0472 082 PROSSER LANDSLIDE AREA MP92.GPJ ENTERPRISE DATA TEMPLATE.GDT 8/27/13
Internal Use Only

Washington State Department of Transportation

LOG OF TEST BORING

Start Card RE-08861

Job No. MT-0472 gp07 SR 082 Elevation No data

HOLE No. H-101vwp-13

Sheet 1 of 3

Project I-82 Prosser Landslide Area Vic. MP92

Driller Shepherd, Robert Lic# 2710

Component

Inspector Fetterly, Jamie #2507

Start August 21, 2013 Completion August 21, 2013 Well ID# BHM-881

Equipment CME 850 (9C2-3)

Station Offset Hole Dia (inches) 6

Historical SPT Efficiency Past Rig Efficiency 86.9%

Northing Easting Collected by HQ Geotech Office

Method Wet Rotary

Lat Long Datum NAD 83/91 HARN, NAVD88, SPS (ft)

Drill Fluid Polymer

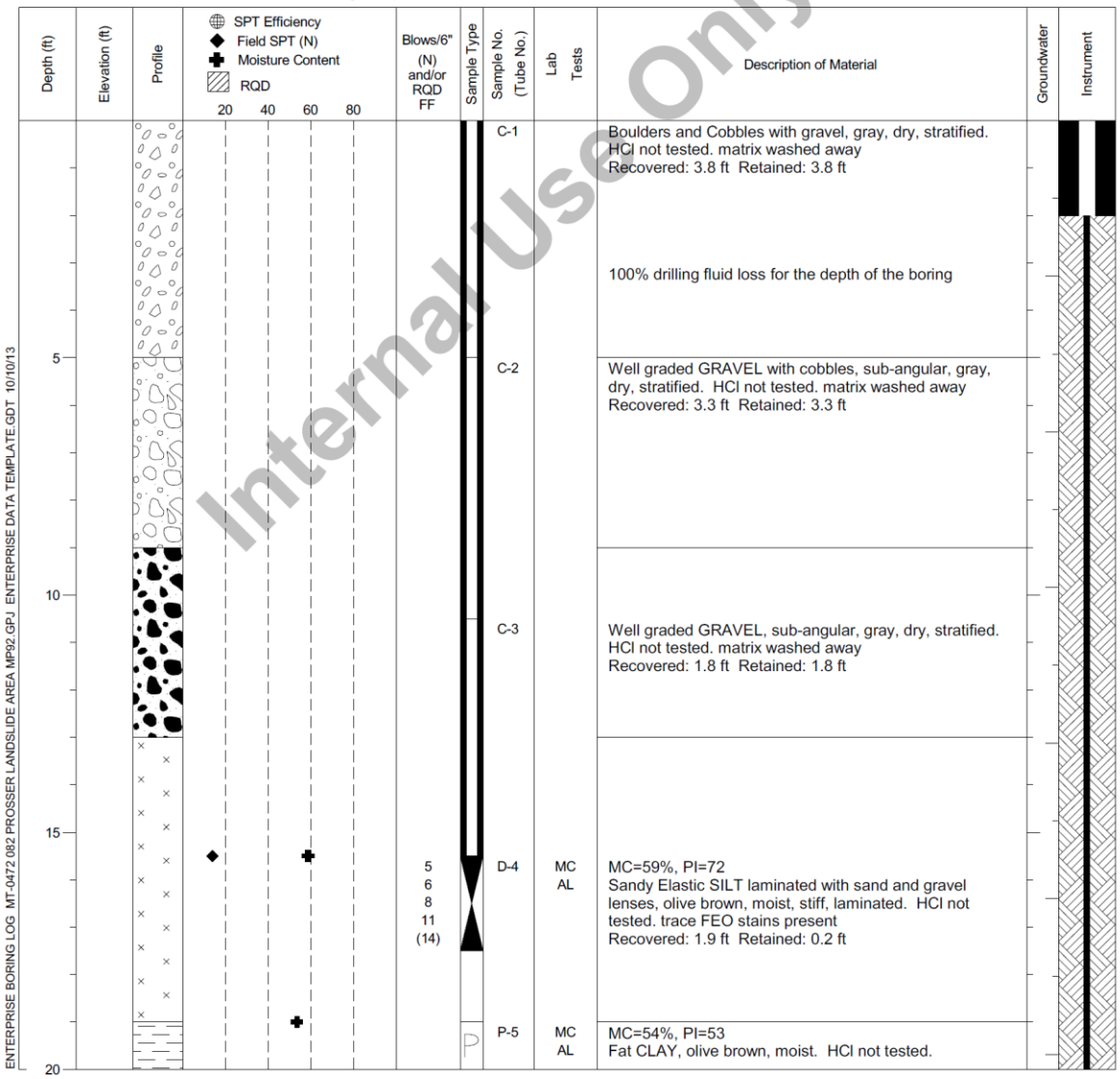

ENTERPRISE BORING LOG MT-0472 082 PROSSER LANDSLIDE AREA MP92.GPJ ENTERPRISE DATA TEMPLATE.GDT 10/10/13

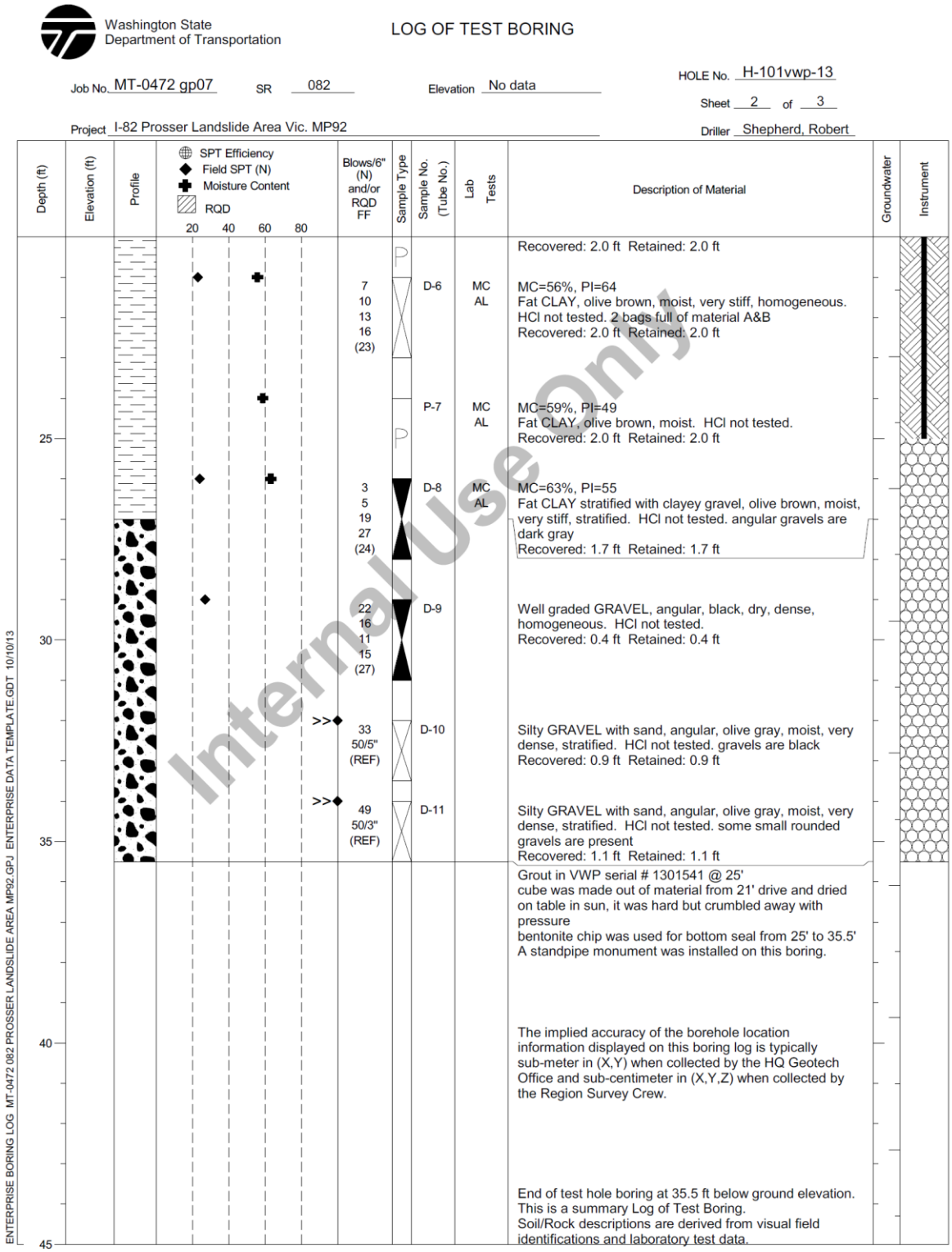
Washington State Department of Transportation
LOG OF TEST BORING
Job No. MT-0472 gp07
SR 082
Elevation No data
HOLE No. H-101vwp-13
Sheet 2 of 3
Project I-82 Prosser Landslide Area Vic. MP92
Driller Shepherd, Robert
Depth (ft)
Elevation (ft)
Profile
SPT Efficiency
Field SPT (N)
Moisture Content
RQD
20 40 60 80
Blows/6" (N) and/or RQD FF
Sample Type
Sample No. (Tube No.)
Lab Tests
Description of Material
Groundwater
Instrument
Recovered: 2.0 ft Retained: 2.0 ft
7 10 13 16 (23) D-6 MC AL
MC=56%, PI=64
Fat CLAY, olive brown, moist, very stiff, homogeneous.
HCl not tested. 2 bags full of material A&B
Recovered: 2.0 ft Retained: 2.0 ft
P-7 MC AL
MC=59%, PI=49
Fat CLAY, olive brown, moist. HCl not tested.
Recovered: 2.0 ft Retained: 2.0 ft
25
3 5 19 27 (24) D-8 MC AL
MC=63%, PI=55
Fat CLAY stratified with clayey gravel, olive brown, moist, very stiff, stratified. HCl not tested. angular gravels are dark gray
Recovered: 1.7 ft Retained: 1.7 ft
22 16 11 15 (27) D-9
Well graded GRAVEL, angular, black, dry, dense, homogeneous. HCl not tested.
Recovered: 0.4 ft Retained: 0.4 ft
30
>> 33 50/5" (REF) D-10
Silty GRAVEL with sand, angular, olive gray, moist, very dense, stratified. HCl not tested. gravels are black
Recovered: 0.9 ft Retained: 0.9 ft
>> 49 50/3" (REF) D-11
Silty GRAVEL with sand, angular, olive gray, moist, very dense, stratified. HCl not tested. some small rounded gravels are present
Recovered: 1.1 ft Retained: 1.1 ft
35
Grout in VWP serial # 1301541 @ 25'
cube was made out of material from 21' drive and dried on table in sun, it was hard but crumbled away with pressure
bentonite chip was used for bottom seal from 25' to 35.5'
A standpipe monument was installed on this boring.
40
The implied accuracy of the borehole location information displayed on this boring log is typically sub-meter in (X,Y) when collected by the HQ Geotech Office and sub-centimeter in (X,Y,Z) when collected by the Region Survey Crew.
End of test hole boring at 35.5 ft below ground elevation.
This is a summary Log of Test Boring.
Soil/Rock descriptions are derived from visual field identifications and laboratory test data.
45
Internal Use Only
ENTERPRISE BORING LOG MT-0472 082 PROSSER LANDSLIDE AREA MP92.GPJ ENTERPRISE DATA TEMPLATE.GDT 10/10/13

Washington State Department of Transportation

LOG OF TEST BORING

Job No. MT-0472 gp07 SR 082 Elevation No data HOLE No. H-101vwp-13

Sheet 3 of 3

Project I-82 Prosser Landslide Area Vic. MP92 Driller Shepherd, Robert

Depth (ft)	Elevation (ft)	Profile	SPT Efficiency / Field SPT (N) / Moisture Content / RQD (20 40 60 80)	Blows/6" (N) and/or RQD FF	Sample Type	Sample No. (Tube No.)	Lab Tests	Description of Material	Groundwater	Instrument
								Note: REF = SPT Refusal		
50										
55										
60										
65										
70										

ENTERPRISE BORING LOG MT-0472 082 PROSSER LANDSLIDE AREA MP92.GPJ ENTERPRISE DATA TEMPLATE.GDT 10/10/13

Appendix B

Atterberg Limit and Shear Ring Testing Results

Testing results in this section were produced by WSDOT after drilling was completed during the summer of 2013. Test results are drafts only. WSDOT has not published official test results at this writing.

Job No. **MT-0472 gp07** Date **October 17, 2013**

Hole No. **H-101vwp-13** Sheet **1**

Project **I-82 Prosser Landslide Area Vic. MP92**

Laboratory Summary

Washington State Department of Transportation

	Depth (ft)	Sample No.	USCS	Description	MC%	LL	PL	PI	Moist Density (lbs/ft³)	Specific Gravity	Gravel (%)	Sand (%)	Fines (%)	Cc	Cu	D60	D50	D30	D20	D10
●	15.5	D-4		MC & AL Only	59	121	49	72												
■	19.0	P-5		MC & AL Only	54	109	56	53												
▲	21.0	D-6	MH	ELASTIC SILT	68	115	51	64		2.79	0.0	0.4	99.6			0.002	0.00	0.00		
★	24.0	P-7		MC & AL Only	59	113	64	49												
⊙	26.0	D-8		MC & AL Only	63	97	42	55												

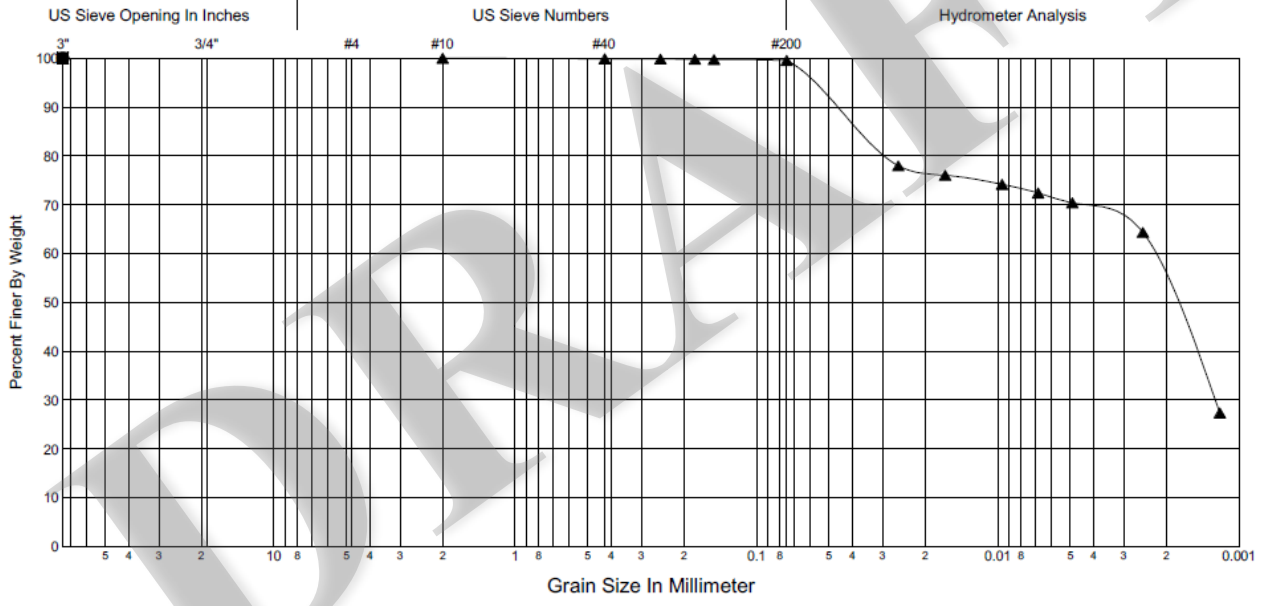

Ring Shear Test Report (ASTM D6467-06a)

Washington State Department of Transportation Geotechnical Division

PROJECT INFORMATION			
Project	Prosser vic. Road Deformation		
Location	SR 82 MP 91.9		
Project Manager	Tom Badger	Sample Number	D-6-A
Project Number	MT-0472	Depth	21' - 23'
Boring Number	H-101vwp-13	Sample Type	Remolded
Description	MH Elastic SILT		

	Specimen			
INITIAL	**A**	**B**	**C**	**D**
Specimen Thickness (in)	0.200	0.200	0.200	0.200
Internal Ring Radius(in)	1.375	1.375	1.375	1.375
External Ring Radius(in)	1.970	1.970	1.970	1.970
Moisture Content (%)	103.0	103.0	103.0	103.0
SHEAR	**A**	**B**	**C**	**D**
Rate of Linear Displacement (in/min)	0.0007	0.0007	0.0007	0.0007
Rate of Angular Displacement (Deg/min)	0.0240	0.0240	0.0240	0.0240
Normal Stress (psi)	7.3	14.3	28.3	42.3
Residual Shear Stress (psi)	0.584	2.100	2.801	6.099
Linear Displacement (in)	0.084	0.028	0.028	0.084
Angular Displacement (Deg)	2.9	1.0	1.0	2.9
FINAL	**A**	**B**	**C**	**D**
Final Moisture Content (%)	80.0	80.0	80.0	80.0
Assumed Cohesion (psi)	0.0	0.0	0.0	0.0
Liquid limit	115.0	115.0	115.0	115.0
Plastic Limit	51.0	51.0	51.0	51.0
Plasticity Index	64.0	64.0	64.0	64.0
Specific Gravity	2.67	2.67	2.67	2.67
Angle of Residual Shear Resistance (Deg)	**7.4**			

COMMENT/REMARKS

In-situ M/C = 69%, Test run at 90% of LL

Tested By	LHB/SW	Date	9/23/2013
Checked By	RDG	Date	10/28/2013

Ring Shear Test Report (ASTM D6467-06a)

Washington State Department of Transportation Geotechnical Division

PROJECT INFORMATION			
Project	Prosser vic. Road Deformation		
Location	SR 82 MP 91.9		
Project Manager	Tom Badger	Sample Number	D-6-A
Project Number	MT-0472	Depth	21' - 23'
Boring Number	H-101vwp-13	Sample Type	Remolded
Description	MH Elastic SILT		

FINAL GRAPHS (1 of 3)

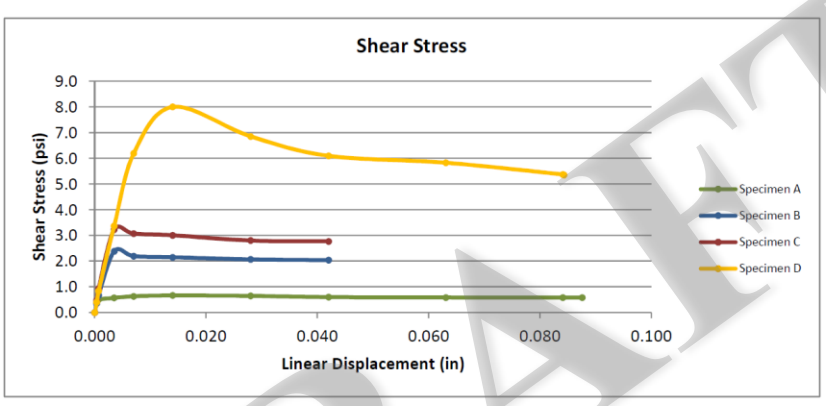

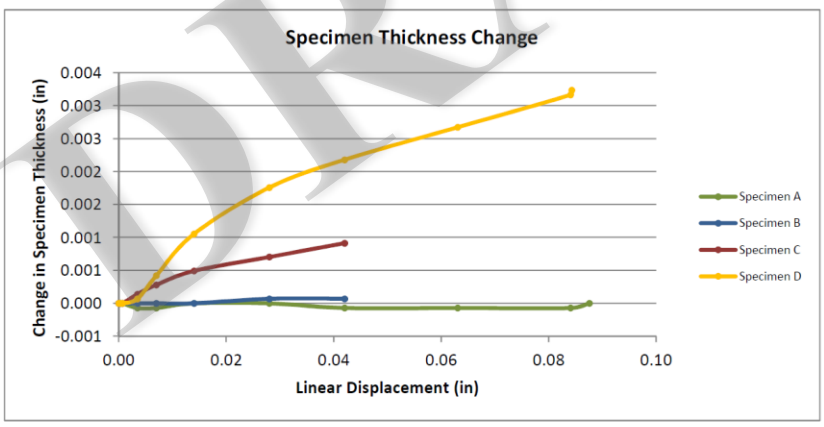

Ring Shear Report (2 of 4)

Ring Shear Test Report (ASTM D6467-06a)

Washington State Department of Transportation Geotechnical Division

PROJECT INFORMATION			
Project	Prosser vic. Road Deformation		
Location	SR 82 MP 91.9		
Project Manager	Tom Badger	Sample Number	D-6-A
Project Number	MT-0472	Depth	21' - 23'
Boring Number	H-101vwp-13	Sample Type	Remolded
Description	MH Elastic SILT		

FINAL GRAPHS (2 of 3)

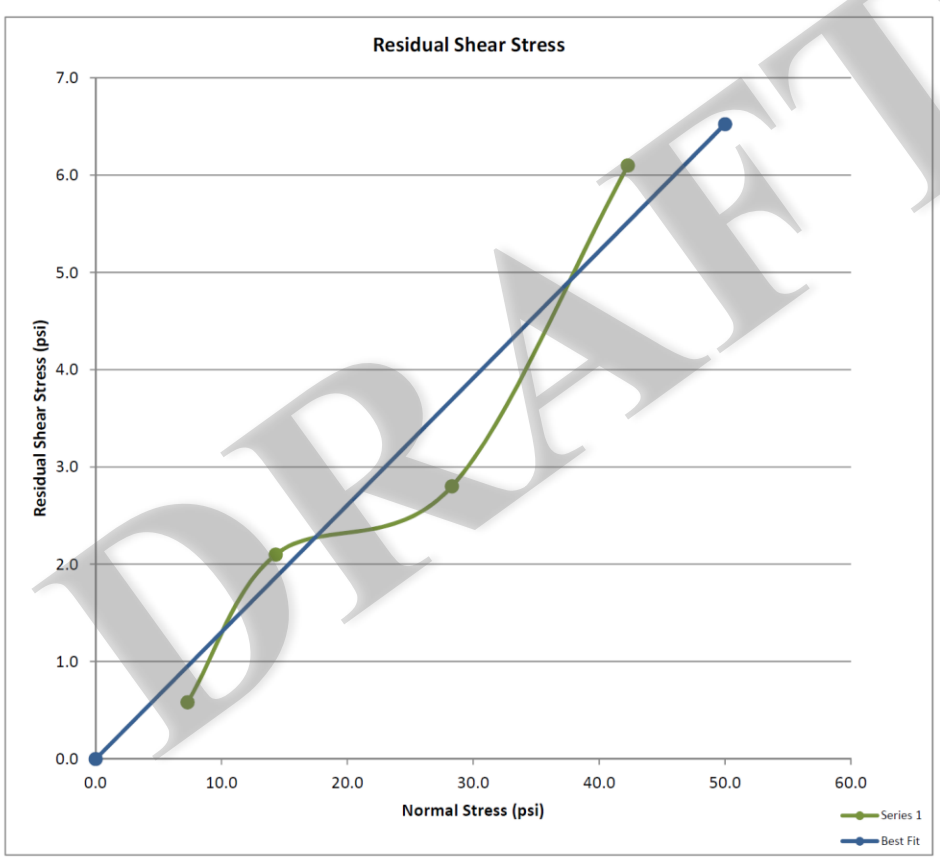

Ring Shear Report (3 of 4)

Ring Shear Test Report (ASTM D6467-06a)

Washington State Department of Transportation Geotechnical Division

PROJECT INFORMATION			
Project	Prosser vic. Road Deformation		
Location	SR 82 MP 91.9		
Project Manager	Tom Badger	Sample Number	D-6-A
Project Number	MT-0472	Depth	21' - 23'
Boring Number	H-101vwp-13	Sample Type	Remolded
Description	MH Elastic SILT		

FINAL GRAPHS (3 of 3)

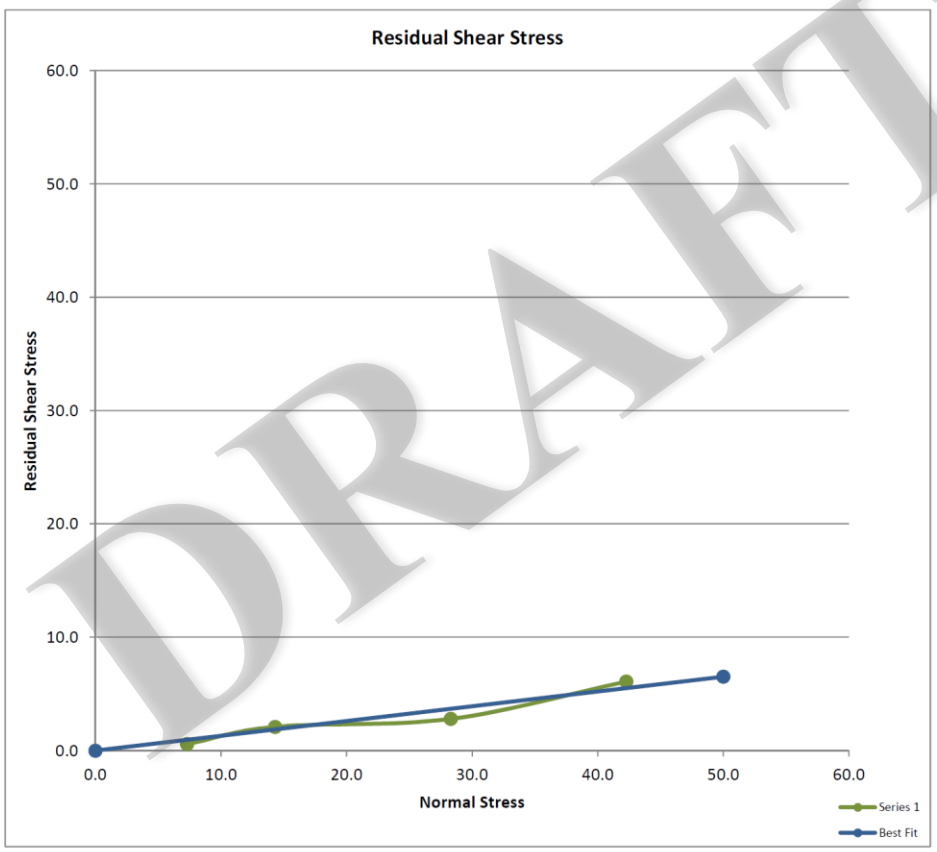

Ring Shear Report (4 of 4)

Ring Shear Test Report (ASTM D6467-06a)

Washington State Department of Transportation Geotechnical Division

PROJECT INFORMATION			
Project	Prosser vic. Road Deformation		
Location	SR 82 mP 91.9		
Project Manager	Tom Badger	Sample Number	D-6-A
Project Number	MT-0472	Depth	21' - 23'
Boring Number	H-101vwp-13	Sample Type	Remolded
Description	MH Elastic SILT		

	Specimen			
INITIAL	A	B	C	D
Specimen Thickness (in)	0.200	0.200	0.200	0.200
Internal Ring Radius(in)	1.375	1.375	1.375	1.375
External Ring Radius(in)	1.970	1.970	1.970	1.970
Moisture Content (%)	92.0	92.0	92.0	92.0
SHEAR	**A**	**B**	**C**	**D**
Rate of Linear Displacement (in/min)	0.0007	0.0007	0.0007	0.0007
Rate of Angular Displacement (Deg/min)	0.0240	0.0240	0.0240	0.0240
Normal Stress (psi)	6.7	13.8	27.8	41.8
Residual Shear Stress (psi)	0.550	1.400	3.000	4.650
Linear Displacement (in)	0.084	0.126	0.042	0.084
Angular Displacement (Deg)	2.9	4.3	1.4	2.9
FINAL	**A**	**B**	**C**	**D**
Final Moisture Content (%)	82.0	82.0	82.0	82.0
Assumed Cohesion (psi)	0.0	0.0	0.0	0.0
Liquid limit	115.0	115.0	115.0	115.0
Plastic Limit	51.0	51.0	51.0	51.0
Plasticity Index	64.0	64.0	64.0	64.0
Specific Gravity	2.67	2.67	2.67	2.67
Angle of Residual Shear Resistance (Deg)	**6.2**			

COMMENT/REMARKS
In-situ M/C = 69%, Test run at 80% of LL

Tested By	LHB/SW	Date	10/14/2013
Checked By	RDG	Date	10/28/2013

Ring Shear Report (1 of 4)

Ring Shear Test Report (ASTM D6467-06a)

Washington State Department of Transportation Geotechnical Division

PROJECT INFORMATION			
Project	Prosser vic. Road Deformation		
Location	SR 82 mP 91.9		
Project Manager	Tom Badger	Sample Number	D-6-A
Project Number	MT-0472	Depth	21' - 23'
Boring Number	H-101vwp-13	Sample Type	Remolded
Description	MH Elastic SILT		

FINAL GRAPHS (1 of 3)

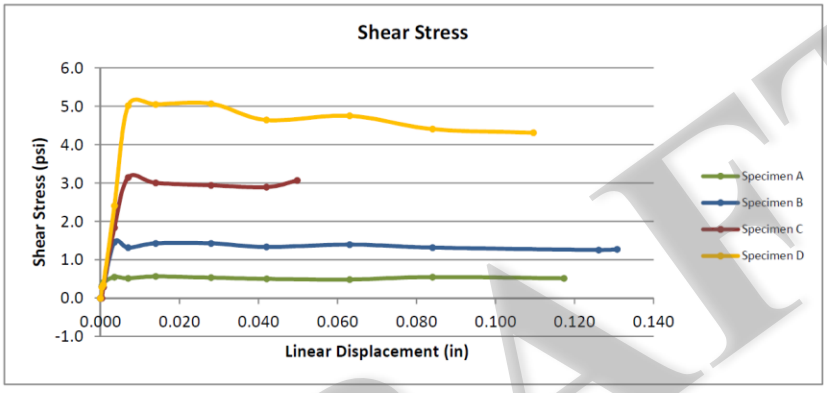

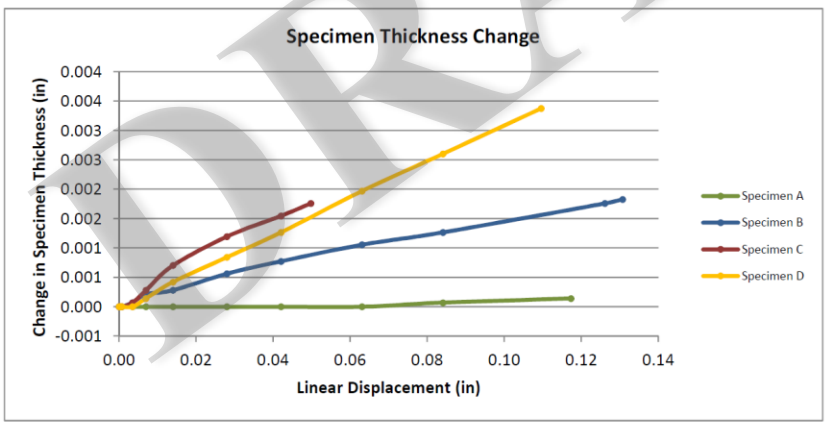

Ring Shear Report (2 of 4)

Ring Shear Test Report (ASTM D6467-06a)

Washington State Department of Transportation Geotechnical Division

PROJECT INFORMATION			
Project	Prosser vic. Road Deformation		
Location	SR 82 mP 91.9		
Project Manager	Tom Badger	Sample Number	D-6-A
Project Number	MT-0472	Depth	21' - 23'
Boring Number	H-101vwp-13	Sample Type	Remolded
Description	MH Elastic SILT		

FINAL GRAPHS (2 of 3)

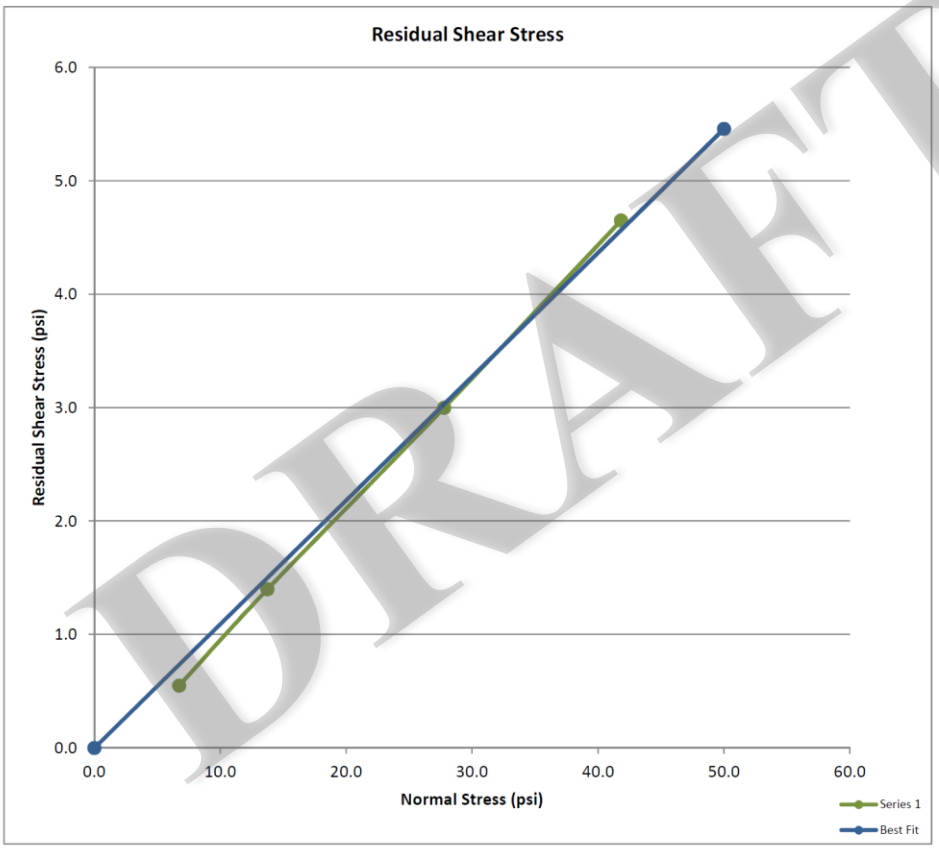

Ring Shear Report (3 of 4)

Ring Shear Test Report (ASTM D6467-06a)

Washington State Department of Transportation Geotechnical Division

PROJECT INFORMATION			
Project	Prosser vic. Road Deformation		
Location	SR 82 mP 91.9		
Project Manager	Tom Badger	Sample Number	D-6-A
Project Number	MT-0472	Depth	21' - 23'
Boring Number	H-101vwp-13	Sample Type	Remolded
Description	MH Elastic SILT		

FINAL GRAPHS (3 of 3)

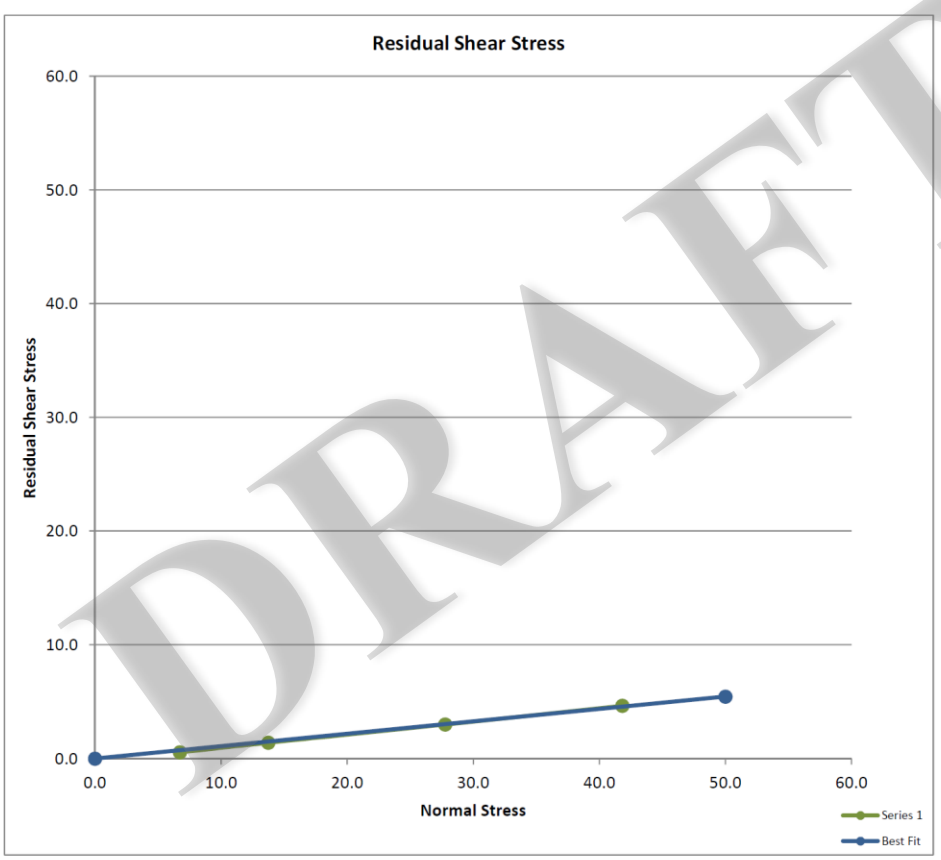

Ring Shear Report (4 of 4)

Ring Shear Test Report (ASTM D6467-06a)

Washington State Department of Transportation Geotechnical Division

PROJECT INFORMATION			
Project	Prosser vic. Road Deformation		
Location	SR 82 MP 91.9		
Project Manager	Tom Badger	Sample Number	D-6-B
Project Number	MT-0472	Depth	21' - 23'
Boring Number	H-101vwp-13	Sample Type	Remolded
Description	MH Elastic SILT		

	Specimen			
INITIAL	**A**	**B**	**C**	**D**
Specimen Thickness (in)	0.200	0.200	0.200	0.200
Internal Ring Radius(in)	1.375	1.375	1.375	1.375
External Ring Radius(in)	1.970	1.970	1.970	1.970
Moisture Content (%)	86.0	86.0	86.0	86.0
SHEAR	**A**	**B**	**C**	**D**
Rate of Linear Displacement (in/min)	0.0007	0.0007	0.0007	0.0007
Rate of Angular Displacement (Deg/min)	0.0240	0.0240	0.0240	0.0240
Normal Stress (psi)	7.3	14.3	28.3	42.3
Residual Shear Stress (psi)	0.348	1.240	3.260	4.930
Linear Displacement (in)	0.063	0.063	0.063	0.042
Angular Displacement (Deg)	2.2	2.2	2.2	1.4
FINAL	**A**	**B**	**C**	**D**
Final Moisture Content (%)	72.0	72.0	72.0	72.0
Assumed Cohesion (psi)	0.0	0.0	0.0	0.0
Liquid limit	115.0	115.0	115.0	115.0
Plastic Limit	51.0	51.0	51.0	51.0
Plasticity Index	64.0	64.0	64.0	64.0
Specific Gravity	2.67	2.67	2.67	2.67
Angle of Residual Shear Resistance (Deg)	**6.4**			

COMMENT/REMARKS
In-situ M/C = 69%, Test run at 75% of LL

Tested By	LHB/SW	Date	10/24/2013
Checked By	RDG	Date	10/28/2013

Ring Shear Report (1 of 4)

Ring Shear Test Report (ASTM D6467-06a)

Washington State Department of Transportation Geotechnical Division

PROJECT INFORMATION			
Project	Prosser vic. Road Deformation		
Location	SR 82 MP 91.9		
Project Manager	Tom Badger	Sample Number	D-6-B
Project Number	MT-0472	Depth	21' - 23'
Boring Number	H-101vwp-13	Sample Type	Remolded
Description	MH Elastic SILT		

FINAL GRAPHS (1 of 3)

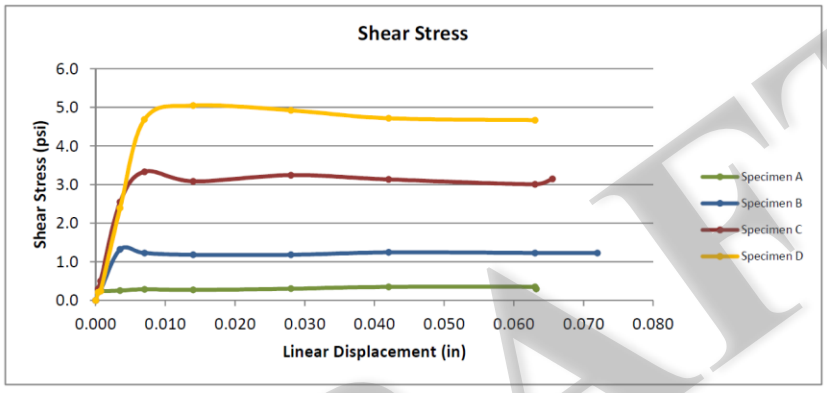

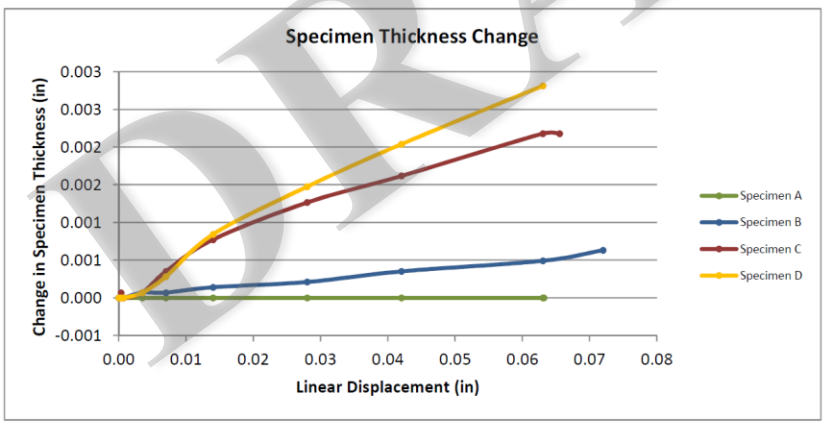

Ring Shear Report (2 of 4)

Ring Shear Test Report (ASTM D6467-06a)

Washington State Department of Transportation Geotechnical Division

PROJECT INFORMATION			
Project	Prosser vic. Road Deformation		
Location	SR 82 MP 91.9		
Project Manager	Tom Badger	Sample Number	D-6-B
Project Number	MT-0472	Depth	21' - 23'
Boring Number	H-101vwp-13	Sample Type	Remolded
Description	MH Elastic SILT		

FINAL GRAPHS (2 of 3)

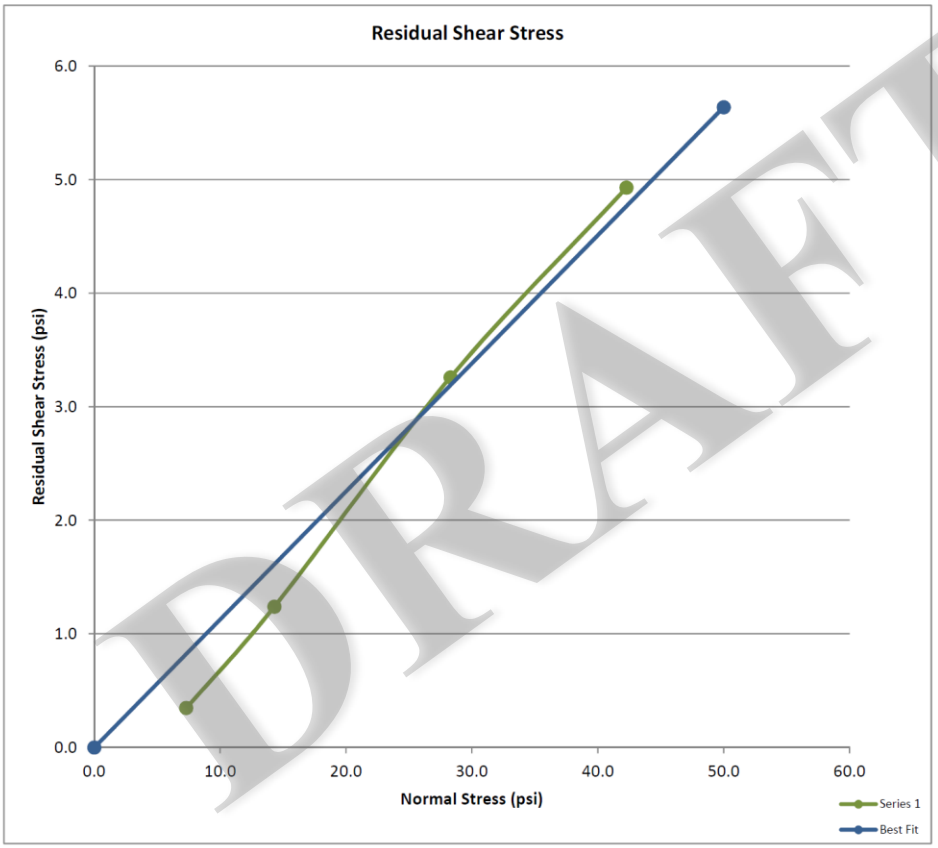

Ring Shear Report (3 of 4)

Ring Shear Test Report (ASTM D6467-06a)

Washington State Department of Transportation Geotechnical Division

PROJECT INFORMATION			
Project	Prosser vic. Road Deformation		
Location	SR 82 MP 91.9		
Project Manager	Tom Badger	Sample Number	D-6-B
Project Number	MT-0472	Depth	21' - 23'
Boring Number	H-101vwp-13	Sample Type	Remolded
Description	MH Elastic SILT		

FINAL GRAPHS (3 of 3)

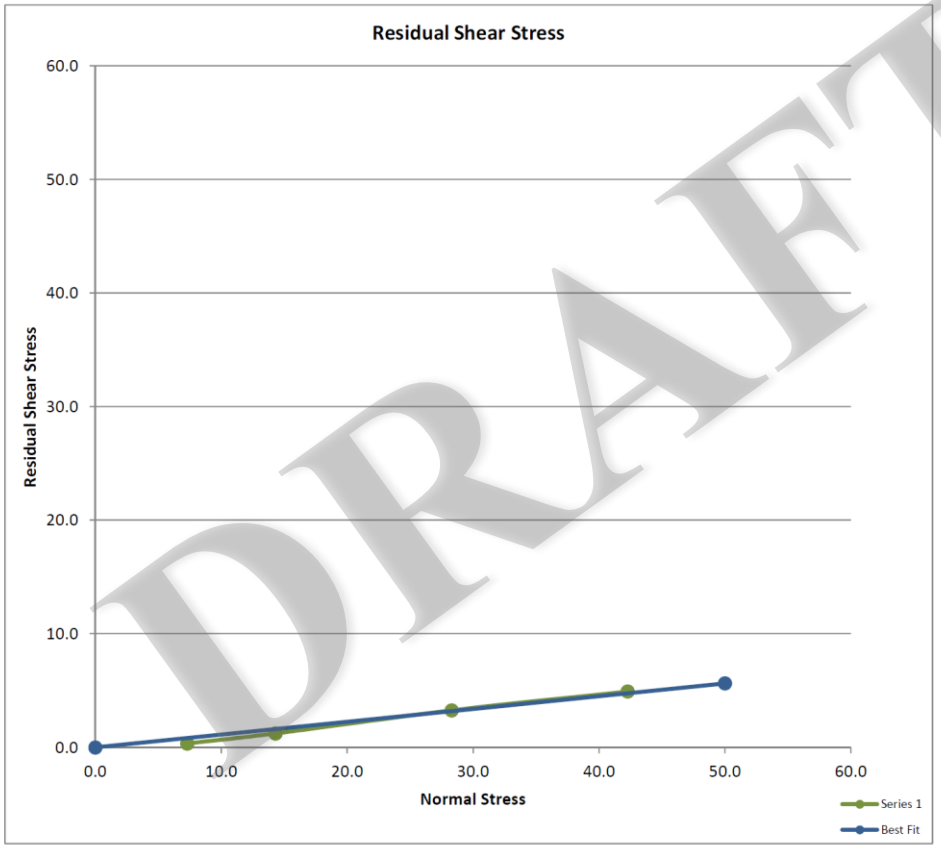

Ring Shear Report (4 of 4)

Ring Shear Test Report (ASTM D6467-06a)

Washington State Department of Transportation Geotechnical Division

PROJECT INFORMATION			
Project	Prosser vic. Road Deformation		
Location	SR 82 MP 91.9		
Project Manager	TOM BADGER	Sample Number	D-6-B
Project Number	MT-0472	Depth	21' - 23'
Boring Number	H-101vwp-13	Sample Type	Remolded
Description	MH Elastic SILT		

	Specimen			
INITIAL	**A**	**B**	**C**	**D**
Specimen Thickness (in)	0.200	0.200	0.200	0.200
Internal Ring Radius(in)	1.375	1.375	1.375	1.375
External Ring Radius(in)	1.970	1.970	1.970	1.970
Moisture Content (%)	69.0	69.0	69.0	69.0
SHEAR	**A**	**B**	**C**	**D**
Rate of Linear Displacement (in/min)	0.0007	0.0007	0.0007	0.0007
Rate of Angular Displacement (Deg/min)	0.0240	0.0240	0.0240	0.0240
Normal Stress (psi)	6.8	13.8	27.8	41.8
Residual Shear Stress (psi)	0.442	1.430	3.190	4.300
Linear Displacement (in)	0.063	0.168	0.126	0.134
Angular Displacement (Deg)	2.2	5.8	4.3	4.6
FINAL	**A**	**B**	**C**	**D**
Final Moisture Content (%)	76.0	76.0	76.0	76.0
Assumed Cohesion (psi)	0.0	0.0	0.0	0.0
Liquid limit	115.0	115.0	115.0	115.0
Plastic Limit	51.0	51.0	51.0	51.0
Plasticity Index	64.0	64.0	64.0	64.0
Specific Gravity	2.67	2.67	2.67	2.67
Angle of Residual Shear Resistance (Deg)	**6.0**			

COMMENT/REMARKS

Tested at in-situ moisture - 69%

Tested By	LHB/SW	Date	10/31/2013
Checked By	RDG	Date	11/1/2013

Ring Shear Test Report (ASTM D6467-06a)

Washington State Department of Transportation Geotechnical Division

PROJECT INFORMATION			
Project	Prosser vic. Road Deformation		
Location	SR 82 MP 91.9		
Project Manager	TOM BADGER	Sample Number	D-6-B
Project Number	MT-0472	Depth	21' - 23'
Boring Number	H-101vwp-13	Sample Type	Remolded
Description	MH Elastic SILT		

FINAL GRAPHS (1 of 3)

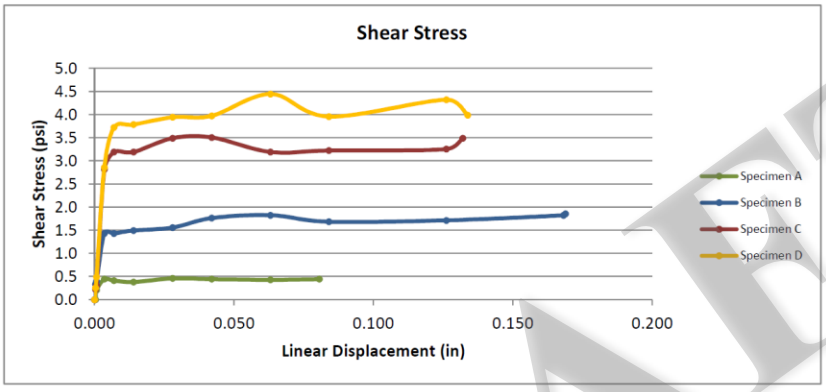

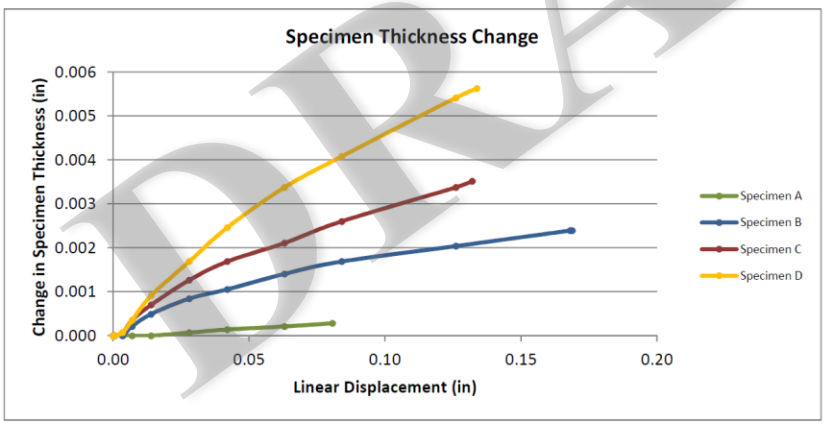

Ring Shear Report (2 of 4)

Ring Shear Test Report (ASTM D6467-06a)

Washington State Department of Transportation Geotechnical Division

PROJECT INFORMATION			
Project	Prosser vic. Road Deformation		
Location	SR 82 MP 91.9		
Project Manager	TOM BADGER	Sample Number	D-6-B
Project Number	MT-0472	Depth	21' - 23'
Boring Number	H-101vwp-13	Sample Type	Remolded
Description	MH Elastic SILT		

FINAL GRAPHS (2 of 3)

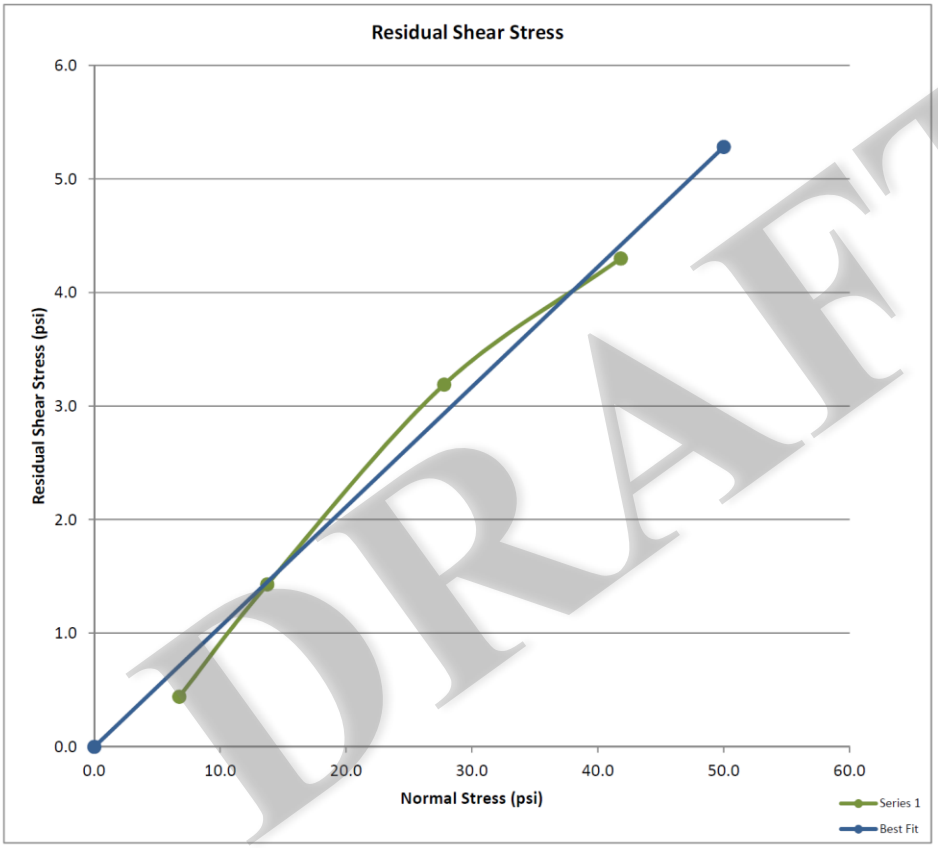

Ring Shear Report (3 of 4)

Ring Shear Test Report (ASTM D6467-06a)

Washington State Department of Transportation Geotechnical Division

PROJECT INFORMATION			
Project	Prosser vic. Road Deformation		
Location	SR 82 MP 91.9		
Project Manager	TOM BADGER	Sample Number	D-6-B
Project Number	MT-0472	Depth	21' - 23'
Boring Number	H-101vwp-13	Sample Type	Remolded
Description	MH Elastic SILT		

FINAL GRAPHS (3 of 3)

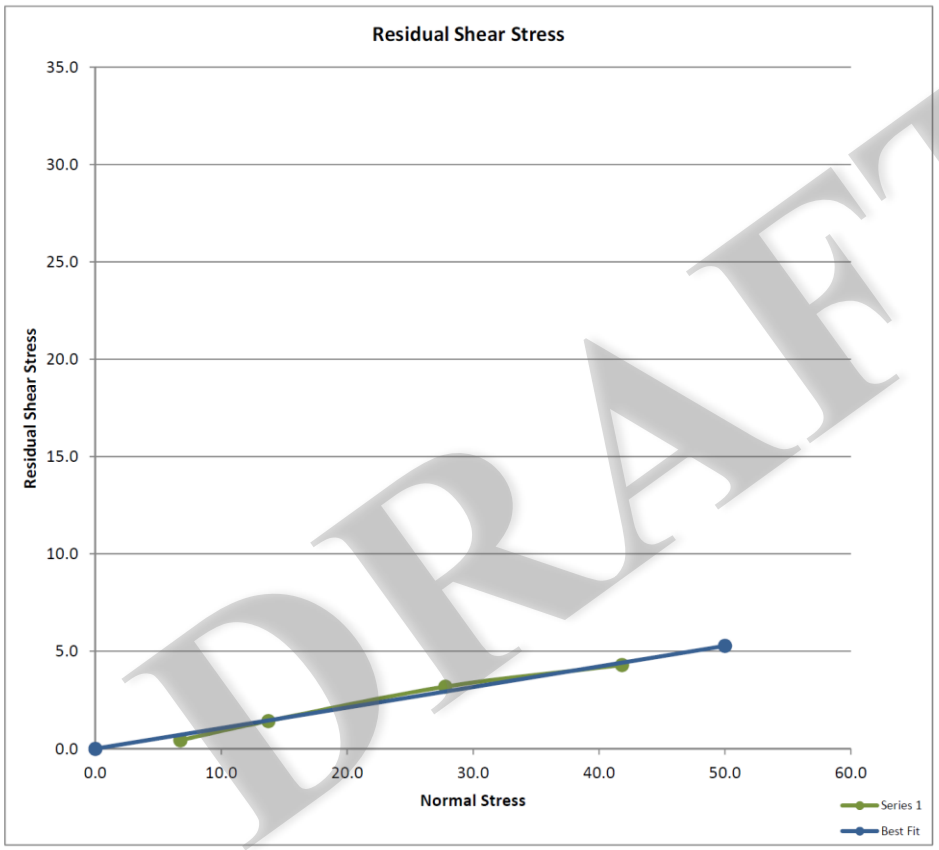

Ring Shear Report (4 of 4)

Appendix C
X-Ray Diffraction Mineralogy

Appendix C: X-Ray Diffraction Mineralogy

Introduction

Presented here are comparisons of the sample XRD peak pattern to standard peak patterns of clay mineral species. The x-axis indicates 2θ angle which increases to a maximum of 65º on the right. The y-axis is the peak intensity. Peaks indicate a 2θ angle which is incident on a crystal plane.

Common clay minerals are presented here for comparison, including three common smectite-group minerals, illite, and mixed layered clays containing a smectite and a non-smectite layer.

Smectite-Group Clay Minerals

Smectite-group minerals are expansive clay minerals (Moore and Reynolds, 1989) largely formed from the decomposition of illite and mica (Moore and Reynolds, 1989; Selley, Cocks, and Pliner, 2005; Bain, 1971).

Figure C.1 - Montmorillonite

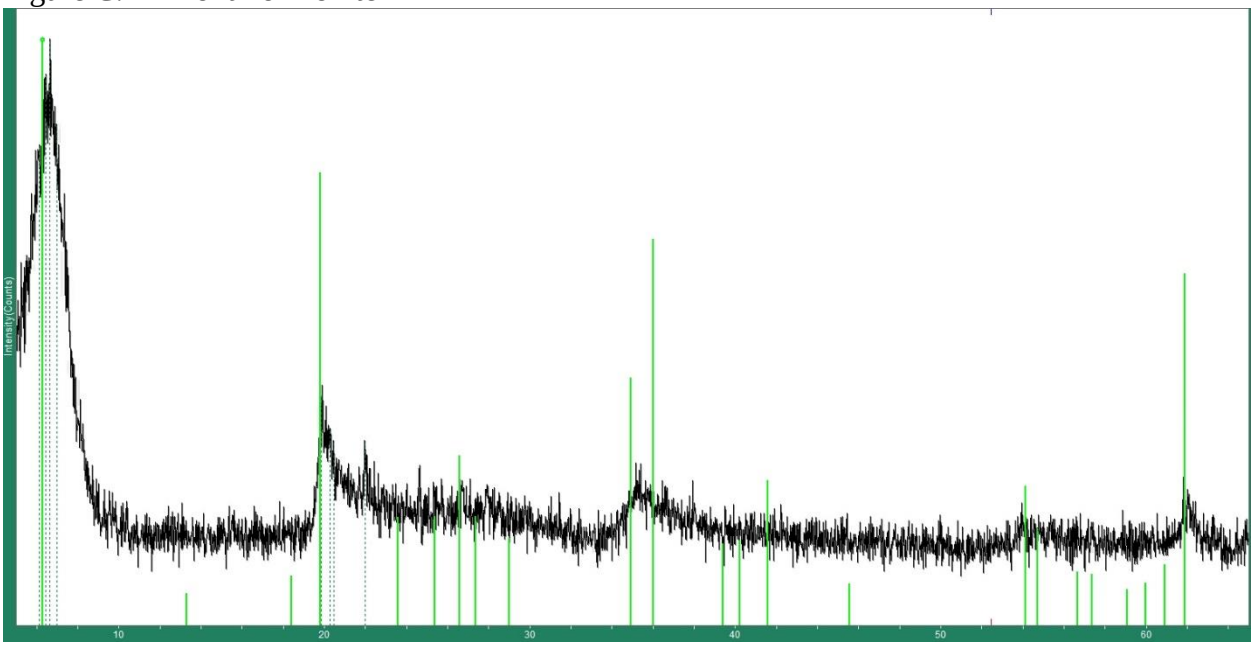

According to Reynolds and Moore (1989) montmorillonite (air-dried, non-solvated) has major peaks at between 4º and 6º 2θ, at around 18º 2θ and between 62.22º and 61.67º 2θ. The green peak pattern given by PDF 00-060-0318 shows good correlation at the 20º 2θ peak, peaks near 35º 2θ, and the peak at 62º 2θ. MDI Jade calculated that the large, low angle peak at between º6 and 7º 2θ as statistically being a 100% match to montmorillonite. MDI Jade also calculated a 77% match on the 20º 2θ peak.

Figure C.2 - Saponite

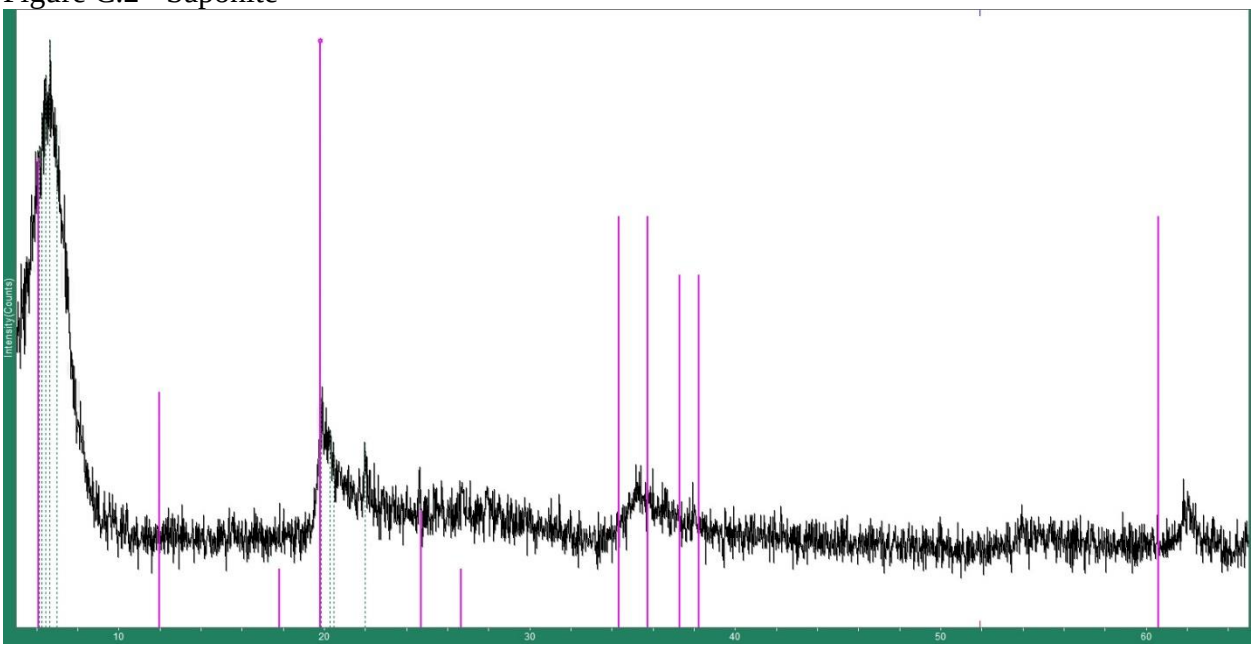

The saponite peak pattern for PDF 00-030-0789 (pink) shows good visual matches at the 20º 2θ peak. Weaker matches are seen at the low angle 2θ peak and near the 35º 2θ. MDI Jade calculated an 80% match for the low angle 2θ peak and a 100% match at the 20º 2θ peak.

Figure C. 3 - Nontronite

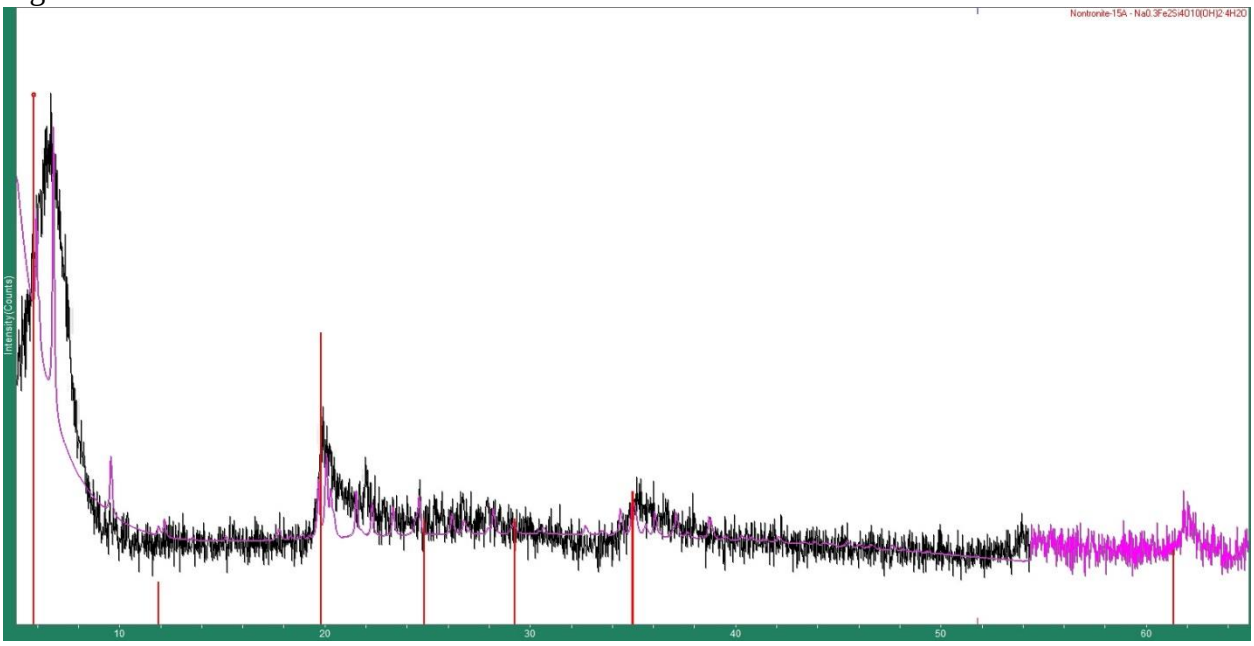

For nontronite PDF 00-029-1497 (dark red), a strong visual match can be seen with the 20º 2θ peak. A weak match can be seen at the 35º 2θ peak. MDI Jade matched the low angle 2θ peak at 100% correlation.

Illite

Illite is a non-expansive clay related to muscovite and smectite minerals (Moore and Reynolds, 1989; Selley, Cocks, and Pliner, 2005). While illite can be plastic, it does not possess the expansion potential or high plasticity of the smectite-group minerals it generates (Bain, 1971).

Figure C.4 - Illite

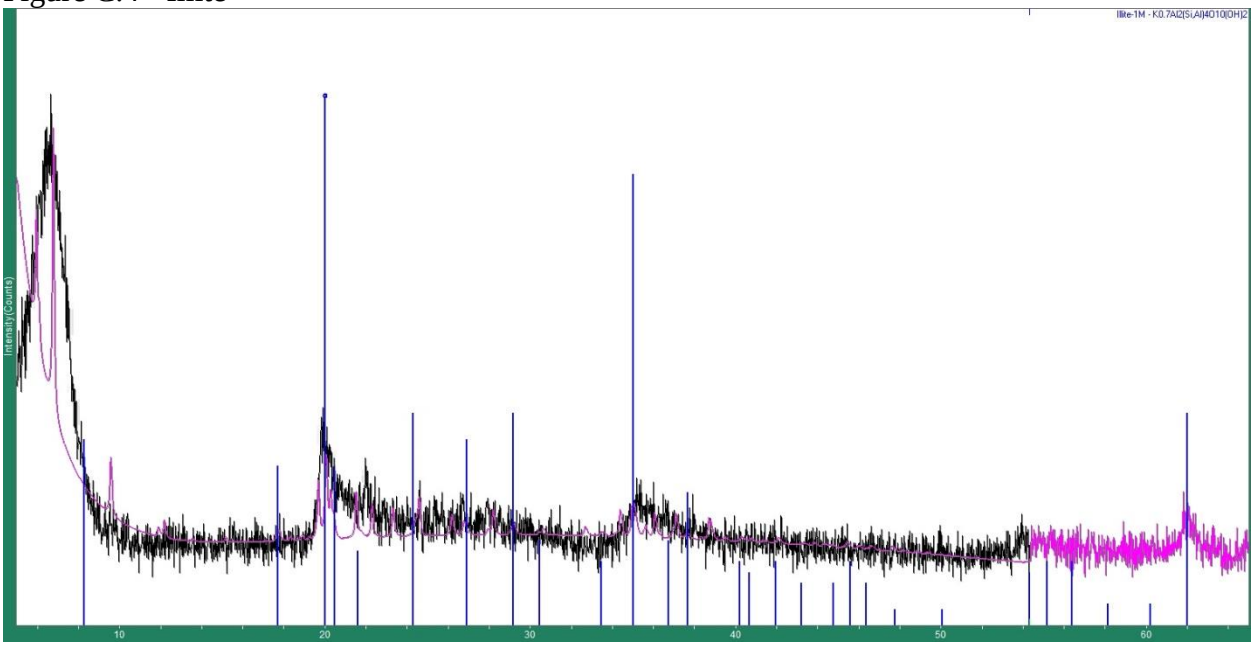

For illite PDF 00-029-1496, strong visual matches can be seen at 20º 2θ, 35º 2θ, and 62º 2θ. MDI Jade matched the 20º 2θ peak at 100%.

Vermiculite and kaolinite were also compared, however no visual or statistical matches between the sample pattern and the standard PDFs could be identified.

Mixed Layer Species

Mixed layer species are clays which incorporate 2 (or possibly more) different clay mineral sheets into the crystal lattice (Moore and Reynolds, 1989). The alternating sheets different clay minerals can be random or ordered (Moore and Reynolds, 1989). Ordered sheet mixed layer clays are named

Figure C.5 - Illite-Montmorillonite

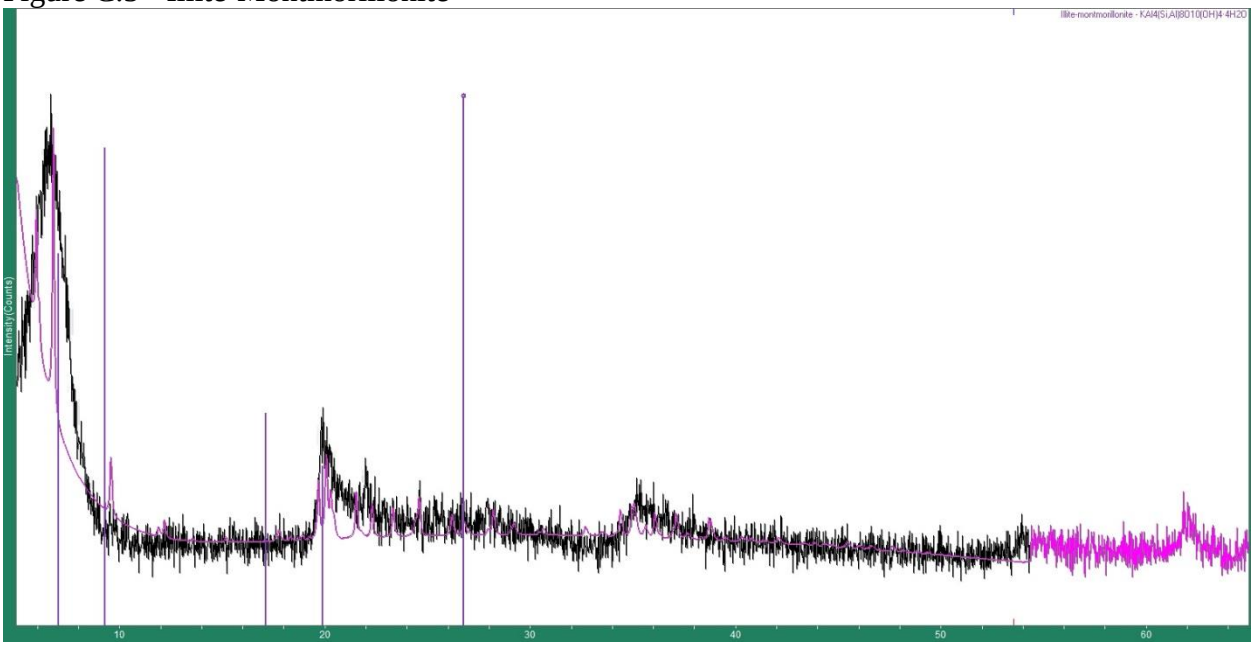

Illite-montmorillonite is a common mix of clay minerals (Moore and Reynolds, 1989). For this sample (PDF 00-035-0652), a strong visual match can be seen at near 20º 2θ, however, MDI Jade did not identify any matches.

Figure C.6. - Rectorite

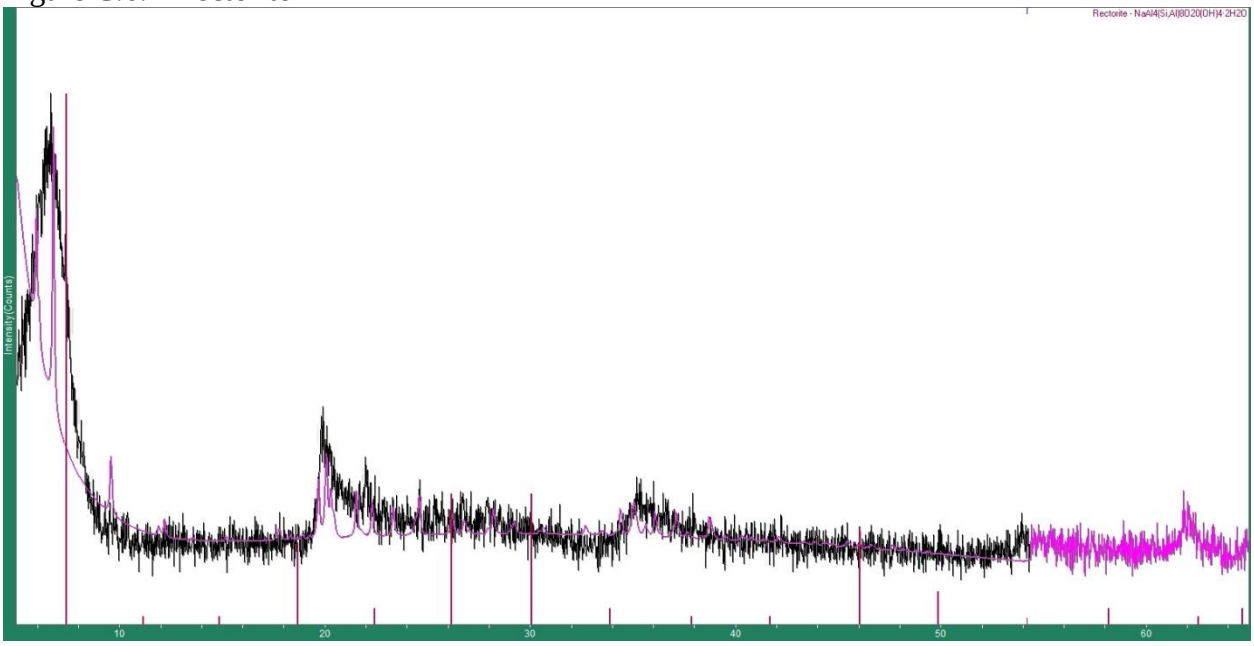

Rectorite is a regularly alternating (1:1) mixed clay consisting of a mica species and smectite (Moore and Reynolds, 1989). With this peak pattern (PDF 00-025-0781) a weak visual correlation may be made with the low angle 2θ peak. MDI Jade did not identify any statistical matches.

Figure C.7 - Kaolinite-Montmorillonite

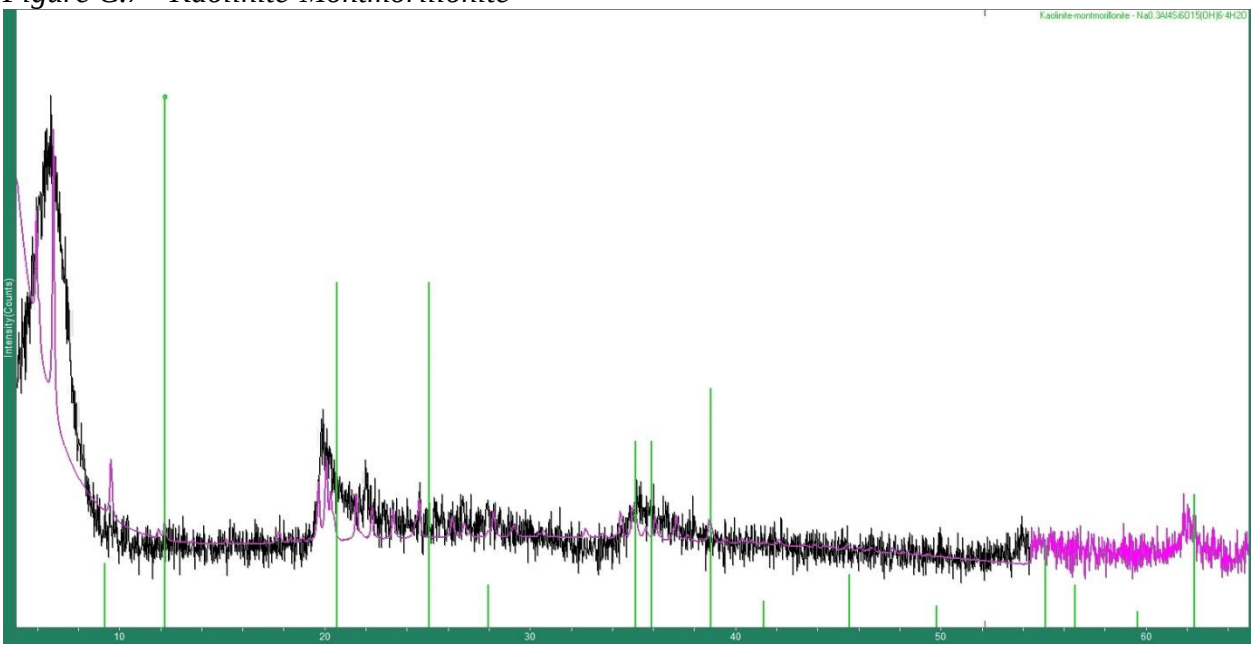

Kaolinite-montmorillonite mixes kaolinite, which is non-expansive, with montmorillonite, which can be highly expansive (Moore and Reynolds, 1989; Bain, 1971). With this peak pattern (PDF 00-029-1490), a mediocre visual match may be seen at near 35º 2θ. MDI Jade did not identify any statistical matches.

Appendix D
Stability Modeling Results

Appendix D: Stability Modeling Results

Introduction

Stability Modeling Results for the large landslide and small landslide scenarios are presented here. Factors of Safety below 1 indicate slope instability. Factors of Safety at or above on indicate stability. The construction status of the buttress (fully keyed, partially keyed, having an absent key) is indicated in the left column (See Figures 28 and 29 for what each condition represents.

Large Landslide

At a φ angle of 10° in the Gravels-with-matrix, the following Factors of Safety were produced:

Table D.1. Factors of Safety when using a 10° φ angle

	Bishop Simplified	GLE/Morgenstern-Price
Full Key	0.977	0.966
Partial Key	0.967	0.957
Absent Key	0.967	0.958

Increasing the φ angle of the silty clay unit to 10°, the same as the Gravels-with-matrix unit, produces the following Factors of Safety:

Table D.2. Results of increasing the φ angle of the silty clay unit to 10°

	Bishop Simplified	GLE/Morgenstern-Price
Full Key	1.000	0.988
Partial Key	0.987	0.974
Absent Key	0.986	0.973

Adding lenses of the Clean Gravels unit into the stratigraphy produced the following Factors of Safety:

Table D.3. Factors of Safety when clean gravel lenses are added

	Bishop Simplified	GLE/Morgenstern-Price
Full Key	1.078	1.071
Partial Key	1.057	1.045
Absent Key	1.057	1.046

A small perched water table was modeled above the clay unit. The Factors of Safety produced in this scenario are as follows:

Table D.4. The effects of a perched water table on the Factor of Safety

Factor of Safety	Bishop Simplified	GLE/Morgenstern-Price

Full Key	0.969	0.958
Partial Key	0.950	0.939
Absent Key	0.950	0.939

Small Landslide

Increasing the φ angle of the Gravels-with-matrix to 35° produces the following Factors of Safety:

Table D.5. Factors of Safety with increased φ angle in the gravels-with-matrix unit

Factor of Safety	Bishop Simplified	GLE/Morgenstern-Price
Full Key	1.297	1.368
Partial Key	0.933	0.939
Absent Key	0.933	0.939

Decreasing the φ angle of the Gravels-with-matrix to 15° produces the following Factors of Safety:

Table D.6. Factors of Safety with a φ angle of 15° in the gravels-with-matrix unit

Factor of Safety	Bishop Simplified	GLE/Morgenstern-Price
Full Key	1.135	1.200
Partial Key	0.795	0.806
Absent Key	0.794	0.806

Decreasing the φ angle of the Gravels-with-matrix to 10° produces the following Factors of Safety:

Table D.7. Factors of Safety with a φ angle of 10° in the gravels-with-matrix unit

Factor of Safety	Bishop Simplified	GLE/Morgenstern-Price
Full Key	0.890	0.940
Partial Key	0.754	0.772
Absent Key	0.754	0.769

Modeling a perched water table above the clay unit produces the following Factors of Safety:

Table D.8. The effects of a perched water table on the Factor of Safety

Factor of Safety	Bishop Simplified	GLE/Morgenstern-Price
Full Key	1.128	1.199
Partial Key	0.798	0.803
Absent Key	0.797	0.804